

AD _____

Award Number: W81XWH-05-1-0340

TITLE: DREW-UCLA Breast Cancer Research and Training Program: Molecular/Cellular Pathogenesis Model

PRINCIPAL INVESTIGATOR: Jaydutt Vadgama, Ph.D.

CONTRACTING ORGANIZATION: Charles R. Drew University of Medicine & Science, Inc.
Los Angeles, California 90059-3057

REPORT DATE: March 2007

TYPE OF REPORT: Annual Summary

PREPARED FOR: U.S. Army Medical Research and Materiel Command
Fort Detrick, Maryland 21702-5012

DISTRIBUTION STATEMENT: Approved for Public Release;
Distribution Unlimited

The views, opinions and/or findings contained in this report are those of the author(s) and should not be construed as an official Department of the Army position, policy or decision unless so designated by other documentation.

REPORT DOCUMENTATION PAGE

Form Approved
OMB No. 0704-0188

Public reporting burden for this collection of information is estimated to average 1 hour per response, including the time for reviewing instructions, searching existing data sources, gathering and maintaining the data needed, and completing and reviewing this collection of information. Send comments regarding this burden estimate or any other aspect of this collection of information, including suggestions for reducing this burden to Department of Defense, Washington Headquarters Services, Directorate for Information Operations and Reports (0704-0188), 1215 Jefferson Davis Highway, Suite 1204, Arlington, VA 22202-4302. Respondents should be aware that notwithstanding any other provision of law, no person shall be subject to any penalty for failing to comply with a collection of information if it does not display a currently valid OMB control number. **PLEASE DO NOT RETURN YOUR FORM TO THE ABOVE ADDRESS.**

1. REPORT DATE (DD-MM-YYYY) 01-03-2007		2. REPORT TYPE Annual Summary		3. DATES COVERED (From - To) 1 Mar 2005 – 28 Feb 2007	
4. TITLE AND SUBTITLE DREW-UCLA Breast Cancer Research and Training Program: Molecular/Cellular Pathogenesis Model				5a. CONTRACT NUMBER	
				5b. GRANT NUMBER W81XWH-05-1-0340	
				5c. PROGRAM ELEMENT NUMBER	
6. AUTHOR(S) Jaydutt Vadgama, Ph.D. E-Mail: javadgam@cdrewu.edu				5d. PROJECT NUMBER	
				5e. TASK NUMBER	
				5f. WORK UNIT NUMBER	
7. PERFORMING ORGANIZATION NAME(S) AND ADDRESS(ES) Charles R. Drew University of Medicine & Science, Inc. Los Angeles, California 90059-3057				8. PERFORMING ORGANIZATION REPORT NUMBER	
9. SPONSORING / MONITORING AGENCY NAME(S) AND ADDRESS(ES) U.S. Army Medical Research and Materiel Command Fort Detrick, Maryland 21702-5012				10. SPONSOR/MONITOR'S ACRONYM(S)	
				11. SPONSOR/MONITOR'S REPORT NUMBER(S)	
12. DISTRIBUTION / AVAILABILITY STATEMENT Approved for Public Release; Distribution Unlimited					
13. SUPPLEMENTARY NOTES					
14. ABSTRACT Objective: The overarching goals of this partnership between Charles R. Drew University of Medicine and Science (Drew) and the University of California Los Angeles Jonsson Comprehensive Cancer Center (UCLA-JCCC) are to develop Drew faculty into independent and competitive investigators and in turn, provide Drew with the necessary capacity to establish a breast cancer research program with a focus on minority and underserved populations. We have generated significant progress toward the following objectives: 1. We have created a Cancer Cluster at Drew that brings together various investigators engaged or have interest in Cancer Research, Education, Training, and Treatment. This Cluster group has enabled us to identify senior, mid-level, and junior faculty who can be partnered with established breast cancer investigators at UCLA as senior mentors or research collaborators. 2. We have created an educational experience and mentored research environment that fosters breast cancer research and offers substantive training to Drew (HBCU/MI) faculty and postdoctoral fellows. 3. We have created opportunities for Drew faculty, fellows and students to access UCLA-JCCC and Drew shared resources. 4. We have generated exciting data that identifies novel genes that may be associated with HER2/neu overexpressing breast tumors. In particular, candidate genes that may be associated with resistant to Trastuzumab treatment.					
15. SUBJECT TERMS Breast Cancer Research; Established Mentor/Trainee partners; recruited new investigators; initiated innovative research project on HER2/neu overexpressing Breast Cancer; Created training opportunities for Postdocs, Residents, Clinical Fellows and Students					
16. SECURITY CLASSIFICATION OF:			17. LIMITATION OF ABSTRACT	18. NUMBER OF PAGES	19a. NAME OF RESPONSIBLE PERSON
a. REPORT	b. ABSTRACT	c. THIS PAGE			USAMRMC
U	U	U	UU	124	19b. TELEPHONE NUMBER (include area code)

Table of Contents

	<u>Page</u>
Introduction.....	4
Body.....	5-6
Key Research Accomplishments.....	7
Reportable Outcomes.....	7
Conclusion.....	7-9
References.....	9
Appendices.....	9

Introduction:

Minority populations are more likely to suffer advanced forms of breast cancers, have limited access to standard of care, and have almost no access to state-of-the art clinical trials for treatment protocols. These communities have poor outcomes and survival. Historically Black Colleges and Universities/Minority Serving Institutions (HBCU/MI), created to serve these communities, often are unable to provide quality education, training, and care necessary for treatment and eradication of the disease in their communities. This is primarily due to poor infrastructure, limited investigators in breast cancer research, and lack of resources to launch a credible clinical trials program.

Objective: The overarching goals of this partnership between Charles R. Drew University of Medicine and Science (Drew) and the University of California Los Angeles Jonsson Comprehensive Cancer Center (UCLA-JCCC) are to develop Drew faculty into independent and competitive investigators and in turn, provide Drew with the necessary capacity to establish a breast cancer research program with a focus on minority and underserved populations.

Specific Objectives: This will be accomplished through three objective and two sub-objectives:

1. Create an educational experience and mentored research environment that fosters breast cancer research and offers substantive training to Drew (HBCU/MI) faculty and postdoctoral fellows.
 - a. Create a trainee/mentor relationship between Drew trainees and UCLA researchers whereby Drew trainees will learn research techniques, concepts, and theories, which will be applied to their own independent research projects.
 - b. Implement an extensive program that focuses on transferring knowledge to Drew faculty regarding biology, etiology, prevention, detection, diagnosis, and treatment of breast cancer.
2. Make available UCLA-JCCC and Drew shared resources through which collaborative projects between Drew and UCLA will be supported, thereby strengthening the training and mentoring experience for HBCU/MI faculty and fellows; and
3. Conduct a substantive research that will focus on cell and molecular biology, detection, diagnosis, etiology, and treatment of HER-2/neu expressing breast tumors in minority and underserved women, which will lead to sustained training, education, publications, and competitive funding for Drew.

BODY:

The following table outlines the summary of our research accomplishments from the initial funding date in March 2005 to April 2007. Essentially it narrates the progress made in two years as per the Statement of Work. The framework of this table was created in the original application to assess our communication/evaluation process. It describes the program's specific activities, the frequency of communication, and the method of communication.

<u>Activity</u>	<u>Frequency of Communication</u>	<u>Progress to Date</u>
PIs to set up a series of planning and evaluation meetings to discuss and organize the training activities and tasks	Every 3 months	Established several opportunities. Activity is ongoing
PIs to identify research training activities	Weekly seminars and Journal Club presentations. Mentors/Mentee's have been identified	Several research projects have been initiated. See Appendix
PIs to publicize training opportunities on the Drew and UCLA web sites	Have established a Cancer Cluster at Drew. Opportunities at UCLA and Drew are disseminated via e-mail and personal contacts.	Excellent. This is an ongoing activity. We will continue to identify more mentors and training opportunities
PIs to generate inter- and intra-communication systems that describe the Drew-UCLA partnership and opportunities for training and research collaborations	Daily/Weekly activities	Ongoing
PIs to identify educational training activities	Weekly/Monthly	Ongoing
PIs to identify research training activities	Weekly/Monthly	Ongoing
Drew PI to identify trainees/faculty investigators for additional training	Monthly and also during research in progress- weekly meetings	Ongoing
PIs to pair trainees/faculty investigators with UCLA research projects	Initially weekly. Now every 2 months	Have identified several collaborative projects
PIs to assign trainees to academic training opportunities	Weekly/Monthly	Completed for 3 trainees. Ongoing for others
Trainees/faculty investigators to work alongside UCLA co-investigators on ongoing research projects	Weekly/Monthly	Ongoing
PIs to assign components/specific aims of innovative research project to trainees/faculty investigators	Weekly during the first 6 months. Several trainees have been assigned	Excellent. One manuscript published, 1 under review

<u>Activity</u>	<u>Frequency of Communication</u>	<u>Progress to Date</u>
		and at least 2 more to be submitted. Other components of Specific aims are ongoing
Dr. Vadgama to solicit feedback from trainees/faculty investigators regarding efficacy of training program, progress of research program, and identification of any problems.		
Dr. Slamon to solicit feedback from UCLA investigators regarding trainee's progress and efficacy of training program. Investigators will report any problems/issues to Dr. Slamon.		
Trainees/faculty investigators to work under Drs. Vadgama and Slamon on the innovative research program.	Daily	Ongoing. See Appendix for details.
With the help of their co-investigator, trainees/faculty investigators to develop publications and grants applications	Every 3-6 months	Ongoing
Trainees/faculty investigators to initiate independent breast cancer research projects applying the knowledge learned through academic and research training activities	Monthly	Have generated 3 new projects
Drew and UCLA to identify shared resource opportunities and make them available to training participants	Daily/Weekly	Ongoing
PIs to meet and discuss progress, milestones, problems, evaluations, etc.	Every 3 months	Ongoing
PIs to complete review of training programs and prepare a final report	N/A	N/A
Trainees and investigators to prepare and submit manuscripts	Every 2-3 months	1 published, 1 under review and 2 to be submitted
Drew investigators to apply for independent funding through MBRS, RCMI, RO1, T32 and K mechanisms.	2 with RCMI, 2 MBRS, 2 with NCI U56. Preparing for U54 application.	Under review. U54 to be submitted in 2008. 1-3 RO1's, and K awards to be submitted by October 2007

KEY RESEARCH ACCOMPLISHMENTS:

We have generated significant progress toward the following objectives:

1. We have created a Cancer Cluster at Drew that brings together various investigators engaged or have interest in Cancer Research, Education, Training, and Treatment. This Cluster group has enabled us to identify senior, mid-level, and junior faculty who can be partnered with established breast cancer investigators at UCLA as senior mentors or research collaborators.
2. We have created an educational experience and mentored research environment that fosters breast cancer research and offers substantive training to Drew (HBCU/MI) faculty and postdoctoral fellows.
3. We have created opportunities for Drew faculty, fellows and students to access UCLA-JCCC and Drew shared resources.
4. We have generated exciting data that identifies novel genes that may be associated with HER2/neu overexpressing breast tumors. In particular, candidate genes that may be associated with resistant to Trastuzumab treatment.

Reportable Outcomes

- (1) Publications. Please see attached published manuscripts as well as those in review and preparation – in Appendix A-C
- (2) Original data on identification of novel genes associated with Akt1 and Her2/neu overexpression in breast tumor cell lines. Please see attached Appendix D.
- (3) Created a Drew Cancer Cluster Group. Please see Appendix E.
- (4) Research grants applied for and under review. Please see attached Appendix F and F1.
- (5) Participation in research meetings, seminars, and workshops. We have made good progress in getting Drew students, fellows, and faculty to participate in these activities. Please see Appendix F.
- (6) Made substantial progress in engaging fellows and students into cancer research. Please see Appendix F.

Conclusion

In conclusion we have made the following progress as per our “Statement of Work”

Under Task 1

- (1) We have created an educational experience and mentored research environment that fosters breast cancer research and offers substantive training to Drew (HBCU/MI) faculty and postdoctoral fellows. This activity is ongoing. The evaluation meetings are ongoing, We have partnered a few Drew trainees with UCLA researchers. We will continue to seek and establish more partnerships.

(2) We have generated inter and intra communication systems at both Drew and UCLA campuses that describe and advertise the Drew-UCLA partnership and opportunities for training and research collaborations. We will continue to improve these communication systems.

(3) Drew investigators have begun training on large-scale topics through skill-building workshops and seminars on grantsmanship. We have encouraged Drew investigators to participate in seminars and workshops at the AACR meetings as well as at UCLA. The workshops include: career development, proteomic and genomic research, translational research. Several Drew investigators have attended scientific meetings. We have ongoing participation in weekly journal clubs, and research seminars. We will continue this activity throughout the life of our grant and beyond.

(4) Drew trainees, have begun applying techniques and theories to independent projects with a special emphasis in addressing the unequal burden of cancer in underserved communities. We are confident that given the current enthusiasm with the Drew investigators, we will make significant progress in addressing the problem of unequal burden of cancer in underserved communities.

(5) Some of the Drew trainees have presented abstracts of findings at AACR and other cancer meetings. We will ensure that we have more individuals who can participate in these scholarly activities.

(6) As evident from the data in the appendices, several trainees have begun to write publications. We plan to increase these numbers substantially in the next year.

Under Task 2.

(1) We have made available shared resources of UCLA-JCCC and Drew. Collaborative projects between Drew and UCLA faculty have begun, and more are on their way toward development. HBCU/MI faculty will continue to obtain outstanding training.

(2) We have created a Cancer Cluster. The goals and the objectives of this cluster are soon to be placed on the Drew Web and may also be placed on the UCLA-JCCC web site. This will identify who at Drew are involved in cancer research, and what types of partners or collaborations they are seeking.

(3) With the help of the UCLA mentors, Drew trainees and mentors have begun to utilize shared resources such as the Drew Tissue Repository and the UCLA-JCCC shared core facilities. We are in the process of developing several research projects.

Under Task 3.

(1) We have initiated significant progress on our innovative project. This project focuses on cell and molecular biology, detection, diagnosis, etiology, and treatment of HER-2/neu overexpressing breast tumors in minority and underserved women. Please see Appendix B and C – for preliminary data. This is an ongoing activity.

(2) We will soon begin to correlate IHC data with FISH analysis. Here, our task is to correlate the IHC data with the FISH data on HER2 tumors from minority women at Drew. A total of 380 samples will be analyzed. Drew investigators will be trained to perform the FISH method. Drew investigators have already begun learning to perform tissue microarrays analysis in Dr. Slamon's laboratory at UCLA. We will continue this activity in years 3-4.

(3) We provide preliminary report that evaluate the clinical correlation between tissue overexpression of HER2 and Akt phosphorylation (activated Akt) in African American and Hispanic women with breast cancer. Please see Appendix D. This activity is ongoing.

(4) We have developed in vitro and in vivo models to study the regulation and function of Akt in the development and pathogenesis of breast tumors. Please see Appendix B and C – for 1 manuscript under review. Additional manuscripts will be generated on this activity.

(5) We have begun investigational studies to understand the mechanisms of anti-HER2 antibodies (Herceptin, and 2C4), alone and in combination with chemotherapy drugs on cell proliferation and apoptosis in breast cancer cells expressing HER2. Preliminary data are presented in a manuscript under review. Please see Appendix B.

(6) In the next two years, we plan to implement the training opportunity for Drew investigators to participate in the conduct of clinical trials using targeted therapy for HER-2 positive tumors.

References (in the manuscripts submitted in the Appendices.

Appendices

The following appendices are attached:

- (A) Apoptosis paper (published)
- (B) HER2/neu/Akt paper (under review)
- (C) Akt1 clinical correlation
- (D) Preliminary data: Identification of novel genes using Tissue Micro Array Technology. Akt1 associated genes.
- (E) Cancer Cluster Members
- (F) Summary of Progress on: Training opportunities; Seminar and Workshop participation; Grant Applications/Funding; Student Training
- (F-1) List of grant applications

Taxol induced apoptosis regulates amino acid transport in breast cancer cells

Yanyuan Wu · Dejun Shen · Zujian Chen ·
Sheila Clayton · Jaydutt V. Vadgama

Published online: 29 December 2006
© Springer Science + Business Media, LLC 2006

Abstract A major outcome from Taxol treatment is induction of tumor cell apoptosis. However, metabolic responses to Taxol-induced apoptosis are poorly understood. In this study, we hypothesize that alterations in specific amino acid transporters may affect the Taxol-induced apoptosis in breast cancer cells. In this case, the activity of the given transporter may serve as a biomarker that could provide a biological assessment of response to drug treatment. We have examined the mechanisms responsible for Taxol-induced neutral amino acid uptake by breast cancer cells, such as MCF-7, BT474, MDAMB231 and T47D. The biochemical and molecular studies include: (1) growth-inhibition (MTT); (2) transport kinetics; (3) substrate-specific inhibition; (4) effect of thiol-modifying agents NEM and NPM; (5) gene expression of amino acid transporters; and (6) apoptotic assays. Our data show that Taxol treatment of MCF-7 cells induced a transient increase in Na^+ -dependent transport of the neutral amino acid transporter B0 at both gene and protein level. This increase was attenuated by blocking the transporter in the presence of high concentrations of the substrate amino acid. Other neutral amino acid transporters such as ATA2 (System A) and ASC were not altered. Amino acid starvation resulted in the expected up-regulation of System A (ATA2) gene, but not for B0 and ASC. B0 was significantly down regulated. Taxol treatment had no significant effect on

the uptake of arginine and glutamate as measured by System y^+ and X^-_{GC} respectively. TUNEL assays and FACS cell cycle analysis demonstrated that both Taxol- and doxorubicin-induced upregulation of B0 transporter gene with accompanying increase in cell apoptosis, could be reversed partially by blocking the B0 transporter with high concentration of alanine, and/or by inhibiting the caspase pathway. Both Taxol and doxorubicin treatment caused a significant decrease in S-phase of the cell cycle. However, Taxol-induced an increase primarily in the G2 fraction while doxorubicin caused increase in G1/G0 together with a small increase in G2. In summary, our study showed that Taxol induced apoptosis in several breast cancer cells results in activation of amino acid transporter System B0 at both gene and protein level. Similar response was observed with another chemotherapeutic agent Doxorubicin, suggesting that this increase is in response to apoptosis, and not only due to changes in cell cycle related events.

Keywords Breast cancer · Apoptosis · MCF7 · T47D · MDAMB231 · Chemotherapy · Taxol · Doxorubicin · Amino acid transport · Transporter gene B0 · ATA2 · ASC

Introduction

Breast cancer is a leading cancer in American women and it is estimated that there will be more than 200,000 new breast cancer cases diagnosed in 2005 and this accounts for more than 30% of all cancers diagnosed in U.S. women in the year [1]. Taxol is an anticancer agent originally isolated from the bark of the pacific yew, *Taxus brevifolia* and has been clinically used for both early stage breast cancer, and for refractory or metastatic breast cancers [2, 3]. Taxol binds

Drs. Wu and Shen contributed equally to this study.

Y. Wu · D. Shen · Z. Chen · S. Clayton · J. V. Vadgama (✉)
Division of Cancer Research and Training, Department of
Medicine, Charles R. Drew University of Medicine and Science,
Hawkins Building, MP 30, 1731 E. 120th Street,
Los Angeles, CA 90059, and David Geffen UCLA School of
Medicine
e-mail: javadgam@cdrewu.edu

to and promotes the assembly of microtubules from tubulin dimers and stabilizes microtubules by preventing depolymerization [4, 5]. Both events inhibit or destroy the normal dynamic reorganization of microtubule network essential for mitotic apparatus, block the cells at G2/M phase and eventually lead to cell apoptosis [6–8]. Since microtubules are important cellular organelles related to multiple functions such as control of cell division by mitosis, cell morphology change, and material transport within cells, it is important to study the effect of Taxol on the basic cellular functions such as cellular transport of nutrients. It is also important to understand metabolic processes associated with Taxol resistance.

Carrier-mediated amino acid transport across plasma membrane is one of the most important functions of living cells and the interactions among different transport systems may regulate the flows of different amino acids among organs or cells [9]. Our previous studies suggested that some amino acid transport systems such as system A activity might be related to specific stages of cell differentiation and other cellular signals [10]. Therefore, it is possible that cellular distribution of nutrients such as amino acids among different cellular systems may be adjusted according to the functional status of those cells. According to the energy source and substrate specificity, amino acid transporters could be classified into two major categories, including the Na^+ -dependent amino acid transporters system A, ASC, N, B0, X_{AG} , Gly, and β -Alanine/Taurine, and the Na^+ -independent amino acid transporters L, asc, y^+ , b0, y^+ , L and T [9, 10]. Systems y^+ and X_{AG}^- are responsible for the transport of the cationic and anionic amino acid, respectively. Systems A, ASC and L are three major amino acid transport agencies participating in the transport of neutral amino acids with rather extensive overlapping of substrate specificity of short, linear side chain aliphatic amino acids. System N is another important Na^+ -dependent neutral amino acid transporter mainly identified in fetal and adult hepatocytes, some hepatoma cells, and muscle cells [11]. System B0 was recognized as a separate amino acid transport system in rabbit small intestine brush-border and bovine renal epithelial cells with broad uptake specificity of alanine, glutamine, branched and aromatic amino acids [12–14]. The system B0 transporter activity has also been identified in placental plasma membrane vesicles [15]. Both human [16, 17] and mouse [18] genes corresponding to amino acid transporter system B0 have been cloned.

Breast epithelial cells have great potential to transport enormous amounts of amino acids across cell membrane to meet the requirements of milk-protein synthesis during lactating period. However, the knowledge of amino acid transport in mammary cells and its regulation in multiple

physiological and pathological processes such as breast cancer is still limited [19, 20]. In this study, we examined the mechanisms of the amino transporter system B0 in human breast cancer cells MCF-7, and its regulation during cell apoptosis induced by an anticancer agent Taxol. MCF-7 cell line was derived from a pleural effusion taken from a patient with metastatic breast cancer and is a well established *in vitro* model of hormone regulated cell growth and endocrine therapy of breast cancer [21]. We have extended our studies to additional breast cancer cell lines: BT474 (ER +, HER2 +); MDAMB231 (ER–, HER2–); and T47D (ER +, HER2–).

Transport systems A [22] and L [23] and their regulation by estrogen has been reported previously in MCF-7 cells. The model of Taxol-induced apoptosis in MCF-7 breast cancer cells is also well established [24]. The purpose of this study was to investigate the mechanisms associated with Taxol induced apoptosis, as they pertain to the amino acid transporter. Our study tests the hypothesis that Taxol induces apoptosis in breast cancer cells, and consequently induce regulation of certain nutrient transporters. In particular, activation of the amino acid transporter B0 may be a important physiological process that assist breast tumor cells to undergo apoptosis in response to chemotherapeutic drugs such as Taxol and doxorubicin.

Materials and methods

Reagents

All chemicals were of highest commercially available quality from Sigma Chemical Co. (St. Louis, MO) or Fisher Scientific Co. (Pittsburg, PA). ^{14}C -L-alanine, ^{14}C -L-leucine and ^3H -glutamine were purchased from DuPont NEN (Boston, MA). ^{14}C -MeAIB and ^3H -L-threonine were from Amersham Corp. (Arlington Heights, IL). ^3H -L-arginine and ^3H -L-glutamic acid were from ICN pharmaceuticals, Inc (Irvine, CA).

Cell culture

Human breast cancer cell lines MCF-7, MDAMB231, and T47D were obtained from ATCC (Manassas, VA) and maintained in RPMI1640 medium supplemented with 10% fetal bovine serum (Irvine Scientific Co, CA), plus 100 $\mu\text{g}/\text{ml}$ of penicillin and streptomycin (Invitrogen, Carlsbad, CA) each. The culture was placed in 37°C humidified atmosphere with 5% CO_2 and the medium was changed every three days. Usually, cells were treated with Taxol at 50% to 70% confluence.

Amino acid transport assay

Uptake of radio-labeled amino acids was performed in 24-well cluster trays (Costar, Cambridge, MA) when MCF-7 cells were near confluence as previously described [10]. Briefly, cells were washed with choline-KRP (Kreb's Ringer Phosphate) buffer at pH 7.4 and 37°C twice and intracellular amino acids were depleted by incubation with 2 ml of choline-KRP at 37°C for 1 h. The amino acid transport was measured in Na⁺-KRP buffer or choline-KRP buffer (also at pH 7.4, and 37°C) for various times according to the experimental design. Uptake was terminated by two washes of 2 ml cold PBS. The amino acids transported into cells were extracted with 5% TCA for 1 h and radioactivity was monitored by a liquid scintillation counter (Beckman, Fullerton, CA). Attached cells were then dissolved in 1N of sodium hydroxide for at least 1 h and cellular protein amount was measured by Lowry method (Sigma, St. Louis, MO). Activity of all amino acid transport was expressed as transport velocity (nmol/mg protein/min) as described before [10]. The significance in the difference between groups of experiments was calculated using student *t*-test.

MTT assay

Growth inhibition of MCF-7 cells by Taxol was tested by MTT assay as described before [25]. Briefly, MCF-7 or other breast cancer cells were plated in a density of 10⁴ cells/well in a 96 well tray (Costar, Cambridge, MA) overnight and calculated concentration of Taxol were added to each well. After preset culture duration, medium was replaced with 50 μl of 1 mg/ml MTT (Sigma, St Louis, MO) solution and the plate was incubated for another 4 h. The dark-blue formazan crystal precipitate reduced from yellow soluble MTT by viable cells was dissolved in 100 μl of DMSO. The optical density was measured at 560 nm absorbance by a Dynatech MR700 ELISA reader (Dynatech Laboratory Inc., Chantilly VA). The inhibitory rate of Taxol was calculated using the following formula:

$$\text{Inhibition rate (IR\%)} = \frac{\text{OD (control)} - \text{OD (drug treated cells)}}{\text{OD (control)}} \times 100\%$$

Isolation of fragmented DNA

Internucleosomal DNA cleavage was analyzed by the method described before with modification [25]. Briefly, after treatment with Taxol with indicated time, 10⁷ MCF-7 or other breast cancer cells were trypsinized and washed with PBS once. Cell pellet was suspended in lysis buffer (5 mM Tris-

HCL, 20 mM EDTA and 0.5% Triton X-100) and kept on ice for 20 min. After 14,000 RPM centrifugation for 10 min the supernatant was extracted with phenol-chloroform twice. The DNA was precipitated with 2.5 volume of ethanol and the DNA pellet was dissolved in 20 μl of dH₂O and separated on 2% agarose gel with ethidium bromide and visualized under UV light.

TUNEL (Terminal Deoxynucleotidyl transferase Biotin-dUTP nick end labeling) assay

Cells and cell culture medium were collected and spun down at 1900 rpm for 5 min. The cells were then suspended in PBS and adjusted to 3 × 10⁵ cells/ml for preparation of cytospin slide. The slides were fixed with 4% paraformaldehyde in 0.1 M NaH₂PO₄, pH 7.4 for 15 min. To identify apoptotic cells, the biochemical property of apoptosis, endonucleolytic cleavage of chromatin was analyzed by TUNEL assay kit (Cat #17-141, Upstate, NY) according to manufacture's instructions. The biotin-labeled cleavage sites were visualized by reaction with fluorescein conjugated avidin (avidin-FITC). In order to measure the number of apoptotic cells, the slides were mounted with propidium iodide mounting medium (H-1300, Vector Lab Inc., CA) and then counted under a fluorescence microscopy. Five representative areas were randomly selected and TUNEL (nuclear) staining was counted by two experienced individuals. The mean values of five areas were calculated and the percentage of apoptotic cells was determined by using TUNEL staining cells divided with total number cells in the corresponding area.

Cell cycle analysis

The cells and the culture medium were collected by centrifugation at 250 × g for 5 min. Cell number was adjusted to 1 × 10⁶/ml, and fixed with 70% ethanol. The fixed cells were then stained with hypotonic DNA staining buffer (Sodium citrate, 0.25 g; Triton-x 100, 0.75 ml; Propidium iodide, 0.025 g; Ribonuclease A, 0.005 g; and Distilled water 250 ml) for 30 min followed by Cell Cycle analysis on a *one single-laser FACScan analytic flow cytometer*.

RNA extraction and cDNA synthesis

Total RNA was extracted with RNA-Bee (TEL-Test, Inc. Frindswood, TX) according to the manufacture's instruction. cDNA was reverse transcribed from 3 μg of total RNA using random primers and ThermoScript RT-PCR system (# 11146-024, Invitrogen) according to the manufacturer's instructions.

Table 1 Primers for Real-Time-PCR

Gene	Oligonucleotide	Sequences
ASC	5'-primer	5'-AAAGAGACGGTGGACTCTTTCC-3'
	3'-primer	5'-CTTTTCATGGGTACATTTCCA-3'
ATA2	5'-primer	5'-TCTGCGTGAGAATAGAGACCAC-3'
	3'-primer	5'-AATACTGAATCGTCCCATTTCG-3'
ATB ⁰	5'-primer	5'-CTCGATTTCCTGGATCTT-3'
	3'-primer	5'-TTCCGGTGATATTCCTCTCTTC-3'
18S	5'-primer	5'-GATCCATTGGAGGGCAAGTC-3'
	3'-primer	5'-TCCCAAGATCCAACACTACGAG-3'

Table 2 Primers for RT-PCR amplification

PCR primers	Sequence (5' → 3')	Accession number	Predicted size of PCR product (bps)
B0 (ATB ⁰) forward	CAGCAGCCTTTCGCTCATAC	U53347	504
B0 (ATB ⁰) reverse	CCTCCACGCACTTCATCATC		
β -actin forward	GTCTTCCCCTCCATCGT	M10278	313
β -actin reverse	CGTACATGGCTGGGGTGT		

Real-time-PCR

Quantitative real-time PCR was performed with iCycle, iQ real-time PCR detection system (Bio-Rad Lab, Hercules, CA) using SYBR Green Master Mix (#204143, QIAGEN) according to the manufacturer's instructions. The thermal cycling conditions were as follows: 15 min at 95°C, followed by 45 cycles of 94°C for 15 s and 58°C for 30 s for amplification of ATA2 and B0 (ATB⁰) genes. For amplification of ASC, 56°C was used instead 58°C. The primer sequences are listed in Table 1. The target messages in unknown samples were quantified by measuring C_t and adjusted with 18S RNA. Final results were expressed as fold difference in target gene relative to 18 S.

Multiplex quantitative RT-PCR

Total RNA was extracted with Trizol™ reagent (Invitrogen, Carlsbad, CA) according to the manufacturer's instructions. Multi-quantitative RT-PCR was performed using human β -actin as an internal control. The primers were designed by a web-based software, Primer3 (http://frodo.wi.mit.edu/cgi-bin/primer3/primer3_www.cgi) and the sequence information is listed in Table 2. Briefly, 1 μ g of total RNA was reverse-transcribed into cDNA using 10 U/ μ l SuperScript™ II reverse transcriptase (Invitrogen, Carlsbad, CA) and random hexamer (250 nM) as primer in following condition: 50 mM Tris-HCl (pH8.3), 75 mM KCl, 3 mM MgCl₂, 5 mM DTT, 1 U/ μ l of RNase inhibitor and 500 μ M of each dNTPs, and incubated at 42°C for 1 h. The reverse transcriptase was then inactivated by heating the reaction at 99°C for 5 min and RNA was eliminated by treating the reaction with 2.5 U of RNase H at 37°C for 15 min. Typically 1 μ l of cDNA was used as template for a 50 μ l of PCR reaction in the fol-

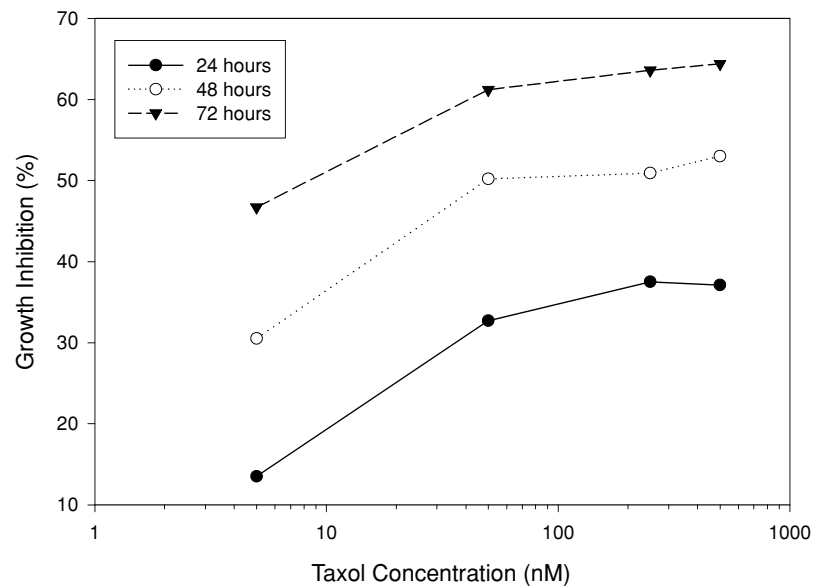
lowing conditions: 10 mM Tris-HCl, pH 8.3, 50 mM KCl, 1.5 mM MgCl₂, 200 μ M of each dNTPs, 1.5 U of Taq DNA polymerase (Perkin Elmer, Branchburg, NJ). Optimal primer concentrations for co-amplification of B0 with β -actin were determined by testing different combinations of different concentration of primers. Primer concentration of 75 nM for β -actin and 400 nM for ATB⁰ were selected for all the multiplex RT-PCR reactions. The logarithmical amplification of target genes was determined by monitoring the concentration increment of PCR product during different PCR cycles. PCR was performed in a Perkin Elmer 480 thermal cycler (Perkin-Elmer, Norwalk, CT) in the following conditions: initial denaturation at 94°C for 2 min, then cycle at 94°C for 1 min, 58°C for 1 min and 72°C for 1 min for 28 cycles and finally extension at 72°C for 7 min. Ten microliters of PCR products were separated on 2% agarose gels with ethidium bromide and visualized under UV light. 100bp DNA ladder (Gibco BRL, Gaithersburg, MD) was used as DNA size reference.

Results

Taxol inhibits proliferation and induces apoptosis in MCF-7 breast cancer cells

MTT assay was used to measure the inhibitory effect of Taxol on proliferation of MCF-7 breast cancer cells. Taxol demonstrated a time- and dose-dependent inhibition of MCF-7 cell growth (Fig. 1). The most significant change occurred between 10 and 50 nm and after 24 and 48 h of Taxol treatment. The maximal inhibitory effect was observed with 500 nm Taxol at 24 h (37%), 48 h (54%) and 72 h (64%). The dosage of Taxol at 50% inhibition rate (IC₅₀) in 48 h and 72 h were 50 nM and 10 nM, respectively (Fig. 1).

Fig. 1 Growth inhibition of MCF-7 breast cancer cells by Taxol. MCF-7 cells were plated in 96-well trays at a density of 10^4 cells/well. The next day, cells were exposed to the indicated concentration of Taxol for 24, 48 and 72 h, respectively. Treated MCF-7 cells were subjected to MTT assay as described in methods. Taxol-mediated growth inhibition was expressed as the percentage inhibition of control MCF-7 cells without Taxol treatment. Each data point is the average of six replica and the stand error are within 10%



Effect of taxol-induced apoptosis on DNA fragmentation pattern

Apoptotic DNA was detected after 48 h of Taxol treatment at 10 nM concentration (Fig. 2). With increased dosage of Taxol, enhanced DNA fragmentation was observed. These results are consistent with the previous report [24] and suggest that Taxol's action on MCF-7 breast cancer cells include inhibition of cell growth and induction of cell apoptosis.

Effect of Taxol on Amino acid transport in MCF-7 cells

In order to study the metabolic changes during Taxol-induced apoptosis, we examined its effect on amino acid transporters in MCF-7 cells. Figure 3 showed that exposure of MCF-7 cells to 100 nM Taxol for 18 h caused an increase in Na^+ -dependent uptake of alanine and leucine. In contrast, the Na^+ -dependent arginine uptake was down-regulated. Taxol had no significant effect on Na^+ -dependent system A transport, as measured by the uptake of MeAIB, a system A-specific substrate. Similarly, Taxol had no effect on Na^+ -independent uptake of arginine, alanine, leucine, threonine and glutamate (data not shown).

Since alanine is an important gluconeogenic amino acid and the change in Na^+ -dependent alanine uptake by Taxol treatment was most prominent in our preliminary data, we selected the alanine transport activity as a marker to further study the regulation of amino acid transporter B0 in MCF-7 cells undergoing Taxol-induced apoptosis. Figures 4 and 5 showed a time- and dose-dependent effect of Taxol on Na^+ -dependent and Na^+ -independent alanine uptake, respectively. The data demonstrated a significant stimulation in Na^+ -dependent alanine uptake at 6 h of Taxol treatment,

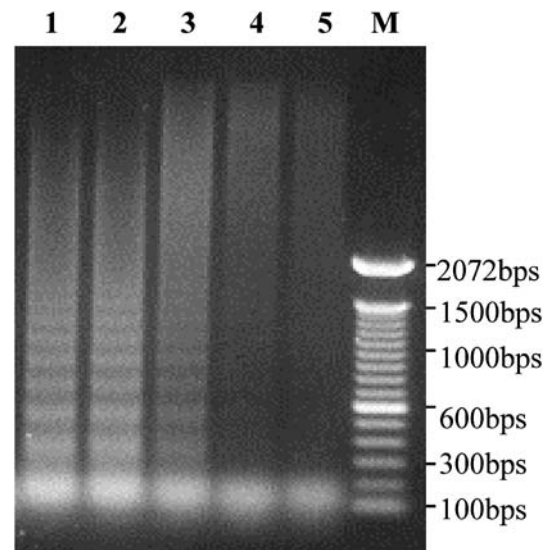


Fig. 2 Taxol-induced apoptosis in MCF-7 breast cancer cells, assessed by DNA fragmentation assay. Near confluent MCF-7 breast cancer cells were treated with different concentrations of Taxol for 48 h. Cells were trypsinized and washed with PBS once. Cells were then lysed in lysis buffer and fragmented DNA was isolated and purified by centrifugation, phenol-chloroform extraction and separated on 2% agarose gel. Concentrations of Taxol are: Lane 1. 1000 nM, 2. 100 nM, 3. 10 nM, 4. 1 nM, 5. Control with no Taxol. M. 100 bp DNA marker (Gibco BRL, Gaithersburg, MD)

with no further increase at 24 h (Fig. 4). In addition, there was a significant stimulation in Na^+ -independent alanine uptake with 10 nM Taxol treatment, with optimal stimulation at 100 nM (Fig. 5). A kinetic study of alanine transport in Taxol-treated MCF-7 cells (Fig. 6) revealed no significant change in K_m , but there was an increase in V_{max} after Taxol treatment. The values are, before Taxol treatment (filled circles): $K_m = 0.14 \pm 0.0185$ mM and $V_{max} = 17.87 \pm$

Fig. 3 *Effect of Taxol on Na⁺-dependent transport of different amino acids in MCF-7 breast cancer cells.* Near confluent MCF-7 breast cancer cells were treated with 100 nM Taxol for 18 h and uptake of 10 μ M of each indicated amino acid was measured in Na⁺ or Choline KRP's-Ringer Phosphate (KRP) buffer at pH 7.4 and 37°C. Na⁺-dependent component is obtained by subtracting the uptake in Choline KRP from the total uptake in Na⁺ buffer. Values are a mean \pm S.E.M of three determinations. *indicates $p < 0.05$. Open columns represent untreated and shaded columns taxol treated cells

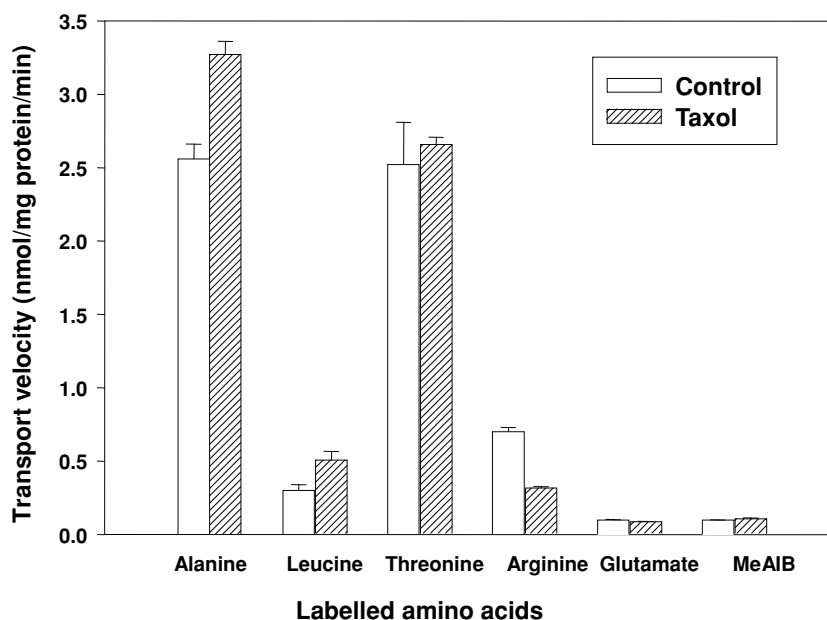
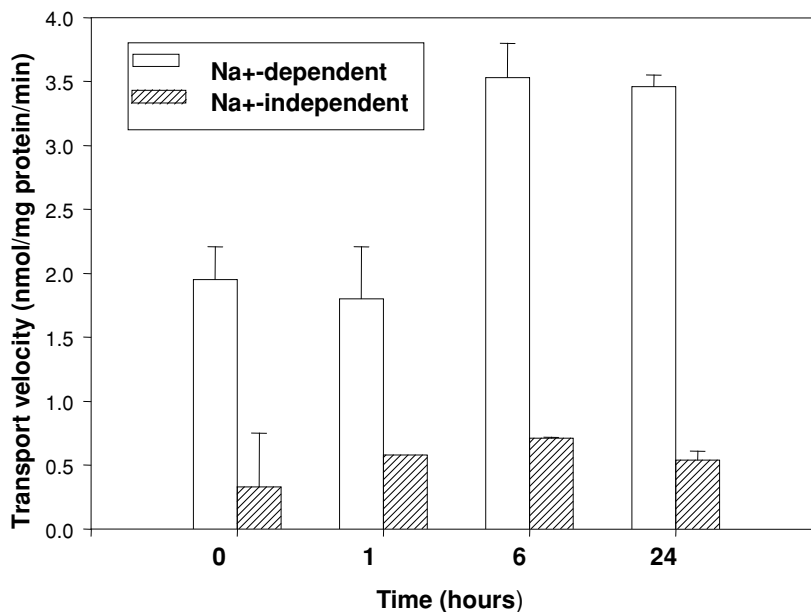


Fig. 4 *Time course of Taxol treatment on alanine transport in MCF-7 breast cancer cells.* Near confluent MCF-7 breast cancer cells were treated with 100 nM of Taxol for indicated time. Uptake of 10 μ M of alanine was measured in Na⁺ or Choline KRP, pH 7.4, at 37°C. Values are a mean \pm S.E.M. of three determinations. *indicates $p < 0.05$ between groups at 6 h of Taxol treatment and control (untreated)



0.761 nmol/mg protein/min; after Taxol treatment (open circles), the values are: $K_m = 0.17 \pm 0.0184$ mM and $V_{max} = 23.38 \pm 0.903$ nmol/mg protein/min.

Inhibition of various Amino acids on Sodium Dependent Alanine uptake

Alanine could be transported by several different agencies, including transport systems A, ASC, B0 or L [9]. In order to delineate the specificity of transport system for alanine uptake and its regulation by Taxol in MCF-7 cells, we mea-

sured alanine uptake in the presence of various amino acids as inhibitors. Figure 7 showed the Na⁺-dependent uptake of 10 μ M alanine in the presence of different amino acids at 10 mM concentration. The results demonstrated that alanine, leucine, threonine and tryptophan were strong inhibitors of Na⁺-dependent alanine transport, while MeAIB, arginine and glutamate had no significant effect. Almost identical inhibitory profile was observed in Taxol-treated MCF-7 cells (shaded bars), suggesting that Taxol treatment might not alter the specificity of proteins responsible for alanine transport.

Fig. 5 Dose-dependent effect of Taxol treatment on alanine transport in MCF-7 breast cancer cells. Near confluent MCF-7 breast cancer cells were treated with indicated concentration of Taxol for six hours. Uptake of $10 \mu\text{M}$ of alanine was measured in Na^+ or Choline KRP, pH 7.4, at 37°C . Values are a mean \pm S.E.M. of three determinations. *indicates $p < 0.05$ between groups of 10 nM Taxol treated and untreated (control)

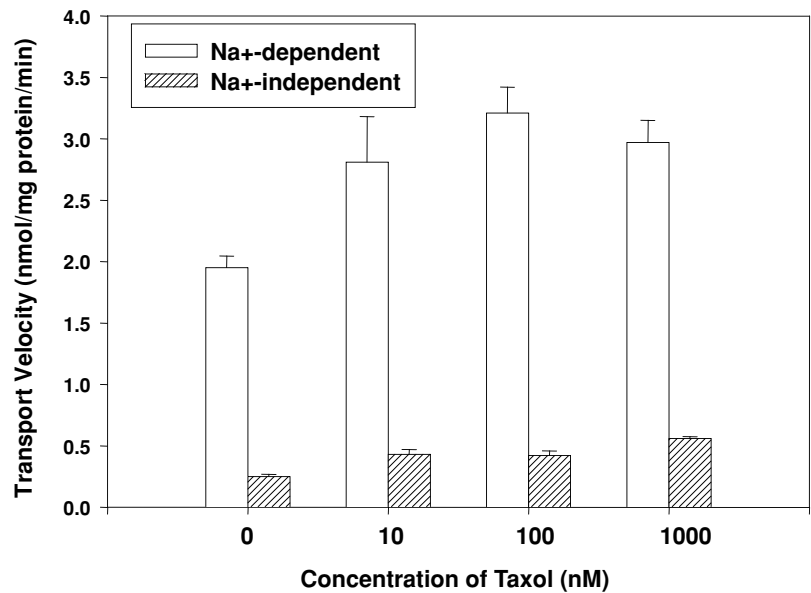
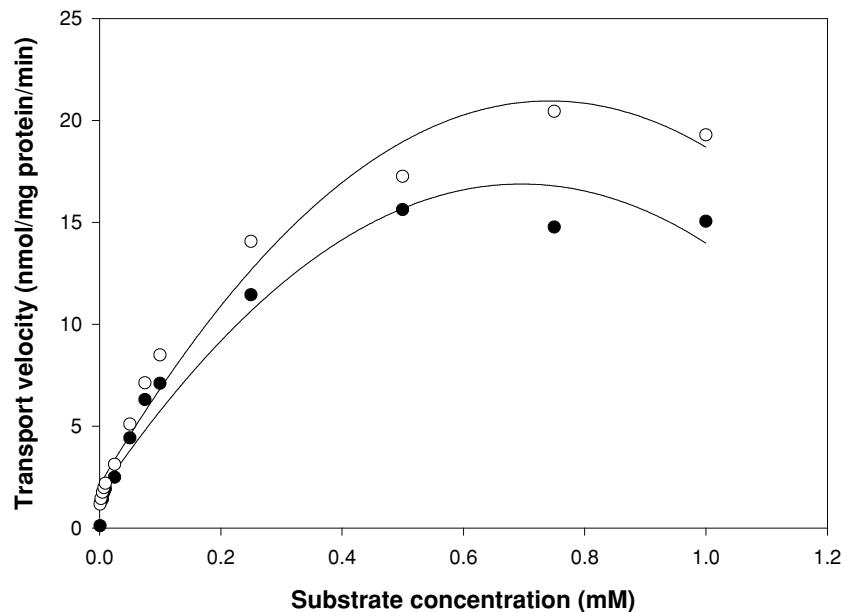


Fig. 6 Kinetic analysis of sodium-dependent alanine transport in Taxol-treated MCF-7 cells. Near confluent MCF-7 breast cancer cells were treated with 100 nM Taxol for 18 h. Uptake of alanine at indicated concentration was measured in Na^+ or Choline KRP, pH 7.4, at 37°C . Values are a mean of two determinations. The kinetic values before Taxol treatment are: $K_m = 0.14 \pm 0.0185 \text{ mM}$ and $V_{\text{max}} = 17.87 \text{ nmol/mg protein/min}$; and after Taxol treatment, $K_m = 0.17 \pm 0.0184 \text{ mM}$ and $V_{\text{max}} = 23.38 \pm 0.903 \text{ nmol/mg protein/min}$



Regulation of Alanine transport in MCF-7 cells treated with Taxol by thiol-group modifying reagents

Due to structural differences, different amino acid transport proteins may functionally display differential responses to various chemical modifications such as treatments with thiol-group modifying reagents. Thiol-modifying reagents such as N-phenylmaleimide (NPM), N-ethylmaleimide (NEM) and iodoacetamide (IA) were reported to have differential effects on different amino acid transport proteins including system B₀, ASC and A [13, 26]. While the function of both systems ASC and B₀ was inhibited similarly by NPM, system B₀

is less sensitive to NEM treatment than system ASC [13]. Figure 8 demonstrated that two thiol-modifying reagents, NPM and NEM, inhibited the alanine transport in MCF-7 breast cancer cells in a dose-dependent manner. However, MCF-7 cells treated with Taxol were less sensitive to NEM treatment compared with those treated with NPM.

Gene expression of transport system B₀ is up-regulated upon Taxol treatment

We further examined the expression of the amino acid transporter gene B₀. MCF-7 cells were treated with

Fig. 7 Inhibition of $10 \mu\text{M}$ ^{14}C -L-alanine uptake by different amino acids into MCF-7 breast cancer cells. Near confluent MCF-7 breast cancer cells were treated with 100 nM Taxol for 18 h. Uptake of $10 \mu\text{M}$ ^{14}C -L-alanine was measured in Na^+ or Choline KRP, pH 7.4, at 37°C for 1 min, in the absence and presence of different amino acids at 10 mM concentration. Values are a mean of 3 determinations. Unless otherwise indicated, the S.E.M was $< 10\%$

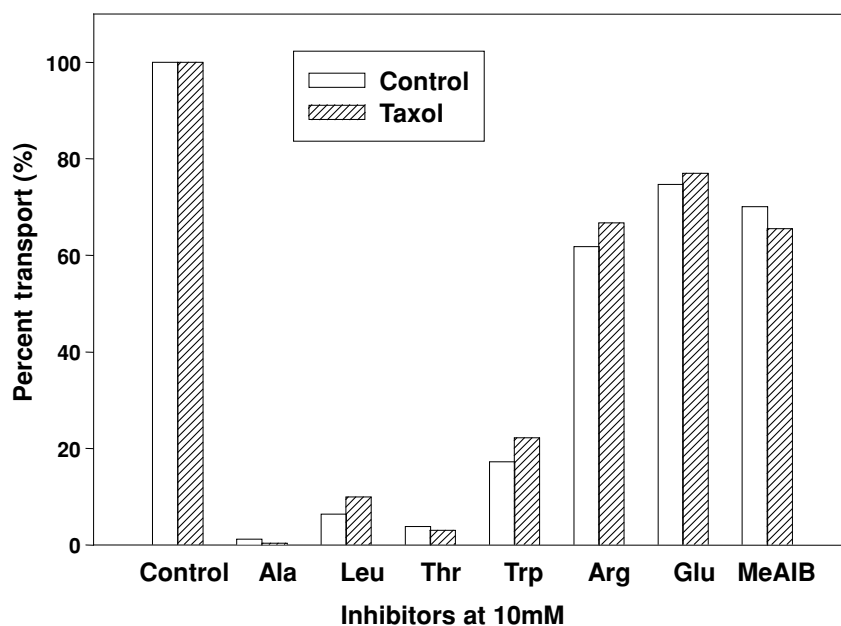
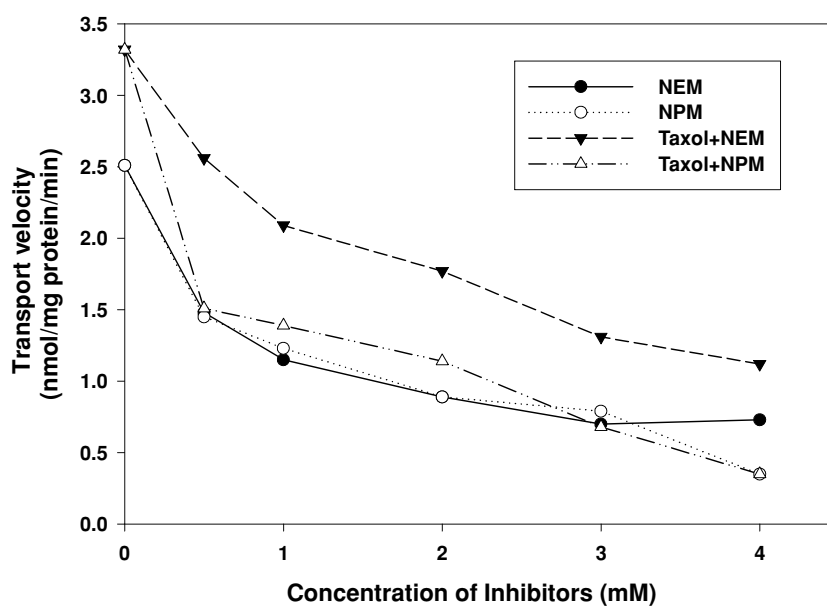


Fig. 8 Inhibition of alanine transport by *N*-ethylmaleimide (NEM) and *N*-phenylmaleimide (NPM) in MCF-7 breast cancer cells treated with Taxol. Uptake of $10 \mu\text{M}$ of ^{14}C -L-alanine into MCF-7 breast cancer cells treated or not treated with Taxol was measured in Na^+ or Choline KRP pH 7.4, at 37°C with or without treatment by indicated concentration of *N*-ethylmaleimide and *N*-phenylmaleimide for 10 min. Values are a mean of 3 determinations. Unless otherwise indicated, the S.E.M. was $< 10\%$ for each mean value



different anticancer agents including Taxol; Vinblastin, another microtubule-targeting anticancer agent; and a non-microtubule-targeting anticancer agent, Mitomycin-C (MMC). The B0 gene expression was measured using a multiplex RT-PCR approach. The results showed that B0 gene expression was upregulated in both Taxol- and Vinblastin-treated cells but not in MMC-treated cells (Fig. 9(A)). With the increased dosage of Taxol, the expression of B0 gene was also enhanced (Fig. 9(B)). The increase in gene expression pattern with Taxol dose escalation in Fig. 9(B) complements the increase in transport activity, shown in Fig. 5.

Effect of Taxol, Doxorubicin, and Amino acid starvation on gene expression of transporters B0, ATA2, and ASC, in (A) MCF7, (B) T47D, and (C) MDAMB231 breast cancer cells

Figure 10, shows the effect of Taxol, Doxorubicin, and Amino Acid starvation on gene expression of System B0, ATA2 (System A), and ASC in MCF7 cells. Expression of each transporter gene is corrected with 18S RNA expression. Our data confirm that as with the transport activity, gene expression of B0 increased upon treatment with both Taxol and Doxorubicin (Fig. 10(A)). Both chemo agents induce

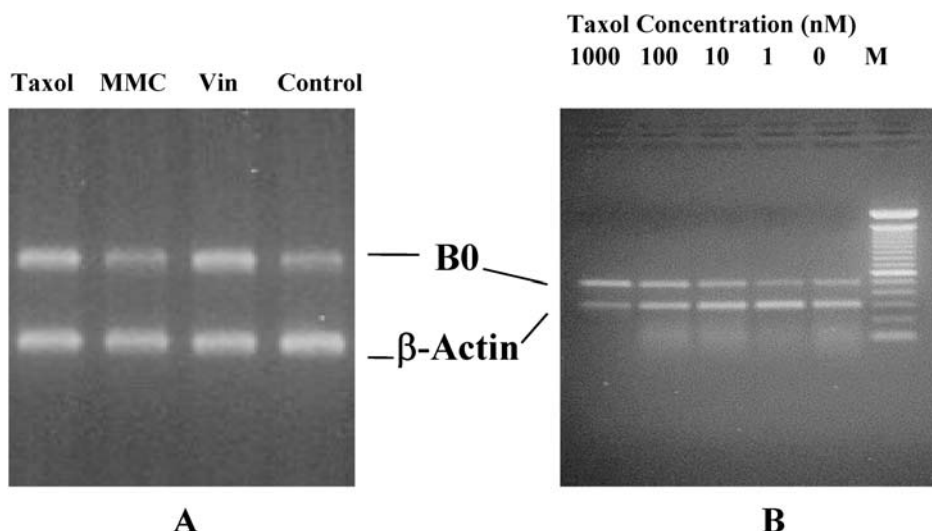


Fig. 9 Multiplex RT-PCR amplification of *B0* (*ATB⁰*) gene upon Taxol treatment in MCF-7 breast cancer cells. Near confluent MCF-7 cells were treated with indicated drugs for 16 h and total RNA was extracted as described in the methods section. Quantitative multiplex RT-PCR

was performed to compare the system *B0* expression by co-amplifying *B0* and β -actin. PCR was run for 28 cycles. Figure A, shows *B0* expression upon treatment with different anticancer agents. B, shows System *B0* gene expression upon different concentration of Taxol treatment

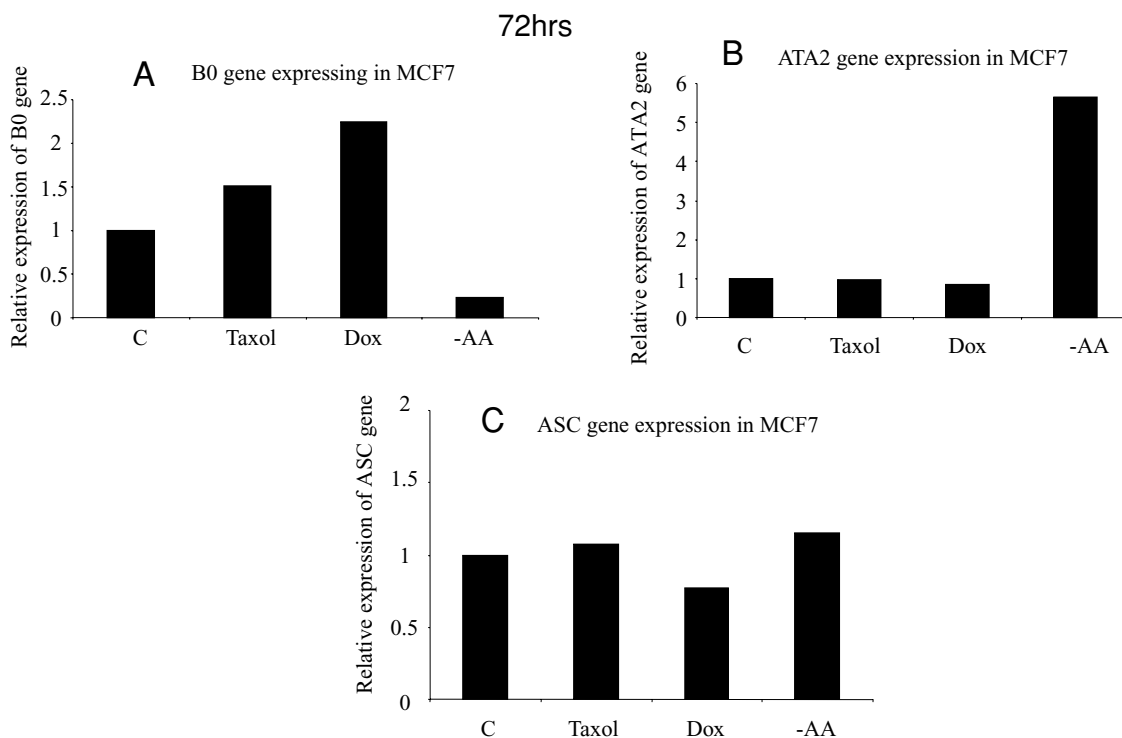


Fig. 10 Effect of Taxol and Doxorubicin on *B0*, *ATA2* and *ASC* transporter gene expression in MCF-7 cells. MCF-7 cells were grown in DMEM/F12 media containing 10% FCS. After 70% confluence, cells were treated with Taxol (10 nM) or Doxorubicin (Dox) 100 ng/ml for 72 h, or changed to amino acid free media EBSS (Earle’s Balanced Salt Solution) containing 5% DFCS (dialyzed fetal calf serum) for 18 h.

The cell culture medium and cell pellets were collected and spun down at 1900 rpm for 5 min. Total RNA was isolated and Real-time RTPCR were performed with a primers specific for *B0* (A), *ATA2* (B) and *ASC* (C) genes. The fold changes were compared with untreated cells and adjusted with 18S RNA. The bars indicate mean \pm SD of 3 different determinations

apoptosis in cancer cells. *B0* gene expression decreased in cells subjected to amino acid starvation. In contrast, System *ATA2* or System A transporter gene was not affected by Taxol or Doxorubicin (Fig. 10(B)). However, the *ATA2* or

System A transporter gene increased by 6 fold upon amino acid starvation. The increase in System A transporter gene to amino acid starvation is consistent with its increase in transport activity, observed in many cell types (ref). In con-

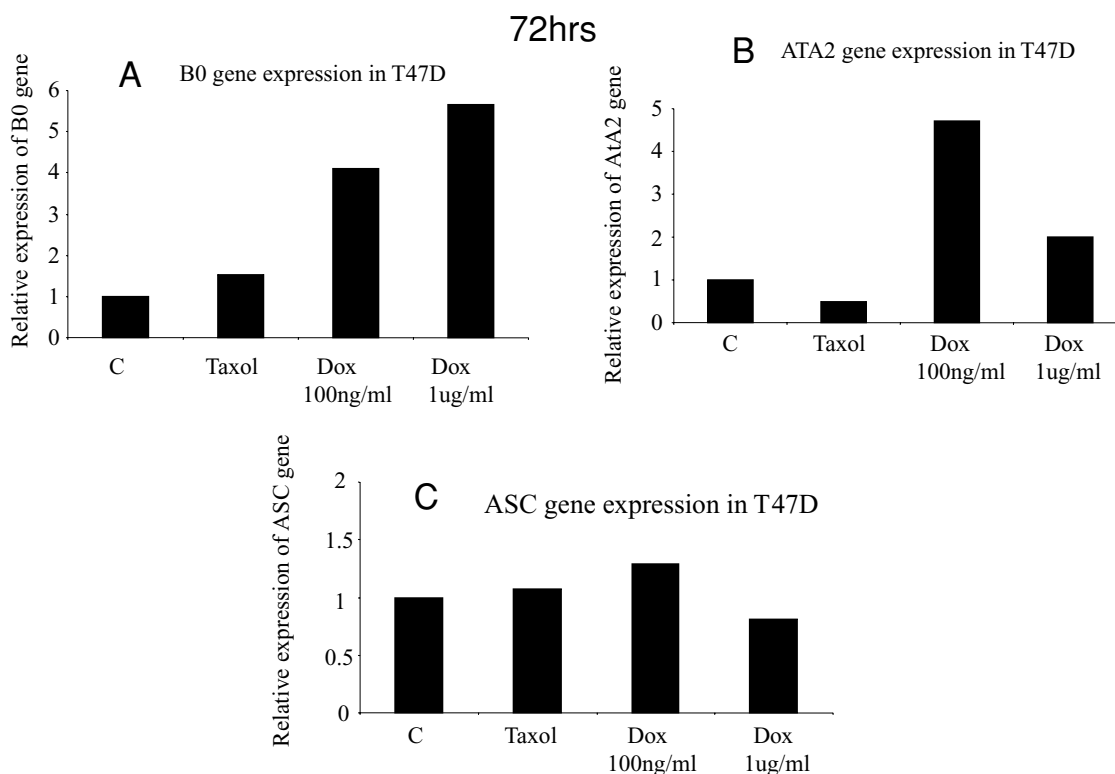


Fig. 11 Effect of Taxol and Doxorubicin on B0, ATA2 and ASC transporter gene expression in T47D cells. T47D cells were grown in DMEM/F12 media containing 10% FCS. After 70% confluence, cells were either treated with Taxol (10 nM) or Doxorubicin (Dox) 100 ng/ml for 72 h, or changed to EBSS containing 5% DFCS for 18 h. The cell culture medium and cell pellets were collected and spun down at

1900 rpm for 5 min. Total RNA was isolated and Real-time RTPCR were performed with a primers specific for B0 (A), ATA2 (B) and ASC (C) genes. The fold changes were compared with untreated cells and adjusted with 18S RNA. The bars indicate mean \pm SD of 3 different determinations

trast to System B0, the ASC transport gene did not change upon Taxol or Doxorubicin treatment, and upon amino acid starvation (Fig. 10(C)). These data suggest that only System B0 transport gene is sensitive to chemo agents that induce apoptosis.

Figure 11 expands on the role of chemo agents Taxol and Doxorubicin in a dose dependent manner on expression of transport genes B0, ATA2, and ASC in T47D breast cancer cells. The data confirm that both Taxol and Doxorubicin up-regulated System B0 gene by 2 to 6 fold (Fig. 11(A)). Doxorubicin treatment up-regulated B0 gene expression in a dose dependent manner by 4.2 and 6 fold at 100 ng/ml and 1 μ g/ml respectively. In contrast to its effect on MCF7 cells (Fig. 10(B)), doxorubicin increased ATA2 gene expression to 5 fold with 100 ng/ml doxorubicin, which came down to 2 fold with high concentration of doxorubicin at 1 μ g/ml (Fig. 11(B)). Figure 11(C) confirm that neither Taxol or Doxorubicin altered System ASC gene expression in T47D cells. These data provide further evidence that only System B0 gene is up-regulated by the two apoptosis-inducing agents Taxol and Doxorubicin in two different breast cancer cells MCF7 and T47D. This response was Doxorobucin dose-dependent in T47D cells.

System ATA2 is only up-regulated by doxorubicin in T47D cells.

Figure 12 tests the specificity of Taxol-induced up-regulation of System B0 in T47D cells. It also compares the activity of transport genes ATA2 and ASC in response to Taxol with and without high concentrations of alanine. The data in Fig. 12(A) demonstrate a 1.8 fold increase in B0 gene expression upon Taxol treatment. However, the presence of 10 mM alanine attenuated the Taxol response. These data confirm that blocking the B0 transporter with high concentration of the substrate amino acid can repress the Taxol-induced increase in B0 gene expression. Taxol treatment had no effect on System ATA2 in both MCF7 and T47D cells (Figures 10 and 11). Hence, the presence of high concentration of alanine had no additional effect on ATA2 gene expression in T47D (Fig. 12(B)). In the case of System ASC in T47D cells, the combination treatment with alanine and Taxol caused a marginal increase in ASC gene expression.

Apoptotic changes as measured by the TUNEL assay

Figure 13 demonstrates apoptotic changes in response to Taxol in the presence or absence of high concentration of

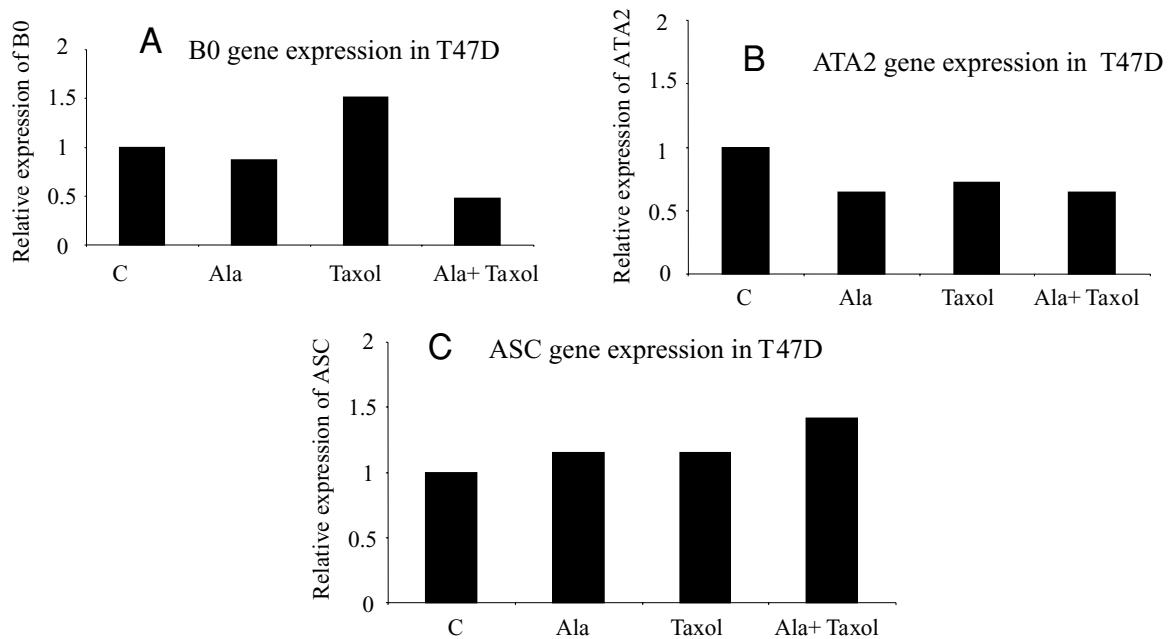


Fig. 12 Effect of L-Alanine on Taxol regulated B0, ATA2, and ASC transporter gene expression. T47D cells were grown in DMEM/F12 media containing 10% FCS. After 70% confluence, cells were treated with L-Alanine (10 mM, 72 h), Taxol (10 nM, 72 h) or pre-incubated with L-Alanine for 2 h, and then treated with Taxol for 72 h. The cell culture medium and cell pellets were collected and spun down at

1900 rpm for 5 min. Total RNA was isolated and Real-time RTPCR were performed with a primers specific for B0 (A), ATA2 (B) and ASC (C) genes. The fold changes were compared with untreated cells and adjusted with 18S RNA. The bars indicate mean \pm SD of 3 different determinations

alanine (10 mM) in MCF7 cells. The rationale was to confirm that the apoptotic changes as assessed by increase in nuclear damage or granulation upon Taxol treatment could be inhibited or reversed by inhibiting or blocking System B0. The data show a clear change in nuclear morphology as assessed by PI uptake, and in the simultaneous uptake of the FITC labeled dUTP in MCF7 cells. From a pool of 10^6 cells that were analyzed, the number of apoptotic cells increased from 30,000 to almost 90,000 upon Taxol treatment. Treatment with high concentrations of alanine in the presence of Taxol decreased the number of apoptotic cells to 50,000. The morphological changes in Fig. 13 confirm this. Similar changes were seen with T47D (Fig. 14) and MDAMB231 (Fig. 15) breast cancer cells. That is, Taxol induced significant increase in apoptosis of both T47D and MDAMB231 cells as measured by increase in nuclear damage/granulation, followed by increase in FITC labeled d-UTP uptake. Blocking the B0 transporter in the presence of high concentration of alanine, reversed the nuclear damage, and decreased FITC

labeled uptake in both T47D and MDAMB231 cells. The extent of protection from apoptosis in the presence of high concentration of alanine, was stronger in T47D (Fig. 14(B)) compared to MCF7 (Fig. 13(B)) cells. Hence, by blocking or inhibiting System B0, the apoptotic effect of Taxol is significantly reduced.

Amino acid starvation and apoptosis

Figure 16 demonstrates that amino acid starvation also results in increase in apoptotic cells (Fig. 16(A) and (B)). In this case, System A or the ATA2 transporter gene is up-regulated by 2 to 6 fold (Fig. 16(C)). This is a characteristic feature of System A that is ubiquitously expressed in most mammalian cells. It is a functional criteria that is often used to identify and characterize System A transporter from other neutral amino acid transporters (9,10). Amino acid starvation also caused some apoptosis (Fig. 16(A) and B), but unlike the ATA2 transporter gene, B0 was down regulated (Fig. 16(C)). These

Table 3 Shows FACS flow analysis on MCF-7 cells treated with various agents for 24 h, and associated changes in B0 and ATA2 gene expression

Condition	G0-G1	S	G2-M	B0 gene expression	System A or ATA2 gene expression
MCF7 Untreated	59%	24%	17%	Normal	Normal
MCF7 – AA 24 h	72%	16%	12%	Decrease by 2–5 fold	Increase by 2–5 fold
MCF7 + Taxol 24 h	4%	4%	92%	Increase by 1.5–4 fold	No change
MCF7 + RA 24 h	80%	8%	12%	No change	Decrease

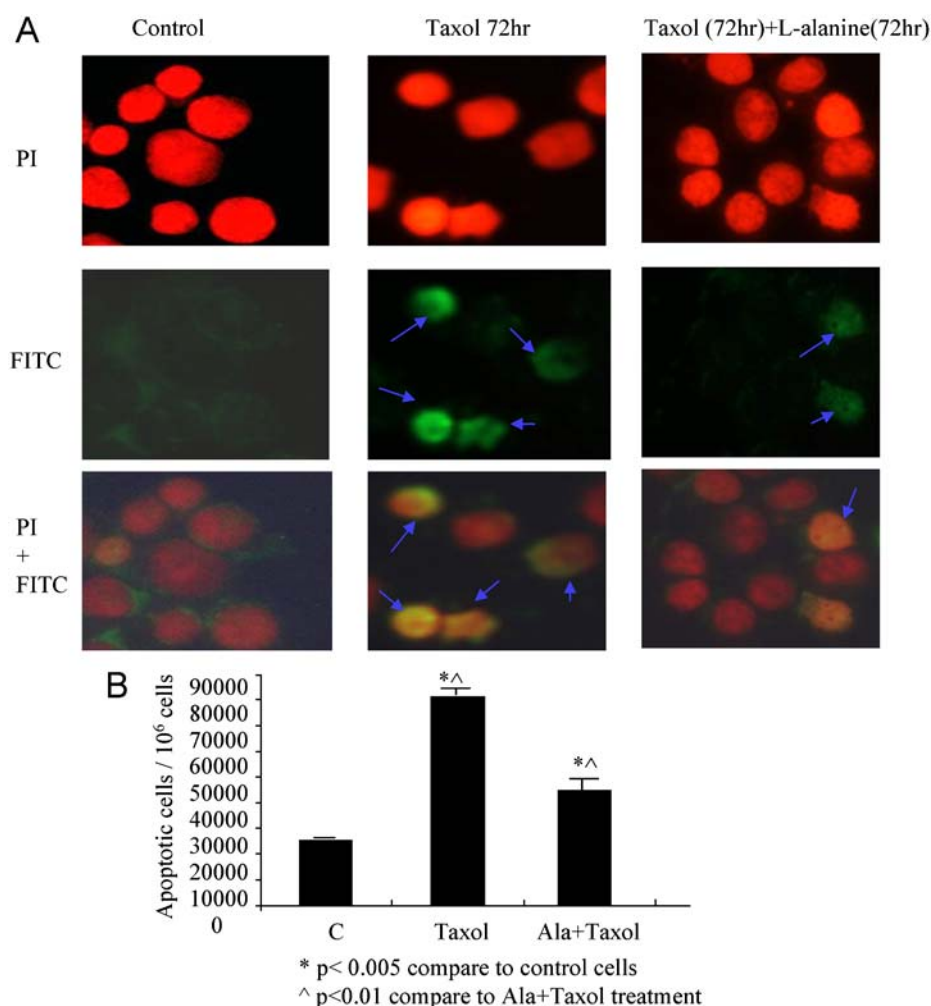


Fig. 13 Effect of L-Alanine on Taxol induced apoptosis in MCF7 cells. MCF-7 cells were grown in DMEM/F12 media containing 10% FCS. After 70% confluence, cells were treated with L-Alanine (10 mM, 72 h), Taxol (10 nM, 72 h) or pre-incubated with L-Alanine for 2 h, and then treated with Taxol for 72 h. Cell culture medium and cell pellets were collected and spun down at 1900 rpm for 5 min. (A) Cell number was counted and adjusted to 1×10^6 /ml. A total 50 μ l of cell suspension from each condition was used for preparation of cytospin slides. The slides were fixed with 4% paraformaldehyde in 0.1 M NaH_2PO_4 ,

pH 7.4 for 15 min then TUNEL assay was used to detect the apoptotic cells according to manufacture's instruction. The slides were mounted with a medium containing Propidium Iodide (PI) and photographed under a fluorescence microscope. The top panel indicate total cells (red), and medial panel indicate apoptotic cells (green). The bottom panel (yellow) shows the cells with merged PI and FITC. (B) The number of apoptotic cells was counted from five different random areas and the bars show mean \pm SD. The statistical significance was determined by student-*t* test

observations provide further evidence that Taxol-induced up-regulation of System B0 is a specific metabolic response to Taxol-induced apoptosis.

Effect of Taxol, Retinoic acid and Amino acid starvation on B0 and system A (ATA2) transporter genes in association with cell cycle changes in MCF-7 breast cancer cells

Results from Table 3 confirm the following: (1) Amino acid starvation leads to an increase in G1/G0, with a decrease in S-phase. The G2/M fraction decreased slightly. B0 transporter decreased, while System A (ATA2) increased by 2–5 fold. However, treatment with Taxol for 24 h caused a significant increase in G2/M phase with anticipated decrease in

G1 and S fractions. This is a typical response expected upon Taxol treatment. Here, B0 gene expression increased by 1.5 to 4 fold, while ATA2 expression did not change. In contrast, treatment with Retinoic acid, known to inhibit MCF-7 and other breast tumor cells at G0/G1, caused the anticipated increase in G0/G1 fraction, with a significant drop in S-phase, and no remarkable change in G2/M. Retinoic acid treatment resulted in a decrease in ATA2, but not B0 transport activity (data not shown). These observations suggest that the Taxol-induced up-regulation of B0 may be partially associated with increase in G2/M phase, but not with G1/G0.

Next, we tested if Taxol and doxorubicin induced apoptosis was (a) cell cycle dependent; (b) caspase-dependent; and (c) sensitive to high concentration of alanine (10

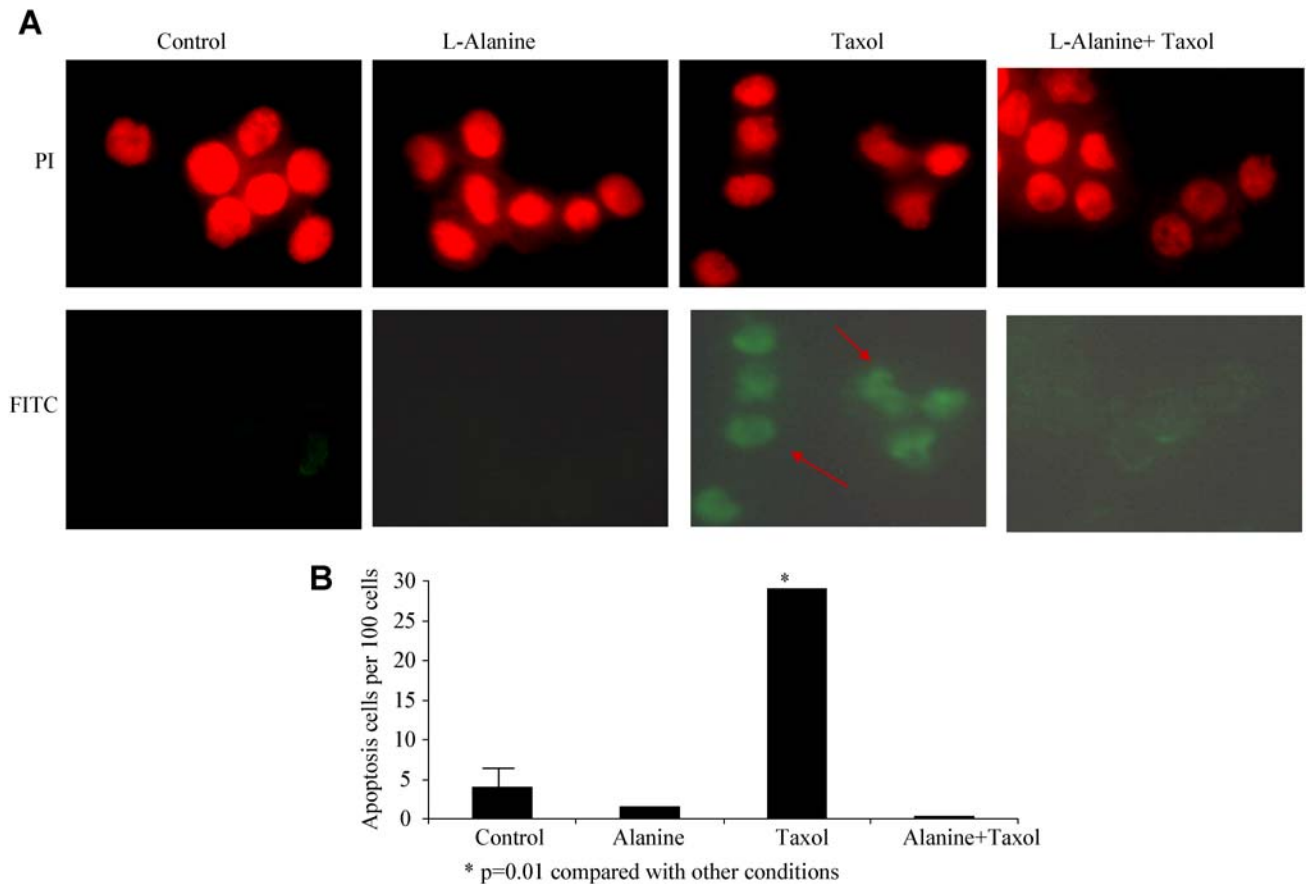


Fig. 14 Effect of L-Alanine on Taxol induced apoptosis in T47D cells. T47D cells were grown in DMEM/F12 media containing 10% FCS. After 70% confluence, cells were treated with L-Alanine (10 mM, 72 h), Taxol (10 nM, 72 h) or pre-incubated with L-Alanine for 2 h, and then treated with Taxol for 72 h. Cell culture medium and cell pellets were collected and spun down at 1900 rpm for 5 min. (A) Cell number was counted and adjusted to 1×10^6 /ml. A total 50 μ l of cell suspension from each condition was used for preparation of cytospin slides. The slides were fixed with 4% paraformaldehyde in 0.1 M NaH_2PO_4 , pH

7.4 for 15 min then TUNEL assay was used to detect the apoptotic cells according to manufacture's instruction. The slides were mounted with a medium containing Propidium Iodide (PI) and photographed under a fluorescence microscope. The top panel indicate total cells (red), and medial panel indicate apoptotic cells (green). (B) The number of apoptotic cells was counted from five different random areas and the bars are mean \pm SD. The statistical significance was determined by student-*t* test

mM). In particular, we examined if blocking the caspase pathway or the B0 transporter with high concentration of alanine would interfere with either Taxol and/or doxorubicin induced apoptosis and up-regulation of B0 transport gene.

Effect of caspase inhibitor and alanine on Taxol-induced apoptosis of MCF-7 cells

Cell cycle data in Fig. 17 demonstrate the following: (a) Taxol treatment resulted in a significant decrease in S-phase, with accompanying increase in the G2 fraction. In the panel below, the data from TUNEL assay, confirm increase in apoptotic cells as measured by FITC uptake. Presence of the Caspase inhibitor IV or alanine (10 mM) inhibited the Taxol-induced apoptosis, as assessed by the TUNEL assay (Fig. 17, panel c). The reversal in apoptosis with the Caspase inhibitor

was more pronounced compared to high concentration of alanine. These observations suggest that based on the TUNEL assay, Taxol-induced apoptosis is partially Caspase-dependent, and alanine sensitive. In contrast to the TUNEL assay data, the FACS results show marginal reversal in the decrease in S phase, and increase in G2 fraction, suggesting that Taxol-induced apoptosis involves caspase dependent and independent pathways.

Effect of caspase inhibitor and alanine on Doxorubicin-induced apoptosis of MCF-7 cells

Figure 18 shows that doxorubicin treatment caused a significant inhibition in S-phase growth of the MCF-7 cells, with accompanying increase in G1 and G2 fractions. The increase in G2 fraction is not as significant as that observed for Taxol treatment. The TUNEL assay shows complementing increase

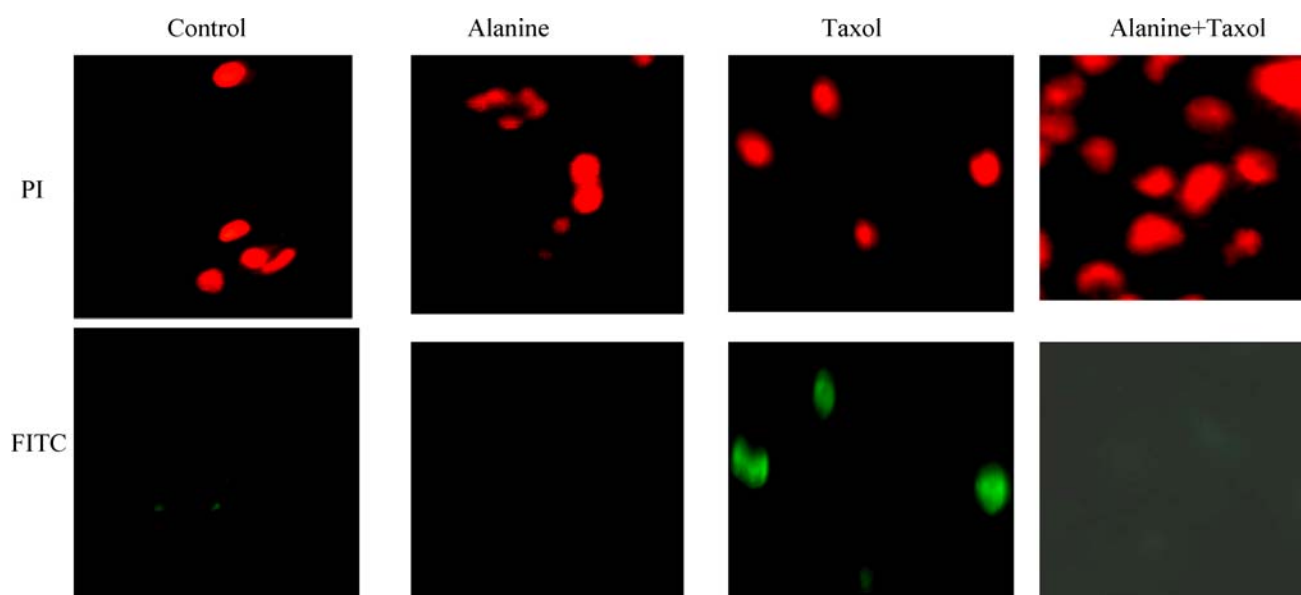


Fig. 15 Effect of L-Alanine on Taxol induced apoptosis in MDA-MB231 cells. MDA-MB231 cells were grown in DMEM/F12 containing 10% FCS. After 70% confluence, cells were treated with L-Alanine (10 mM, 72 h), Taxol (10 nM, 72 h) or pre-incubated with L-Alanine for 2 h, and then treated with Taxol for 72 h. Cell culture medium and cell pellets were collected and spin down at 1900 rpm for 5 min. Cell number was counted and adjusted to 1×10^6 /ml. A total 50 μ l of

cell suspension from each condition was used for preparation of cytospin slides. The slides were fixed with 4% paraformaldehyde in 0.1 M NaH_2PO_4 , pH 7.4 for 15 min then TUNEL assay was used to detect the apoptotic cells according to manufacture's instruction. The slides were mounted with a medium containing Propidium Iodide (PI) and photographed with a fluorescence microscope. The top panel indicated total cells (red), and medial panel indicated apoptotic cells (green)

in FITC labeled apoptotic cells (Fig. 18 panel below). Unlike its response to Taxol treatment (Fig. 17), the presence of Caspase inhibitor did not reverse the doxorubicin-induced increase in apoptotic cells (Tunel assay, Fig. 18 panel below), or in the S, and G1 fractions of the cell cycle. On the contrary, the presence of the caspase inhibitor caused further increase in G2 fraction.

Similar to its response with Taxol, treatment with alanine (10 mM) caused a significant reversal in the FITC labeled apoptotic cells assessed by the Tunel assay. In addition, alanine treatment caused a partial reversal in doxorubicin-induced inhibition of the S-phase. It had no significant effect on doxorubicin-induced increase in the G1 and G2 fractions. These observations suggest that as measured by the Tunel assay, there is some difference in mechanisms leading to apoptosis by Taxol compared to Doxorubicin treatment.

Discussion

Programmed cell death or apoptosis is known as one of the primary mechanisms underlying actions of multiple anti-cancer agents [27, 28]. A series of molecular and biochemical events have been defined during cell apoptosis process, including activation of death receptor or checkpoint genes; apoptotic signaling; activation of caspases; and nucleosomal cleavage of DNA. Morphologically the apoptotic cells are characterized by condensed nucleus and formation of

apoptotic body. The biochemical features underlying these morphological changes include protein cleavage by caspases, protein cross-linking by activated transglutaminase, and internucleosomal cleavage of DNA by Ca^{++} and Mg^{++} dependent endonuclease [29]. Taxol-induced cancer cell apoptosis was first described by Bhalla and colleagues in leukemia cells [8]. Multiple studies have indicated that the mechanisms of Taxol-induced apoptosis were related to the dosage of Taxol administrated [30–33]. At low Taxol concentration, apoptosis might occur after an aberrant mitosis by a Raf-1 independent pathway, whereas cell death may be the result of a terminal mitotic arrest occurring by a Raf-1 dependent pathway at higher Taxol concentration [32]. In the present study, the effect of Taxol on MCF-7 breast cancer cells was confirmed by a time- and dose-dependent growth inhibition (Fig. 1) and cell apoptosis (Fig. 2). Examination of biochemical changes during Taxol-induced apoptosis by measuring the transport of various amino acids demonstrated an increased sodium-dependent uptake of alanine in a time- and dose-dependent manner upon Taxol treatment. Interestingly, Taxol also exhibited partial inhibition of sodium-dependent arginine transport. However, no effect on sodium-dependent transport of glutamate and MeAIB was observed. Although the mechanism and significance of this transient up-regulation of sodium-dependent alanine transport during Taxol-induced cell apoptosis is not clear, it is possible that this event might be part of the concerted metabolic responses during cell apoptosis induced by Taxol.

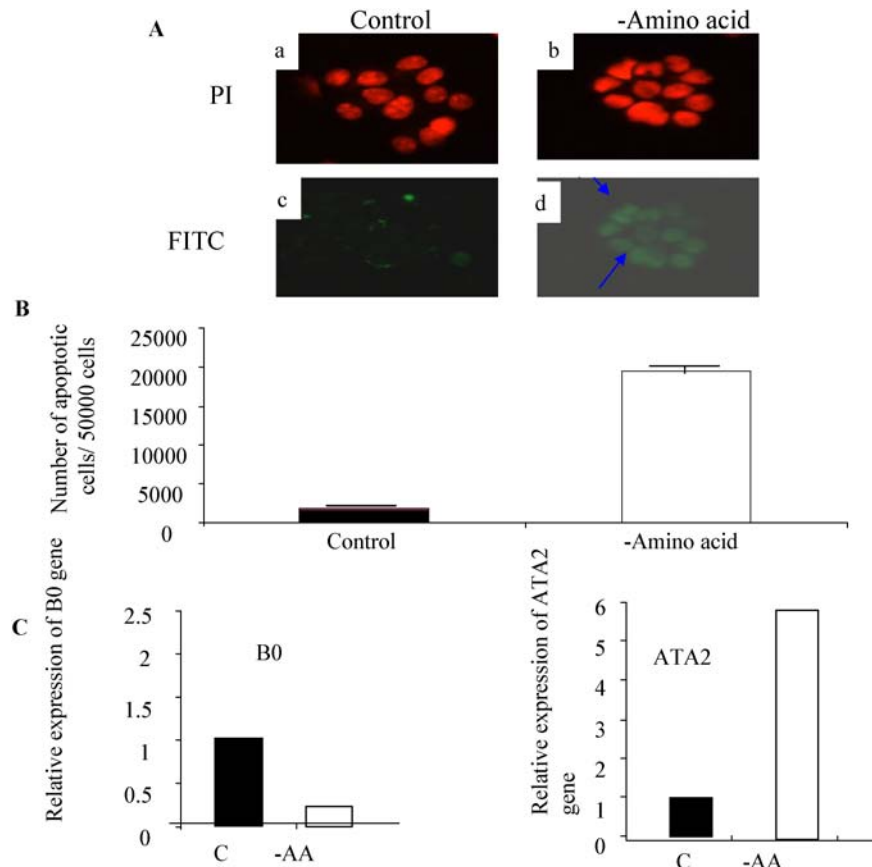


Fig. 16 Effect of amino acid starvation on cell apoptosis. MCF-7 cells were grown in DMEM/F12 media containing 10% FCS. At 80% confluence, the monolayers were washed with PBS and incubated in amino acid-free media (Earle's Balanced Salt Solution, EBSS) containing 5% DFCS for 18 h. (A) Cell culture medium and cell pellets were collected after 18 h starvation, spun down at 1900 rpm for 5 min. Cell number was counted and adjusted to 1×10^6 /ml. A total 50 μ l of cell suspension from each condition was used for preparation of cytospin slides. The slides were fixed with 4% paraformaldehyde in 0.1 M NaH_2PO_4 , pH 7.4 for 15 min. TUNEL assay was used to detect apoptotic cells

according to manufacture's instructions. The slides were mounted with a medium containing Propidium Iodide (PI) and photographed under a fluorescence microscope. The arrows indicate apoptotic cells. (B) The number of apoptotic cells was counted from five different random areas and the bars were mean \pm SD from 3 slides. (C) Total RNA was isolated and RT-Real-Time PCR was performed with the indicated gene primers. The bars indicate fold change in gene copy for System B0 and ATA2 from 3 different determinations compared to untreated cells. The values are adjusted with 18S gene expression. The statistical significance was determined by student-*t* test

It is well known that alanine is one of the most important gluconeogenic amino acids flowing to the liver [9]. The serum concentration of alanine ranks at second highest only after glutamine [20]. Kubota et al. reported that the plasma level of alanine was significantly increased in patients with breast cancer and some other cancers [34]. In mammalian cells alanine is transported via multiple mechanisms including sodium-dependent amino acid transport systems A, ASC and B0, as well as sodium-independent transport system L [9]. Sharma et al. found that, in the mammary glands of lactating mouse, L-alanine uptake was mediated by three Na^+ -dependent and one Na^+ -independent systems [35]. The Na^+ -dependent systems include system A and two others with broad transport specificities. In our study, we have demonstrated that a breast cancer cell line MCF-7 constitutively expresses activity of amino acid transport system B0, whose expression was further induced after treatment with Taxol.

System B-like transport activities were first described by Stevens BR and Wright EM et al. in the rabbit intestine brush-border membrane as a separate amino acid transport agency with a broad uptake specificity of alanine, glutamine, branched and aromatic amino acids [12]. McGivan et al. later identified the similar transport system in bovine renal brush-border [13] and in a bovine renal epithelial cell line NBL-1 [14]. In order to highlight the substrate difference with another broad range amino acid transport system $\text{B}^{0,+}$, which interacts with both neutral amino acid and cationic amino acid, Christensen and colleagues proposed to name this transport agency as system B0 [13]. More recently, Ganapathy and co-workers isolated a cDNA (ATB^0) with the transport activity similar to system B0 from a human placental choriocarcinoma cell cDNA library [16], and demonstrated that the same gene was also expressed in human intestine and kidney [17]. A mouse version of system B0 gene was also reported

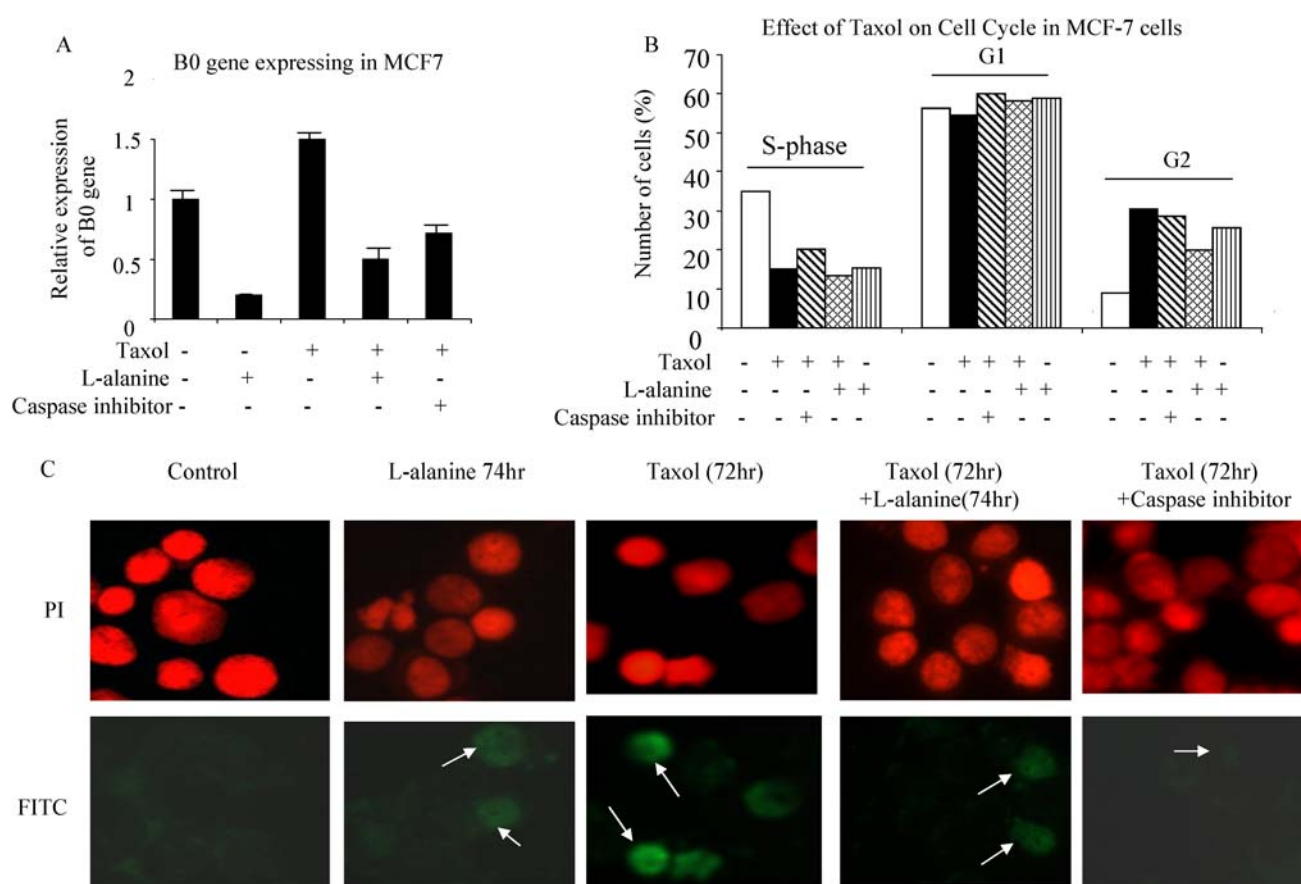


Fig. 17 Taxol up-regulates B0 transporter gene, and induces cell apoptosis in G2-phase in MCF-7 cells. MCF-7 cells were grown in DMEM/F12 containing 10% FCS. After 60%–70% confluence cells were either pre-incubated with L-Alanine (10 mM, 2 h) or Caspase inhibitor IV (10 μ M, 2 h) then add Taxol (10 nM) for additional 72 h or treated with Taxol directly. The cell culture medium and cell pellets were collected and centrifuged at $250 \times g$ for 5 min. (A) Total RNA was isolated and Real-time RT-PCR was performed with a primer specific for B0 gene, and the fold changes were compared with untreated cells and adjusted with 18S. The bars indicated mean of 3 different determi-

nations and plus standard deviation. (B) Cell number was adjusted to 1×10^6 /ml, fixed with 70% ethanol, and stained with hypotonic DNA staining buffer for 30 min followed by Cell Cycle Analysis. (C) A total 50 μ l of cell suspension for each condition was used for preparation of cytospin slides. The slides were fixed with 4% paraformaldehyde in 0.1 M NaH_2PO_4 , pH 7.4 for 15 min then TUNEL assay was used to detect the apoptotic cells according to manufacture's instructions. The slides were mounted with a medium containing Propidium Iodide (PI) and photographed under a fluorescence microscope. The top panel indicate total cells (red), and bottom panel indicate apoptotic cells (green)

recently [18]. It is interesting that ATB⁰ gene was found to serve as the receptor of RD114/simian type D retrovirus [36, 37]. Also, system B0-mediated amino acid transport was up-regulated by several hormones including growth hormone [38], epidermal growth factor (EGF) [39], and glucagon [40].

In this study, we have confirmed that alanine transport was up-regulated during Taxol-induced apoptosis process in MCF-7 and other breast cancer cells. Substrate inhibition analysis indicated the existence of a transport agency with broad substrate specificities in MCF-7 cells. Further analysis of the gene expression revealed that system B0 gene was induced in response to Taxol treatment as well as to another microtubule-targeting anticancer agent Vinblastine, but not to the non-microtubule-targeting anticancer agent MMC. Since microtubules play an important role in cellular

transport process, it will be interesting to investigate whether the increased amino acid transport by system B0 is part of the cellular apoptotic response or simply the result of cellular microtubule disturbance.

Our data demonstrated apoptotic changes in response to Taxol in the presence or absence of high concentration of alanine in MCF7 cells. The rationale was to confirm increase in nuclear damage or granulation upon Taxol treatment, and if this apoptotic change could be inhibited or reversed by inhibiting or blocking System B0. The data show a clear demonstration in both changes in nuclear morphology as assessed by PI uptake, and with simultaneous uptake of the FITC labeled d-UTP in MCF7 cells. Blocking the B0 transporter resulted in a decrease in apoptotic changes in response to Taxol. Protection from Taxol-induced apoptosis in the presence of high concentrations of alanine was also con-

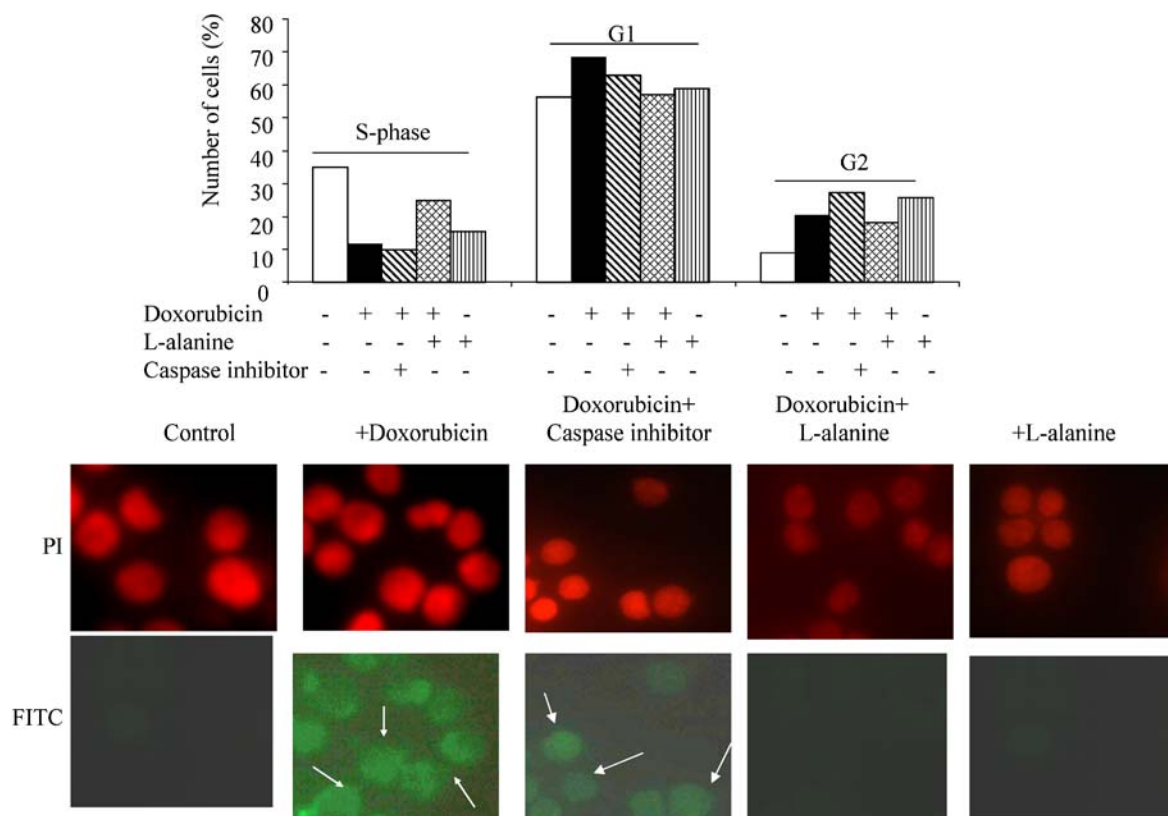


Fig. 18 Doxorubicin induces cell apoptosis in G1-phase in MCF-7 cells. MCF-7 cells were grown in DMEM/F12 containing 10% FCS. After 60%–70% confluence cells were either pre-incubated with L-Alanine (10 mM, 2 h) or Caspase inhibitor IV (10 μ M, 2 h) followed by addition of Doxorubicin (100 ng/ml) for additional 72 h. Another set of cell cultures were treated with Doxorubicin directly. The cell culture medium and cell pellets were collected and spun down at $250 \times g$ for 5 min. Cell number was adjusted to 1×10^6 /ml, fixed with 70% ethanol, and stained with hypotonic DNA staining buffer for 30 min followed

by Cell Cycle Analysis. (B) A total 50 μ l of cell suspension from each condition was used for preparation of cytospin slides. The slides were fixed with 4% paraformaldehyde in 0.1 M NaH₂PO₄, pH 7.4 for 15 min then TUNEL assay was used to detect the apoptotic cells according to manufacture's instructions. The slides were mounted with a medium containing Propidium Iodide (PI) and photographed under a fluorescence microscope. The top panel indicate total cells (red), and bottom panel indicate apoptotic cells (green)

firmed with other breast cancer cells T47D and MDAMB231. That is, Taxol induced significant increase in apoptosis of both T47D and MDAMB231 cells as measured by increase in nuclear damage/granulation, followed by increase in FITC labeled BRDU uptake. Blocking the B0 transporter in the presence of high concentration of alanine, reversed the nuclear damage, and decreased FITC labeled uptake in both T47D and MDAMB231 cells. Our studies speculate that the presence of high concentrations of Alanine in plasma or diet, could inhibit or reduce the chemotherapeutic effect of Taxol by decreasing its apoptotic potential, and this process involves activation and deactivation of B0 transporter. In addition, breast cancer cells with high concentrations of alanine could become resistant to Taxol. Alternatively, activation of System B0 is a critical step in Taxol-induced apoptosis in breast cancer cells MCF7, T47D and MDAMB231. Down regulation of this transporter could result in reducing the Taxol effect, and eventually lead to resistance to Taxol treatment. This hypothesis could be further tested by knocking

down the B0 transporter with Si-RNA against the B0 transporter gene. Further studies are warranted to understand why the B0 transporter should be up-regulated upon apoptosis signals generated in response to chemo agents such as Taxol and Doxorubicin.

The data from amino acid starvation studies show an increase in apoptotic cells (Fig. 16 (A) and (B)). However, only System A or the ATA2 transporter gene was up-regulated by 2 to 6 fold while the B0 gene expression was down regulated. These observations provide further evidence that Taxol-induced up-regulation of System B0 is a specific metabolic response to apoptosis induced by Taxol.

Numerous studies have shown that System A transport activity increases in response to amino acid starvation, a phenomenon known as adaptive regulation. This observation has also been confirmed at the gene level for System A, cloned and identified as ATA2 [8, 10, 11, 19–21, 41]. Why, should the System B0 activity at both transport and gene level go up in response to Taxol-induced apoptosis, but

not during amino acid starvation-induced apoptosis, needs further investigation.

There are several possible mechanisms which could contribute to alanine induced decrease in drug-induced apoptosis. (1) High concentrations of extracellular alanine will block the B0 transporter activity. Consequently, the cells will be deprived of those amino acids which require the B0 transporter to enter the cell and maintain metabolic and ATP requirement for cell survival. Deprivation of these “essential” amino acids could result in apoptosis. This concept has been nicely elucidated in a recent study by Fu et al. [42]. These authors demonstrated that specific amino acid restriction affects the functioning of mitochondria in two prostate cancer cell lines, DU145 and PC3. In particular, restriction of tyrosine and phenylalanine (Tyr/Phe), glutamine (Gln), or methionine (Met), modulated Raf and Akt survival pathways and affected the function of mitochondria in DU145 and PC3. In addition, amino acid restriction has been shown to reduce the amount of ATP in DU145 and PC3 cells. The reduction in ATP was cell and amino acid specific in some cancer types [43]. It is therefore possible that in our current study, inhibition of B0 transporter could restrict the entry of substrate amino acids such as alanine, threonine, and leucine. Depriving these amino acids could compromise the metabolic needs of the tumor cell, resulting in mild to moderate degree of apoptosis.

(2) Down regulation of the transporter, may result in the inhibition of some of the apoptotic molecules that are activated in response to Taxol treatment. Future studies from our lab will test this possibility by using siRNA to knock down B0 transporter. As shown in our data in Fig. 17, inhibition of the caspase pathway by the caspase inhibitor IV, resulted in a decrease in Taxol-induced up-regulation of the B0 transporter gene. In comparison, high concentration of alanine had greater inhibition.

(3) Conversely, cell cultures incubated with high concentration of alanine alone could result in a significant inhibition of the B0 transporter gene via activation or inactivation of the mitogen activated-activated protein kinases (MAPKs) comprising of ERK, p38MAPKs, and c-Jun N-terminal kinase (JNK). Koyama et al. [44] have demonstrated that apoptosis induced by chemotherapeutic agents involves c-Jun N-terminal kinase activation in Sarcoma Cell lines. The activation of JNK was induced by the chemotherapeutic agent cis-diaminedichloroplatinum (cisplatin, CDDP) and doxorubicin (DXR). The authors also investigated whether the ectopic expression of constitutively active (MKK7-JNK1) or dominant-negative form of JNK(dnJNK) influenced apoptosis in response to the CDDP or DXR in sarcoma cell lines MG-63 and SaOS-2. Their results showed that JNK activation is involved in apoptotic cell death in sarcoma cell lines following stimulation with CDDP or DXR. Over-expression of dnJNK prevented drug induced apoptosis.

In a recent study Lee et al. [45] proposed that the sustained activation of ERK1/2 pathway may be involved in the apoptosis induced by anticancer DNA-damaging drugs, including doxorubicin and etoposide. Their data have demonstrated that the differential regulation of the PI3K/Akt, ERK1/2, and p38 MAPK signaling pathways are crucial in the context of DNA-damaging drug-induced apoptosis. Doxorubicin was determined to elicit the apoptosis of NIH3T3 cells in a dose-dependent manner. Prior to cell death, both Akt and p38 MAPK were transiently activated and subsequently inactivated almost wholly, whereas ERK and JNK activation was sustained in response to the drug treatment. The inhibition of PI3K/Akt and p38 MAPK both accelerated and enhanced doxorubicin-induced apoptosis and ERK inhibition apparently exerted negative effect on apoptosis. The modulation of PI3K/Akt activation by treatment of LY294002 or expression of Akt mutants such as Akt-DN or Myr-Akt exerted a significant effect on the activation of ERK1/2.

In conclusion, our data clearly demonstrate that up-regulation of B0 in response to Taxol, is not a simple epiphenomenon of drug treatment, but a process that may promote apoptosis. Up-regulation of B0 by doxorubicin argues against the importance of microtubules per se in regulating B0 transporter levels, as doxorubicin is not known to affect microtubule assembly. It could be argued that since doxorubicin arrests cells in G1 rather than in G2/M, FACS cell cycle analysis of cells treated with paclitaxel or with doxorubicin, should document independence of B0 up-regulation from cell cycle effects. We generated additional data to further explore possible interactions between B0 up-regulation in response to Taxol and doxorubicin in relation to cell cycle changes. In addition, we have tested the presence and absence of alanine and the caspase inhibitor IV on Taxol and doxorubicin induced apoptosis, using both FACS cell cycle analysis and TUNEL assay.

First, FACS cell cycle analysis confirm that significant portion of cells treated with Taxol get arrested at G2 (increase in G2), resulting in a decrease in S-phase fraction. In comparison, doxorubicin treatment resulted in a decrease in S-phase with increase in G1 and a small increase in G2. We now provide additional data to elucidate the differences (if any) in apoptotic signals between Taxol and doxorubicin treatment.

Cell cycle data in Fig. 17 demonstrate the following: (a) Taxol treatment resulted in a significant decrease in S-phase, with accompanying increase in the G2 fraction. In the panel below, the data from TUNEL assay, confirm increase in apoptotic cells as measured by FITC uptake. Presence of the Caspase inhibitor IV or alanine (10 mM) inhibited the Taxol-induced apoptosis, as assessed by the TUNEL assay (Fig. 17, panel c). The reversal in apoptosis with the Caspase inhibitor was more pronounced compared to high concentration of alanine. These observations suggest that

based on the TUNEL assay, Taxol-induced apoptosis is partially Caspase-dependent, and alanine sensitive. In contrast to the TUNEL assay data, the FACS results show marginal reversal in the decrease in S phase, and increase in G2 fraction, suggesting that Taxol-induced apoptosis involves caspase dependent and independent pathways. Figure 18 shows that doxorubicin treatment caused a significant inhibition in S-phase growth of the MCF-7 cells, with accompanying increase in G1 and G2 fractions. The increase in G2 fraction is not as significant as that observed for Taxol treatment. The TUNEL assay shows complementing increase in FITC labeled apoptotic cells (Fig. 18 panel below). Unlike its response to Taxol treatment (Fig. 17), the presence of Caspase inhibitor did not reverse the doxorubicin-induced increase in apoptotic cells (TUNEL assay, Fig. 18 panel below), or in the S, and G1 fractions of the cell cycle. On the contrary, the presence of the caspase inhibitor caused further increase in G2 fraction.

Similar to its response with Taxol, treatment with alanine (10 mM) caused a significant reversal in the FITC labeled apoptotic cells assessed by the TUNEL assay. In addition, alanine treatment caused a partial reversal in doxorubicin-induced inhibition of the S-phase. It had no significant effect on doxorubicin-induced increase in the G1 and G2 fractions.

These observations suggest that as measured by the TUNEL assay, there is some difference in mechanisms leading to apoptosis by Taxol compared to Doxorubicin treatment. However, high concentrations of alanine, reverses the decrease in doxorubicin –induced S-phase fraction, compared to Taxol. In contrast, alanine treatment decreased the Taxol-induced increase in G2 phase. That is, high concentrations of alanine affect doxorubicin-induced apoptosis at the S-phase, while for Taxol it affects the G2/M phase.

Once antibodies to the extracellular portion of B0 become available, it will be possible to demonstrate a direct link between B0 expression and TUNEL positive cells in the sub-G fraction of cells undergoing apoptosis. Studies from Ganapathi's laboratory have used a polyclonal antibody generated against ATB (0/+) in oocyte expression systems and in luminal membranes of tissues such as eyelid, lung, retina, and colon [46, 47]. However, it is not clear if this transporter would have the same transport specificity and antigenic recognition as in our breast cancer cell model.

Acknowledgments Grant Support: NIH/NCI U56 CA101599-01 (J.V.V); CA15083-25S3 (J.V.V); NIH/NIDDK R25 DK067015-01 (J.V.V); Department of Defense (BCRP) BC043180 (J.V.V). MBRS, NIH SO6 GM0685-10-01 (Y. Wu).

References

- Jemal A, Murray T, Ward E et al (2005) Cancer statistics. *CA Cancer J Clin* 55:10–30
- Nowak AK, Wilcken NR, Stockler A, Hamilton D, Ghersi D (2004) Systematic review of taxane-containing versus non-taxane-containing regimens for adjuvant and neoadjuvant treatment of early breast cancer. *Lancet Oncol* 5:372–380
- Crown J, O'Leary M, Ooi WS (2004) Docetaxel and paclitaxel in the treatment of breast cancer: a review of clinical experience. *Oncologist* 9(2):24–32
- Horwitz SB, Cohen D, Rao S, Ringel I, Shen HJ, Yang CP (1993) Taxol: mechanisms of action and resistance. *J Natl Cancer Inst Monogr* 55–61
- Rao S, Orr GA, Chaudhary AG, Kingston DG, Horwitz SB (1995) Characterization of the taxol binding site on the microtubule. 2-(m-Azidobenzoyl)taxol photolabels a peptide (amino acids 217–231) of beta-tubulin. *J Biol Chem* 270:20235–20238
- Milross CG, Mason KA, Hunter NR, Chung WK, Peters LJ, Milas L (1996) Relationship of mitotic arrest and apoptosis to antitumor effect of paclitaxel. *J Natl Cancer Inst* 88:1308–1314
- Yvon AM, Wadsworth P, Jordan MA (1999) Taxol suppresses dynamics of individual microtubules in living human tumor cells. *Mol Biol Cell* 10:947–959
- Bhalla K, Ibrado AM, Tourkina E, Tang C, Mahoney ME, Huang Y (1993) Taxol induces internucleosomal DNA fragmentation associated with programmed cell death in human myeloid leukemia cells. *Leukemia* 7:563–568
- Christensen HN (1990) Role of amino acid transport and countertransport in nutrition and metabolism. *Physiol Rev* 70:43–77
- Vadgama JV, Chan MN, Wu JM (1991) Differential expression of amino acid transport systems A and ASC during erythroleukemia cell differentiation. *Am J Physiol* 260:C392–C399
- Vadgama JV, Christensen HN (1983) Comparison of system N in fetal hepatocytes and in related cell lines. *J Biol Chem* 258:6422–6429
- Stevens BR, Ross HJ, Wright EM (1982) Multiple transport pathways for neutral amino acids in rabbit jejunal brush border vesicles. *J Membr Biol* 66:213–225
- Lynch AM, McGivan JD (1987) Evidence for a single common Na⁺-dependent transport system for alanine, glutamine, leucine and phenylalanine in brush-border membrane vesicles from bovine kidney. *Biochim Biophys Acta* 899:176–184
- Doyle FA, McGivan JD (1992) The bovine renal epithelial cell line NBL-1 expresses a broad specificity Na⁽⁺⁾-dependent neutral amino acid transport system (System B0) similar to that in bovine renal brush border membrane vesicles. *Biochim Biophys Acta* 1104:55–62
- Carbo N, Lopez-Soriano FJ, Argiles JM (1997) Neutral amino acid transport in placental plasma membrane vesicles in the late pregnant rat. Evidence for a B0-like transport system. *Eur J Obstet Gynecol Reprod Biol* 71:85–90
- Kekuda R, Prasad PD, Fei YJ et al (1996) Cloning of the sodium-dependent, broad-scope, neutral amino acid transporter B⁰ from a human placental choriocarcinoma cell line. *J Biol Chem* 271:18657–18661
- Kekuda R, Torres-Zamorano V, Fei YJ et al (1997) Molecular and functional characterization of intestinal Na⁽⁺⁾-dependent neutral amino acid transporter B0. *Am J Physiol* 272:G1463–G1472
- Broer A, Klingel K, Kowalczyk S, Rasko JE, Cavanaugh J, Broer S (2004) Molecular cloning of mouse amino acid transport system B0, a neutral amino acid transporter related to Hartnup disorder. *J Biol Chem* 279:24467–24476
- Bequette BJ, Backwell FR, Crompton LA (1998) Current concepts of amino acid and protein metabolism in the mammary gland of the lactating ruminant. *J Dairy Sci* 81:2540–2559
- Shennan DB (1998) Mammary gland membrane transport systems. *J Mammary Gland Biol Neoplasia* 3:247–258

21. Levenson AS, Jordan VC (1997) MCF-7: the first hormone-responsive breast cancer cell line. *Cancer Res* 57:3071–3078
22. Bhat HK, Vadgama JV (2002) Role of estrogen receptor in the regulation of estrogen induced amino acid transport of system A in breast cancer and other receptor positive tumor cells. *Int J Mol Med* 9:271–279
23. Shennan DB, Thomson J, Gow IF, Travers MT, Barber MC (2004) L-leucine transport in human breast cancer cells (MCF-7 and MDA-MB-231): kinetics, regulation by estrogen and molecular identity of the transporter. *Biochim Biophys Acta* 1664:206–216
24. Saunders DE, Lawrence WD, Christensen C, Wappler NL, Ruan H, Deppe G (1997) Paclitaxel-induced apoptosis in MCF-7 breast-cancer cells. *Int J Cancer* 70:214–220
25. Vadgama JV, Wu Y, Shen D, Hsia S (2000) J. Block, Effect of selenium in combination with adriamycin or Taxol on several different cancer cells. *Anticancer Res* 20:1391–1414
26. Pola E, Bertran J, Roca A, Palacin M, Zorazano A, Testar X (1990) Sensitivity of system A and ASC transport activities to thiol-group-modifying reagents in rat liver plasma-membrane vesicles. Evidence for a direct binding of N-ethylmaleimide and iodoacetamide on A and ASC carriers. *Biochem J* 271:297–303
27. Lowe SW, Ruley HE, Jacks T, Housman DE (1993) P53-dependent apoptosis modulates the cytotoxicity of anticancer agents. *Cell* 74:957–967
28. Thompson CB (1995) Apoptosis in the pathogenesis and treatment of disease. *Nature* 1456–1462
29. Cotran RS, Kumar V, Collins P (1999) Cell injury and cell death. In: Robbins pathologic basis of diseases. Philadelphia. W.B. Saunders Company, 6th Ed. pp. 18–25
30. Jordan MA, Wendell K, Gardiner S, Derry WB, Copp H, Wilson L (1996) Mitotic block induced in HeLa cells by low concentrations of paclitaxel (Taxol) results in abnormal mitotic exit and apoptotic cell death. *Cancer Res* 56:816–825
31. Au JL, Li D, Gan Y et al (1998) Pharmacodynamics of immediate and delayed effects of paclitaxel: role of slow apoptosis and intracellular drug retention. *Cancer Res* 58:2141–2148
32. Torres K, Horwitz SB (1998) Mechanisms of Taxol-induced cell death are concentration dependent. *Cancer Res* 58:3620–3626
33. Blagosklonny MV, Fojo T (1999) Molecular effects of paclitaxel: myths and reality (a critical review). *Int J Cancer* 83:151–156
34. Kubota A, Meguid MM, Hitch DC (1992) Amino acid profiles correlate diagnostically with organ site in three kinds of malignant tumors. *Cancer* 69:2343–2348
35. Sharma R, Kansal VK (1999) Characteristics of transport system of L-alanine in mouse mammary gland and their regulation by lactogenic hormones: evidence for two broad spectrum systems. *J Dairy Res* 66:385–398
36. Rasko JJ, Battini J, Gottschalk RJ, Mazo I, Mille D (1999) The RD114/simian type D retrovirus receptor is a neutral amino acid transporter. *PNAS* 96:2129–2134
37. Tailor CS, Nouri A, Zhao Y, Takeuchi Y, Kabat D (1999) A sodium-dependent neutral-amino-acid transporter mediates infections of feline and baboon endogenous retrovirus and simian type D retrovirus. *J Virol* 73:4470–4474
38. Iannoli P, Miller JH, Ryan CK, Gu LH, Ziegler TR, Sax HC (1997) Human growth hormone induces system B transport in short bowel syndrome. *J Surg Res* 69:150–158
39. Torres-Zamorano V, Kekuda R, Leibach FH, Ganapathy V (1997) Tyrosine phosphorylation-and epidermal growth factor-dependent regulation of the sodium-coupled amino acid transporter B^o in the human placental choriocarcinoma cell line JAR. *Biochem Biophys Acta* 1356:258–270
40. Lim SK, Cynober J, Bandt JD, Aussel C (1999) A Na⁺-dependent system A and ASC-independent amino acid transport system stimulated by glucagon in rat hepatocytes. *Cell Biol Int* 23:7–12
41. Tanaka K, Yamamoto A, Fujita T (2005) Functional expression and adaptive regulation of Na⁺-dependent neutral amino acid transporter SNAT/ATA2 in normal human astrocytes under amino acid starvation condition. *Neuroscience Letters* 378:70–75
42. Fu Y-M, Zhang H, Ding M, Li Y-Q, Fu X, Yu Z-X, Meadows GG (2006) Selective amino acid restriction targets mitochondria to induce apoptosis of androgen-independent prostate cancer cells. *J Cell Physiol* 209:522–534
43. Fu Y-M, Yu XX, Li Y-Q, Ge X, Sanchez PJ, Fu X, Meadows GG (2003) Specific amino acid dependency regulates invasiveness and viability of androgen-independent prostate cancer cells. *Nutr Cancer* 45:60–73
44. Koyama T, Mikami T, Koyama T, Imakirre A, Yamamoto K, Toyota H, Mizuguchi J (2006) Apoptosis induced by chemotherapeutic agents involves c-Jun N-terminal kinase activation in Sarcoma cell lines. *J Orthop Res* 24:1153–1162
45. Lee E-R, Kim J-Y, Kang Y-J, Ahn J-Y, Kim J-H, Kim B-W, Choi H-Y, Jeong M-Y, Cho S-G (2006) Interplay between PI3K/Akt and MAPK signaling pathways in DNA-damaging drug-induced apoptosis. *Biochimica et Biophysica Acta* 1763:958–968
46. Hatanaka T, Haramura M, Fei Y-J, Miyauchi S, Bridges CC, Ganapathy PS, Smith SB, Ganapathy V, Ganapathy ME (2004) Transport of Amino Acid-Based Prodrugs by the Na₊- and Cl₋-Coupled Amino Acid Transporter ATB0, and Expression of the Transporter in Tissues Amenable for Drug Delivery. *JPET* 308:1138–1147
47. Hatanaka T, Nakanishi T, Huang W, Leibach FH, Prasad PD, Ganapathy V, Ganapathy ME (2001) Na- and Cl- coupled active transport of nitric oxide synthase inhibitors via the amino acid transport system ATB0. *J Clin Investig* 107:1035–1043

APPENDIX B

Down regulation of Akt1 is essential for the treatment of HER2/neu overexpressing breast tumors

Yanyuan Wu, Rita Chakrabarti, Amaechi Okafor, Aye Aye Thant, Reiko Sakurai, Dennis Slamon, Jaydutt V. Vadgama*

Divisions of Cancer Research and Training and Hematology/Oncology, Departments of Medicine, David Geffen School of Medicine at UCLA and Charles R. Drew University of Medicine and Science. Los Angeles, CA

Running title:

Targeting Akt1 inhibits HER2/neu overexpressing breast cancer cells

Keywords: HER2/neu; Herceptin; Akt1; Breast Cancer

Please send all correspondence to:

Dr. Jaydutt Vadgama

Division of Cancer Research and Training

Department of Medicine

Charles R. Drew University of Medicine and Science

1731 East 120th Street. Los Angeles, CA 90059

Tel: 323-563-4853

Fax: 323-563-4859

e-mail: javadgam@cdrewu.edu

Abstract

Purpose: Patients with HER2/neu overexpressing breast tumors have poor survival, and frequently become resistant to hormonal, chemo, and antibody therapy. The mechanisms leading to resistance to HER2/neu antibody, Herceptin are poorly understood. We propose that overexpression and increased activation of the PI3/Akt kinase pathway may contribute to Herceptin resistance.

Experimental Design: We investigated mechanisms by which the PI3/Akt kinase pathway can be down-regulated, and thereby improve response to Herceptin treatment. We stable transfected active (myrsilated) or inactive Akt1 (kinase dead) into HER2/neu over-expressing breast cancer cells. Several clones were generated, their growth characteristics determined and response to Herceptin investigated. The function of pAkt1 was examined in these clones and in breast tumor cells with HER2/neu knock down.

Results: Levels of active Akt1 (phospho-Akt1) were highest in HER2/neu overexpressing cells. Cell proliferation was higher in active Akt1 transfectants compared to dominant negative Akt1 and vector only transfectants. Herceptin caused a greater growth inhibition in cells with dominant negative Akt1. Similar results were observed with the PI3 kinase inhibitors LY294002 and Wortmannin. Combination of Herceptin with LY294002 caused further growth inhibition. However, Herceptin had little or no effect on SKBR3 cells transfected with active Akt1. Clones with active Akt1 had increased levels of HER2/neu mRNA. HER2/neu siRNA treatment led to a significant shut down of HER2/neu gene and protein expression in both wild type and myrsilated Akt1 transfectants.

Conclusion: HER2/neu overexpressing breast tumors may be more responsive to Herceptin treatment, after targeting the down regulation of the PI3 kinase pathway, in particular pAkt1.

Introduction

Over-expression of HER2/neu has been shown in 20-30% of patients with breast cancer. The overall survival and the time to relapse for patients whose tumors over-express HER2/neu are significantly shorter (1-3). The malignant phenotypes exhibited by tumor cells, such as those causing metastasis, are also enhanced by HER2/neu over-expression (4-6). Clinical and translational studies from our own laboratory also demonstrated that an increased level of plasma HER2/neu in breast cancer patients who underwent surgery and completed chemotherapy is associated with poor outcome and reduction in disease-free survival (7). It is an aggressive form of breast cancer since HER2/neu over-expressing tumor is more likely to be resistant to treatment with tamoxifen and standard chemotherapy (8-14).

Different therapeutic strategies have been developed against HER2/neu-positive breast cancer over the past decade, which included HER2/neu antisense, tyrosine kinase inhibitors such as emodin, and antibodies against HER2 receptor. In particular, humanized MAb Herceptin (Trastuzumab; Genentech, San Francisco, CA) has been widely used for the treatment of women with HER2/neu overexpressing breast cancers. Herceptin is designed to target the extracellular domain of the HER2/neu tyrosine kinase receptor and block its function (15). In patients with metastatic breast cancer that over-express HER2/neu, Herceptin has been found to be clinically beneficial as first-line chemotherapy (16-17). However, the response rates to Herceptin monotherapy range from 12% to 34% for a median duration of 9 months only (18). Even though current treatment regimens combining Herceptin with the taxane paclitaxel (19-21) or docetaxel (22) increase response rates, greater than 70% of patients with over-expressing HER2/neu show no response to treatment (23). Many possible mechanisms have been proposed to account for the therapeutic effects of Herceptin, including down-modulation of the HER2/neu receptor (15),

interaction with immune system and enhancing cytotoxic activity of tumor-specific CTLs (15, 24), activation of apoptotic signals (25), and inhibition of HER2/neu receptor downstream signal transduction pathway (15, 18, 26).

The phosphatidylinositol-3 kinase (PI-3K) and its associated protein kinase B (Akt) pathway has been demonstrated to be one of the important downstream signaling pathways that play a critical role toward anti-apoptosis and pathogenesis of cancer (27). The PI-3K/Akt pathway can be activated by several growth factors such as insulin-like growth factor (IGF-I), epidermal growth factor (EGF), cytokines, and the HER2/neu network. The activation of Akt results in the downstream regulation of target molecules: glycogen synthase kinase-3 (GSK-3); forkhead transcription factor (FKHR); caspase-9; and pro-apoptotic Bcl-2 family member Bad. The final outcome may result in cellular proliferation or anti-apoptosis (28, 29). The cell lines derived from patients who were resistant to Herceptin treatment has shown upregulation of Akt (30). Activation of Akt followed by loss of p27^{wip} could be one of mechanisms of Herceptin-resistance (31). However, the mechanisms as to why those patients with over-expressing HER2/neu breast tumors do not respond to Herceptin treatment still remain poorly understood. In addition, the differences in tumor phenotype and genotype between the responders and non-responders to the Herceptin monotherapy are unknown.

The present study was designed to understand the role of Akt1 in response to Herceptin treatment and mechanisms of Herceptin actions in inhibiting the HER2/neu receptors and their downstream events. We either overexpressed or inhibited Akt1 in HER2/neu over-expressing breast cancer cells by transfection of myr-Akt1 or dominant negative Akt1 and then compared the differences from cell phenotype to signaling events, as well as responses to Herceptin among these cells expressing myr-Akt1, dominant negative Akt1 and normal Akt1. Our study

demonstrated that increased expression of active Akt1 changes cell phenotype rendered HER2/neu over-expressing tumors resistant to Herceptin. The PI-3Kinase or Akt inhibitors are able to restore the HER2 and Akt1 over-expressing tumor response to Herceptin treatment. Recently RNA interference (RNAi), such as small interfering RNA (siRNA) or short hairpin RNA (shRNA) against HER2 (siHER2) has been used to inhibit HER2 gene expression and modulate HER2 signaling *in vitro* (32). In the current study we also observed that using shRNA against HER2 (shHER2) can effectively block HER2/neu gene expression followed by inhibition of HER2/neu receptor, and down-regulation of Akt protein phosphorylation.

Materials and Methods

Chemicals and antibodies. Lipofectin Reagent and Geneticin (G-418 Sulfate) were purchased from Invitrogen (CA, USA); 3-(4,5-dimethyl-2-thiazolyl)2,5-diphenyl tetrazolium bromide (MTT) was purchased from Sigma (St. Louis, MO); PI-3 kinase inhibitor, LY90024 (#9901), was obtained from Cell Signaling Technology (Beverly MA); Heregulin β -1 (RP-318-PIA) was bought from Neo Markers (Fremont, CA) and Herceptin was received from Genentech (San Francisco, CA). Antibodies used were from the following suppliers: rabbit polyclonal anti-phospho-Akt Ser 473 (pAkt ser473) (#9271 and #9277), anti-Akt (#9272), and phospho-GSK3 β (pGSK-3 β) (#9331) from Cell Signaling Technology; mouse monoclonal anti-phosphor-Tyr (PT03), anti-CyclinD1 (Ab3) (CC12), anti-c-ErbB2/c-Neu (Ab-3) (OP15), rabbit polyclonal anti-c-neu (Ab-1) (PC04) and anti-cerbB3 (Ab-1) (PC27) from Oncogene Science (Cambridge, MA); rabbit polyclonal anti-Neomycin phosphotransferase II (#06-747) from Upstate Biotechnology (Lake Placid, NY); mouse monoclonal anti- β -actin from Sigma; and mouse monoclonal anti-c-erbB-2 (NCL-L-CB11) and CyclinD1 (NCL-L-CYCLIND1-GM) from Novocastra Laboratories (UK). Protein A/G Sepharose was obtained from Oncogene Science. Chemiluminescence reagent for detection of antigen-bound antibody was purchased from Bio-Rad (Hercules, CA).

Construction of Myr-Akt1 and dominant negative Akt1 (K179M). The form of myr-Akt1 contains sequences corresponding to amino-terminal 1-11 of avian *c-src* at 5' end, and a Myc-His tag at the 3' end of the mouse Akt1 ORF (open reading frame), inserted into the Klenow blunted Nhe I and PmeI sites of pUSEamp(+) (Catalog #21-151, Upstate Biotechnology). The activation of Akt1 is accomplished by the presence of the 11 N-terminal

amino acids of avian *c-src* that are required for protein myristoylation at the amino terminus of Akt1. The form of dominant-negative Akt1 (K179M mutant) (#21-152, Upstate Biotechnology) containing a Myc-His tag at the 3' end of the Akt1 ORF and substitution of methionine (ATG) for lysine (AAG) at residue 179 of Akt1 ORF, has been inserted as a Klenow blunted Nhe I and Pme I fragment into the multiple cloning site of pUSEamp(+).

Cell lines and cell culture. Human Breast cancer cell line SKBR3 was obtained from American Type Culture Collection. Unless otherwise stated, monolayer cultures of SKBR3 cells were maintained in DMEM/F12 (Fisher Scientific, CA) medium containing 10% FBS (Invetrogen), 2mM glutamine, 50 units/ml penicillin and 50 µg/ml streptomycin (Fisher Scientific, CA). The cells were grown at 37°C in a humidified incubator containing 5% CO₂.

SKBR3/AA cells were generated by transfection of Myr-Akt1 in SKBR3 cells; SKBR3/DN cells were created by transfection of dominant-negative Akt1 in SKBR3; and SKBR3/V33 was generated by transfection of pUSEamp(+) vector in SKBR3. The transfected cells were maintained in DMEM/F12 medium containing 10% FBS, 2mM glutamine, 50 units/ml penicillin, 50 µg/ml streptomycin and 500µg/ml G-418.

Stable transfection. Transfections were performed using Lipofectin reagent per manufacturer's instructions. Briefly, cells (1×10^5) were cultured in 60mm cell culture dish with 2ml DMEM/F12 containing 10% fetal calf serum, and incubated at 37° C in a CO₂ humidified incubator until 40-60% confluent. The cells were transfected with the pUSEamp vector or the vector containing either activated Akt1 or dominant-negative Akt1. After 48 hrs of transfection, the transfectants were selected by exposure to 500µg/ml G-418. The positive transfectants were selected by RT-PCR, Quantitative real-time PCR, as well as Western blot analysis.

Reverse transcriptase-polymerase chain reaction (RT-PCR). RNA was extracted using RNA-Bee (TEL-Test, Inc. Frindswood, TX) according to the manufacture's instructions. cDNA was reverse transcribed from 3 µg of total RNA using random primers and ThermoScript RT-PCR system (# 11146-024, Invitrogen) according to the manufacturer's instructions. PCR was performed with primers that contain a partial (21bp) Myc-Tag sequence in the reverse primer (5'-TCAATGGTGATGGTGATGATG-3') and a partial (20bp) Akt1-ORF: nt 2346-2365 (5'-TCCCCCAGTTCTCCTACTCA-3') in the forward primer. Activated Akt1 transfected clones were further confirmed by PCR with primers that contain a partial (21bp) Myr-Akt1 sequence in the reverse primer (5'-TTCTAGACTTGGGCTTGCTCTT-3') and a partial (22bp) Akt1-ORF: nt 792-903 (5'-CGGTGGGAGGTCTATATAAGCA-3') in the forward primer. Dominant-negative Akt1 (K179M mutant) transfected clones were further confirmed by PCR with primers that contained the mutant (ATG) sequence in the reverse primer and near to 3' end (5'-GAGGATCATCATGGCCATAGTAGC-3') and a partial (23bp) Akt1-ORF: nt 1361-1383 (5'-GACCATGAACGAGTTTGAGTACC-3') in the forward primer and sequenced by Retrogen, Inc. (San Diego, CA).

Quantitative real-time RT-PCR. Quantitative real-time PCR was performed with iCycle iQ real-time PCR detection system (Bio-Rad Lab, Hercules, CA) using SYBR Green Master Mix (#204143, QIAGEN). Reactions are characterized at the point during cycling when amplification of the PCR product is first detected. The mRNA levels of Akt1 and HER2/neu were quantified by measuring the threshold cycle (*C_t*) and adjusted with the level of 18S for each sample. The primers for Akt1 (forward primer '5-TCCTCAAGAAGGAAGTCATCGT-3' and reverse primer '5-CGTACTCCATGACAAAGCAGAG-3'), HER2/neu (forward primer '5-GACGAGACAGAGTACCATGCAG-3' and reverse primer '5-

AACTCCACACATCACTCTGGTG-3' and 18S (forward primer '5-GATCCATTGGAGGGCAAGTC-3' and reverse primer 5'-TCCCAAGTACCAACTACGAG-3') were purchased from Retrogen, Inc. (San Diego, CA).

shRNA transfection. The HER2 shRNA (short hairpin RNA) and negative control shRNA were expression ArrestTM short hairpin RNA constructs, cloned into pSHAG-MAGIC2c (pSM2c) retroviral vector and were purchased from Open Biosystems (Huntsville, Al). The shRNA for HER2/neu (Cat#: RHS1764-9692793 and RHS1764-9209568) were designed corresponding to nucleotides 575 to 595 of the coding region (gccctggccgtgctagacaat) of Homo sapiens ERBB2 transcript variant 1, mRNA sequence (NM_004448, NCBI database), and 2896 to 2917 of the coding region (gctgaactggtgtatgcagatt) of Homo sapiens ERBB2, transcript variant 2, mRNA sequence (NM_001005862, NCBI database) respectively. The plasmid DNA was prepared by using a kit for plasmid DNA extraction (QIAGEN, UHraPure) according to manufacturer's protocol. The transfection was performed by using Arrest-inTM transfection reagent (Open Biosystems) following the manufacture's instructions. Briefly, cells were trypsinized and plated at 1.4×10^5 cells per well in six-well plates 48 hrs prior to transfection in DMEM/F12 containing 10% fetal bovine serum. Two microgram of HER2, or negative shRNA plasmid was transfected in serum free media, and then cells were incubated at 37°C for 6 hours at which time serum were added back to the media. The HER2 mRNA expression after shRNA knock down was determined by Quantitative RT-PCR at 48hrs to 72hrs transfection.

MTT assay. Cells were plated at a density of 6,000 cells/well in different test conditions containing DMEM/F12 with 10% FCS into a 96 well microtitre (Corning). At the end of the experiment a 50 µl MTT (1 mg/ml) solution was added to each well and the incubations

continued for an additional 4 hours. Viable cells turn the yellow color of the MTT reagent to a dark-blue color (formazan crystal). This product was then dissolved in 100 μ l of DMSO and the optical density was read at 560 nm in a microplate reader.

Cell Fractionation. Cells were harvested by trypsinization, washed with PBS, and incubated in hypotonic buffer [10 mM HEPES (pH 7.2), 10 mM KCl, 1.5 mM MgCl₂, 0.1 mM EDTA, 2 μ g/ml leupeptin and aprotinin, 200 μ M Na₃VO₄, 1 mM PMSF, and 10 mM NaF] for 30 min at 4°C. The swollen cells were next homogenized in a Dounce homogenizer with 30 strokes and centrifuged at 12,000 x *g* for 10 min at 4°C. The supernatant was removed and labeled as "cytoplasmic" fraction. The nuclear pellet was washed once in hypotonic buffer, lysed with Triton X lysis buffer [10 mM Tris (pH 7.5), 150 mM NaCl, 5 mM EDTA, 1% Triton X-100, 2 μ g/ml leupeptin and aprotinin, 200 μ M Na₃VO₄, 1 mM PMSF, and 10 mM NaF], sonicated for 1 min in a water bath sonicator (Fisher Scientific), and incubated for 30 min at 4°C. The lysate was centrifuged at 12,000 x *g* for 10 min at 4°C; the supernatant was labeled as "nuclear" fraction.

Immunoblotting and Immunoprecipitation. Cells were lysed in 1X lysis buffer (20mM Tris pH 7.5; 150mM NaCl; 1mM EDTA; 1mM EGTA; 1% Triton X-100; 2.5 mM sodium pyrophosphate; 1mM β -glycerolphosphate; 1 mM Na₃VO₄; 1 μ g/ml leupeptin; 0.1mM PMSF) and protein concentration was measured using BCA dye (Pierce). For immunoblot analysis, total protein (30 μ g to 50 μ g) from cell lysates was resolved on SDS-PAGE followed by transfer to nitrocellulose membrane. The membranes were incubated with specific antibodies according to manufacturer's instruction. Detection of antigen-bound antibody was performed with the

enhance chemiluminescence reagent. For immunoprecipitations, 250µg of protein from whole cell lysates was incubated overnight with primary antibody/protein A/G Sepharose (Oncogene Science) at 4°C while rocking. The precipitates were washed three times with ice-cold PBS, re-suspended in 3X SDS Sample buffer and resolved using SDS-PAGE followed by immunoblot analysis.

Immunofluorescence and Immunohistochemistry (IHC). Cells were grown in eight well chamber slides until 80% confluence and fixed by 4% paraformaldehyde for 10 min at 4°C followed by incubation with 100% methanol for 20 min at -20°C. IHC was performed by incubated with antibody to HER2/neu (NCL-L-CB11, dilution 1:40; Novocastra Laboratories, UK) for 1 hr. Immunostaining was performed using ABC kit (PK-6200, Vector Laboratories, Burlingame, CA) followed by DAB kit (SK-4100, Vector Laboratories) according to the manufacturer's instruction. The immunofluorescence analysis was performed by incubating the cells (10^6 cells) with 20µl anti-HER2/neu fluorescence-conjugated monoclonal antibody (Cat# 340553, Becton Dickinson, CA) for 30 min at room temperature in dark. The cells were washed with 1X PBS and fixed with 1% paraformaldehyde. A 100µl cell suspension was used for preparing cytopsin slide. The slides were mounted with VECTASHIELD mounting medium with propidium iodide (Cat# H-1300, Vector Laboratories, CA) and viewed under a fluorescence microscope. The cells with positive staining were counted in five different areas and adjusted with total number of cells.

Statistical analysis. The values were expressed as mean±SD and/or fold change. The statistical significances of mean values among different cell lines were determined by one-way

ANOVA first, then by Student t test, and the fold changes were analyzed by χ^2 test. P-value \leq 0.05 was considered significant for ANOVA and χ^2 test. P-Value \leq 0.01 was considered significant for Student t test.

Results

An association between expression of HER2 and expression of pAkt in breast tumor cell lines. As shown in figure 1A, SKBR3, and BT474 cells express large amounts of the HER2/neu receptor protein. These cells also show significantly high levels of constitutive active or phosphorylated Akt (pAkt). There is no significant difference in total Akt expression between these cell types. MDA-MB231, MCF7, and T47D cells express low levels or almost undetectable levels of HER2 and pAkt. These cells however, express similar amounts of total Akt as the HER2 over-expressing cells.

To examine the regulation of PI3-kinase/Akt pathway in HER2/neu over-expressing breast cancer cells we induced SKBR3 cells with Heregulin (HRG). Although HRG is a ligand of HER3 and HER4, no direct ligand has been identified for HER2 receptor. There is evidence clearly showing that heterodimerization of HER2 with other family members can be mediated by ligands for HER3/4 receptor, HRG or for EGF receptor, EGF and lead to an efficient signaling complex that can promote enhanced PI3-kinase signal transduction pathway (33). Figure 1B demonstrated that HRG induces phosphorylation of HER3 receptor, formation of HER3/HER2 protein complex, and further phosphorylates HER2 receptor in SKBR3 cells. The pAkt and pGSK-3 β were also induced by HRG, while total Akt was not altered (figure 1C). The increased pAkt and pGSK-3 β were partially inhibited by the PI3-kinase inhibitors, LY294002 and completely blocked by Wortmannin (figure 1C).

Generate and characterize transfectants containing active Akt1 (myrAkt1) and dominant negative Akt1 (mutant K179M that is kinase-dead Akt1). The elevated Akt1 kinase activity has been shown to be important for development and/or proliferation of a subset of human cancers including breast cancer (28). Several laboratories have employed either

transient Akt transfection (34) or stably transfected Akt cell models. In order to understand the mechanisms associated with increased Akt1 in HER2/neu over-expressing cells, we created stable cell transfectants with either myrAkt1 (active Akt1), or K179M (dominant negative mutant) Akt1 (DNAkt1). The empty vector, pUSEamp(+) was also transfected. Since both myrAkt1 and K179M Akt1 contain the Myc-His tag, we first confirmed the presence of Myc-Tag in each clone by RT-PCR with primers specific for Myc-His tag and immunohistochemical analysis with antibody specific against Myc-His tag (data not shown), then followed by using PCR with primers specific for MyrAkt1 or K179M Akt1. Figure 2A shows representative examples of a few clones.. The presence of the dominant negative Akt1 mutant K179M Akt1 with nt 1460 AAG changed to ATG was further confirmed with sequence analysis (Figure 2B). All vector transfectants were confirmed by western blotting with anti-neomycin antibody (data not shown). We obtained 15 clones of myrAkt1 transfectants, 12 clones of K179M transfectants and 8 clones of vector transfectants. The myrAkt1 positive-transfectants confirmed were 4 and K179M positive-transfectants were 6. We also identified 5 positive vector transfectants. For the positive myrAkt1 and K179M Akt1 transfectants we also used quantitative real-time RTPCR (Q-RTPCR) with primer Akt1 to measure the gene expression and adjusted with 18S. Figure 2C shows Akt1 expression was increased almost 7 fold in SKBR3 transfected with myrAkt1 (SKBR3/AA28) than with vector (SKBR3/V33). After confirming Akt1 gene expression, protein level of Akt1 expression was analyzed by western blot analysis with antibodies against pAkt (Ser473) and Akt for all positive clones. Figure 2D shows representation of a few SKBR3 transfectants. SKBR3 transfected with myrAkt1 (SKBR3/AA28, SKBR3/AA29 and SKBR3/AA9) showed a significant increase in pAkt (Ser473) compared with vector (SKBR3/V33) or K179M transfectants (SKBR3/DN8 and SKBR3/DN9) but did not change in

total Akt expression (figure 2D). For all subsequent experiments in this study we tested transfectants SKBR3/AA28, SKBR3/AA29, SKBR3/DN8, SKBR3/DN9, SKBR3/V28, and SKBR3/V33. The following data are shown only for SKBR3/AA28, SKBR3/DN9, and SKBR3/V33.

Characterization of the phenotypes for cells expressing active or dominant negative Akt1. Once the stably transfected clones were isolated and confirmed, we conducted a series of tests to characterize the phenotype of the transfectants. *Cell growth:* As shown in figure 3A, in comparison to vector transfected cells, SKBR3/V33; SKBR3/AA28, and SKBR3/AA29 cells transfected with the active Akt1 showed significant stimulation in growth after 3 days. In contrast, the dominant negative K179M clones, SKBR3/DN9 and SKBR3/DN6 had significant lower growth than SKBR3/V33. In a similar study where growth was measured over a 5-day period, we observed that in comparison to SKBR3/V33 and SKBR3/DN9, SKBR3/AA28 had the highest growth rate (figure 3B).

Next, we compared growth rates of SKBR3/AA28, SKBR3/DN9, and SKBR3/V33 in serum-containing and serum-free growth media. Over a 5-day growth period, SKBR3/V33 and SKBR3/DN9 had a 2-fold increase of growth in normal serum (10%FCS)-containing media; however, the growth in SKBR3/V33 and SKBR3/DN9 did not change in serum-free media. In contrast to SKBR3/V33 and SKBR3/DN9, SKBR3/AA28 cells had a 3.5 fold increase of growth in normal serum-containing medium, and maintained active growth in serum-free media over 5 days. Western blot analysis in figure 3C demonstrated increase in pAkt in the rapidly growing SKBR3/AA28 cells. There was no significant change in the levels of total Akt among SKBR3/V33, SKBR3/AA28, and SKBR3/DN9.

Inhibition of cell proliferation with Herceptin in SKBR3 cells was affected by Akt1.

Our data clearly indicate that Herceptin down-regulates HER2/neu mRNA level (figure 4A), as well as the cytoplasmic and plasma membrane associated HER2/neu protein (figure 4B). The cell growth of SKBR3 was significantly inhibited when treated with Herceptin for 5 days (figure 4C). Next, we examined if SKBR3 cells transfected with active Akt1 (SKBR3/AA28) or dominant-negative Akt1 (SKBR3/DN9) would respond to Herceptin in a similar or different manner. The SKBR3/V33, SKBR3/AA28, and SKBR3/DN9 were treated with Herceptin at 10 μ g/ml for 7 days, and MTT assay was performed on days 2, 3, 5, and 7. In comparison to the SKBR3/V33 and SKBR3/DN9 cells, the anti-proliferation potential of Herceptin decreased significantly over the first 3 days of treatment in cells transfected with active Akt1 (SKBR3/AA28). As shown in figure 4D, during the first 2 to 3 days of Herceptin treatment, the cell growth in SKBR3/V33 was inhibited by 28% to 30%, but less than 10% in SKBR/AA28 cells. In contrast, SKBR3/DN9 demonstrated increased response to Herceptin. Herceptin inhibits cell growth in SKBR3/DN9 up to 42% after 3 days treatment (Figure 4D). Similarly, the cell growth in SKBR3/V33 and SKBR3/DN9 was inhibited more than 40% when treated with PI3-kinase inhibitor, LY294002, however in SKBR3/AA28 was only inhibited 20% (figure 4E). Meanwhile, we tested the effect of Herceptin in combination with LY294002 on cell proliferation. The inhibitory effect of Herceptin on cell proliferation was enhanced significantly by combination treatment with LY294002 (figure 4E).

Effect of Herceptin on PI3-kinase/Akt pathway. Our data clearly indicate that inhibiting the PI3-kinase in SKBR3 cells enhanced anti-proliferation effects of Herceptin. We therefore examined which cell signaling molecules might be involved in this process. Data in figure 5A demonstrate that Herceptin at 10 μ g/ml down-regulated pAkt, pGSK-3 β and cyclinD1

expression in SKBR3 cells after 72 hours of treatment. Figure 5A also shows that once pAkt was up-regulated upon stimulation with Heregulin (HRG), Herceptin was unable to down-regulate the increase in pAkt, pGSK3 β , and cyclin D1. Effect of Herceptin on pAkt and downstream cell signaling in SKBR3/V33 was similar to SKBR3 parental cells (figure 5A). Since the effect of Herceptin on cell proliferation in HER2/neu over-expressing cells transfected with active Akt1 was very little. Herceptin did not further down-regulate the level of pAkt, pGSK-3 β and cyclin D1 in the active Akt1-transfected SKBR3/AA28 cells after 72 hrs treatment (figure 5A). In contrast, SKBR3/DN9 was highly responsive to Herceptin, with respect to down-regulation of pAkt, pGSK-3 β , and cyclin D1 (figure 5A). In summary, data from figure 5A suggest that if active Akt1 is over-expressed in HER2/neu over-expressing cells, these cells become less sensitive to Herceptin treatment. Conversely, if HER2/neu over-expressing cells were transfected with dominant-negative Akt1, these cells become more sensitive to Herceptin treatment.

With these findings we next examined if PI3-kinase and Akt inhibitors could down-regulate the level of pAkt in SKBR3/AA28. Figure 5B demonstrated that neither LY294002 nor Wortmannin can inhibit the level of pAkt in the active Akt1-transfected SKBR3/AA28 cells. The Akt/protein kinase B signaling inhibitor-2 (API-2) has been reported to be a highly selective inhibitor of Akt signaling in human tumor cells with aberrant Akt, leading to decrease in cell growth and induction of apoptosis (35). As shown in figure 5B, API-2 significantly inhibited pAkt expression in SKBR3/AA28 (figure 5B). The total Akt remained similar in SKBR3/AA28 with and without treatment (figure 5B).

Our data confirm that HER2/neu activation results in the activation of the PI3-kinase/Akt pathway, regulates cell cycle protein cyclinD1, and induces cell proliferation. The p27^{kip1}, a

member of the Kip family of cyclin-dependent kinase (Cdk) inhibitors, plays an important role in cell cycle arrest (36). Cytoplasmic translocation of p27^{kip1} has been increasingly recognized to be associated with an aggressive phenotype of tumors, whereas nuclear expression confers a more favorable outcome (37). As shown in figure 5C, p27^{kip1} expression was present in both nuclear and cytoplasm in SKBR3/V33 and SKBR3/DN9 cells; however, the p27^{kip1} was exclusively in the cytoplasmic localization in SKBR3/AA28 cells. It has been shown that Herceptin suppresses the HER2/neu over-expressing breast cancer cells growth through induction of G1 arrest associated with upregulation of p27^{kip1} (38, 39). Our data further confirmed the role of Akt1 in this process, which could be associated with cytoplasmic retention and nuclear export (34, 37, 40).

Next, we asked the question if Herceptin could decrease the HER2/neu mRNA and protein levels in the active Akt1 transfected cells as much as in the non-transfected cells. Figure 5D shows that the basic level of HER2/neu mRNA was increased by 6 fold in SKBR3/AA28 compared with the level in SKBR3/V33. Although after 3 days of treatment, Herceptin effectively decreased the HER2/neu mRNA level in SKBR3/AA28, the level of mRNA in SKBR3/AA28 was still 1.6 fold higher than in SKBR3/V33 and 2 fold higher than in SKBR3/DN9. The increased mRNA level of HER2/neu in active Akt1-transfected SKBR3 cells could make the cells become more aggressive and less sensitive to Herceptin treatment.

Inhibition of HER2/neu with shHER2 downregulates Akt expression in SKBR3 cells. Faltus et al (41) have demonstrated that silencing of the HER2/neu gene by siRNA inhibits proliferation and induces apoptosis in HER2/neu over-expressing breast cancer cells. Using a similar approach we transfected the shHER2 into SKBR3 and SKBR3/AA28 cells. As expected,

shHER2 down-regulated HER2/neu mRNA level after 72 hrs transfection in both SKBR3 and SKBR3/AA28 (figure 6A). The shHER2 also decreased HER2 extracellular membrane receptor in SKBR3 and SKBR3/AA28 (figure 6B and 6C). Next we compared Akt1 mRNA level in SKBR3 and SKBR3/AA28 after silencing of the HER2/neu gene. Figure 6D shows that shHER2 down-regulated Akt1 mRNA level by 60% in SKBR3 and only 30% in SKBR3/AA28 which expresses active Akt1. As shown in figure 5A, Herceptin did not affect the level of pAkt in SKBR3/AA28 after 72 hrs treatment. However, the shHER2 was able to down-regulate pAkt level in SKBR3/AA28 at the same level as in SKBR3 cells after 72 hr transfection (figure 6E and 6F). These data demonstrate that similar to the Herceptin effect, shHER2 downregulated HER2 mRNA and protein levels and inhibits pAkt protein expression in HER2/neu over-expressing SKBR3 cells. In addition shHER2 also down-regulated pAkt level in SKBR3/AA28 cells, which over-expresses HER2/neu and Akt1.

Discussion

In this study, we had proposed that activation of HER2 receptor in HER2/neu overexpressing tumors would result in the activation of the PI3-kinase pathway with increase in phosphorylation of Akt1 as well as its downstream targets, culminating in increase in cell cycle proteins such as cyclinD1 (34, 42). We believe that the constitutively activated PI3/Akt pathway will make certain HER2/neu overexpressing breast cancer cells, resistant to Herceptin treatment. Herceptin is designed to target the extracellular domain of the HER2/neu tyrosine kinase receptor and block its function (15). Herceptin can inhibit PI3/Akt pathway and induce cell apoptosis or anti-proliferation. However, if Akt has been constitutively activated in the HER2/neu positive tumor cells, targeting HER2/neu receptor with Herceptin, may not be enough to suppress HER2-mediated down-stream cell signaling and inhibit cell proliferation or induce cell apoptosis.

We have investigated the phenotype changes in HER2/neu over-expressing breast cancer cells with concurrent expression of active Akt1. We have focused on cell progression regulated by Akt1, and whether Herceptin alone or in combination with PI3-kinase inhibitors, LY294002 or Wortmannin, could better inhibit this signal transduction pathway in HER2/neu over-expressing breast cancer cells. Our results demonstrate that expression of Myr-Akt1 in HER2/neu over-expressing breast cancer cells led to a more aggressive phenotype with respect to cell growth. This increase in growth could be sustained in the absence of serum (figure 3). Furthermore, the Myr-Akt1 transfected cells showed increased HER2/neu mRNA levels compared with parent cells without myr-Akt1 expression (figure 5D). This observation is fairly novel, and suggest that increase in activated Akt1 may have transcriptional influence on HER2/neu gene expression.

Our data confirmed that Herceptin treatment can decrease HER2/neu mRNA and the corresponding HER2/neu extracellular membrane receptor levels (figure 4A and 4B). Herceptin treatment also decreased the levels of pAkt, and pGSK-3 β , resulting in down-regulation of cyclin D1 and inhibition of cell proliferation in SKBR3 cells (figure 5). Herceptin, however, was not able to modulate pAkt, pGSK-3 β , and cyclin D1 levels in SKBR3/AA28 that had activated Akt1 (figure 5A).

The phosphorylation of Akt involves cell cycle progression and cytoplasmic retention of the cyclin-dependent kinase inhibitors p21^{waf1} (43) and p27^{kip1} (34, 37, 38). Nuclear expression of p27^{kip1} confers a more favorable outcome (37); therefore, the cytoplasmic translocation of p27^{kip1} in SKBR3/AA28 (figure 5C) may further indicate the aggressive phenotype of these cells and partially explain the diminished response to Herceptin in SKBR3/AA28 than that in SKBR3/V33 and SKBR3/DN9 (figure 4D). Inhibition of PI3-kinase by LY294002 increased Herceptin suppressing cell growth in both normal and active Akt1 expressing cell (figure 4E). However, the PI3-kinase inhibitors, LY294002 and Wortmannin, failed to down-regulate the pAkt in SKBR3/AA28 that has been stable transfected with myr-Akt1 (figure 5B).

Besides PI3-kinase inhibitors, we also examined the effect of Akt/protein kinase B inhibitor-2 (API-2) on inhibition of pAkt in HER2/neu over-expressing cells with activation of Akt1. The API-2 (NCI identifier, NSC 154020) was first identified to inhibit cell growth in Akt2-transformed but not empty vector LXSIN-transfected NIH3T3 cells (44, 45). Later it was shown to suppress pAkt level without inhibition of PI3-kinase (35). API-2 also has been reported to suppress EGF-induced kinase activity and phosphorylation of Akt1, AKT2, and AKT3 in HEK293 cells transfected with hemagglutinin (HA)-Akt1, HA-AKT2, and HA-AKT3 (Yang et al., 2004). Here, we report that API-2 inhibits pAkt expression significantly in

SKBR3/AA28 that is myr-Akt1 transfected breast cancer cells with HER2/neu over-expression (figure 5B).

Transfection with HER2/neu-specific siRNA (siHER2) in HER2/neu over-expressing breast cancer cells can result in a sequence-specific decrease in HER2/neu mRNA as well as protein levels (41). Silencing of the HER2/neu gene by siRNA demonstrated inhibition of proliferation and induction of apoptosis in HER2/neu over-expressing breast cancer cells (41). Using a similar approach, we transfected shHER2 in SKBR3 and SKBR3/AA28 cells. The shHER2 inhibited HER2/neu mRNA and protein levels; followed by down-regulation of pAkt in a similar manner to Herceptin treatment in SKBR3 cells (figure 6). Compared with Herceptin, shHER2 demonstrated a more robust effect on down-regulation of HER2/neu with a further decrease in pAkt level in active Akt1 expressing cells, SKBR3/AA28. This effect could not be achieved by Herceptin alone (figure 5A and 6E).

Next we examined the effect of Herceptin in HER2/neu over-expressing cells, but had been transfected with dominant-negative Akt1 (K179M). Our data demonstrated that SKBR3 cells transfected with dominant-negative Akt1 (SKBR3/DN) showed less aggressive phenotype and rapid response to Herceptin treatment.

Yakes and colleagues have shown that increase in Akt activity following adenoviral infection of Myr-Akt1 prevented Herceptin-induced cytostasis of BT474 cells and apoptosis in SKBR3 cells (34). In our study, SKBR3 cells with stable transfection of the myr-Akt1 gene demonstrated increased expression of constitutively active Akt1, resulting in an abrogation of the anti-proliferative effects of Herceptin. The inhibition of cell growth and down-regulation of phospho-GSK-3 β by Herceptin was attenuated in cells with constitutively activated Akt1. The

cells transfected with dominant-negative Akt1 can restore the inhibitory effect of Herceptin on cell growth and proliferation (figure 3, 4D, and 5A).

One of the novel finding in this study is that in comparison to Herceptin, shHER2 can effectively down-regulate pAkt in the cells expression myr-Akt1 (figure 6E). Hence, for development of target therapy against HER2/neu over-expressing breast cancers with activated Akt1, application of RNA interference targeting HER2/neu, gene may be another promising strategy.

In this study we report for the first time that the activation of Akt1 in HER2/neu over-expressing SKBR3 cells, leads to an increase in HER2/neu mRNA expression (figure 5D). Although, Herceptin treatment decreased the HER2/neu mRNA expression in SKBR3/AA28 cells, the level of HER2/neu still remained higher than in SKBR3 cells with normal Akt1 expression. Our studies suggest that activation of Akt in HER2/neu over-expressing cells may contribute to increase in mRNA and protein levels for HER2/neu and consequently lead to resistance to treatment.

In summary, our data confirm that Herceptin can inhibit the growth of HER2/neu over-expressing breast cancer cells by inhibiting the PI-3K/Akt pathway. However, in those tumors that over-expressed both HER2/neu and active Akt1, the tumor cells became more resistant to Herceptin treatment. Hence, treatment of these tumors should factor a target therapy that combines anti-HER2/neu and anti-Akt1 agents. In addition, use of use of RNA interference strategies against HER2/neu gene offers promising avenues.

Acknowledgments

Grant Support: NIH/NCI U56 CA101599-01 (J.V.V); CA15083-25S3 (J.V.V);
NIH/NIDDK R25 DK067015-01 (J.V.V); Department of Defense (BCRP) BC043180 (J.V.V);
MBRS, NIH SO6 GM0685-10-01 (Y.Wu).

References

1. Slamon DJ, Godolphin W, Jones LA, et al. Studies of the HER-2/neu proto-oncogene in human breast and ovarian cancer. *Science* 1989; 244:707-12.
2. Hynes NE, Stern DF. The biology of erB-2/neu/HER-2 and its role in cancer. *Biochim Biophys Acta* 1994; 1198:165-84.
3. Ravdin PM, Chamness GC. The c-erbB-2 proto-oncogene as a prognostic and predictive marker in breast cancer: A paradigm for the development of other macromolecular markers – A review. *Gene* 1995; 159:19-27.
4. Yusa K, Sugimoto Y, Yamori T, et al. Low metastatic potential of clone from murine colon adenocarcinoma 26 increased by transfection of activated c-erbB-2 gene. *J Natl Cancer Inst* 1990; 82:1633-6.
5. Yu DH, Hung MC. Expression of activated rat neu oncogene is sufficient to induce experimental metastasis in 3T3 cells. *Oncogene* 1991; 6:1991-6.
6. Yu D, Wang SS, Dalski KM, et al. c-erbB-2/neu over-expression enhances metastatic potential of human lung cancer cells by induction of metastasis-associated properties. *Cancer Res* 1994; 54:3260-6.
7. Wu Y, Khan H, Chillar R, Vadgama JV. Prognostic value of plasma HER-2/neu in African American and Hispanic women with breast cancer. *International J of Oncology* 1999; 14:1021-37.
8. Rosen PP, Lesser ML, Arroyo CD, Cranor M, Borgen P, Norton L. Immunohistochemical detection of HER-2/neu in patients with axillary lymph node negative breast carcinoma. A study of epidemiologic risk factors, histologic features, and prognosis. *Cancer* 1995; 75:1320-26.

9. Carlomagno C, Perrone F, Gallo C, et al. c-erbB2 over-expression decreases the benefit of adjuvant tamoxifen in early stage breast cancer without axillary lymph node metastases. *J Clin Oncol* 1996; 14:2702-8.
10. Ross JS, Fletcher JA. The HER2/neu oncogene in breast cancer: prognostic factor, predictive factor, and target for therapy. *Stem Cells* 1998; 16:413-28.
11. Paik S, Bryant J, Park C, et al. erbB-2 and response to doxorubicin in patients with axillary lymph node-positive, hormone receptor-negative breast cancer. *J Natl Cancer Inst* 1998; 90:1361-70.
12. Ravdin PM, Green S, Albain V. Initial report of the SWOG biological correlative study of c-erbB2 expression as a predictor of outcome in a trial comparing adjuvant CAF-T with tamoxifen (T) alone. *Proc Am Soc Clin Oncol* 1998; 17: 97A.
13. Thor AD, Berry DA, Budman DR, et al. erbB-2, p53, and efficacy of adjuvant therapy in lymph node-positive breast cancer. *J Natl Cancer Inst* 1998; 90:1346-60.
14. Muss H, Berry D, Thor A. Lack of interaction of tamoxifen use and erbB2/HER-2/neu expression in CALGB 8541: a randomized adjuvant trial of three different doses of cyclophosphamide, doxorubicin and fluorouracil in node positive primary breast cancer. *Proc Am Soc Clin Oncol* 1999; 1999: 68A.
15. Sliwkowski MX, Schaefer G, Akita RW, et al. Co-expression of erbB2 and erbB3 proteins reconstitutes a high affinity receptor for heregulin. *J Biol Chem* 1994; 269:14661-5.
16. Baselga J, Tripathy D, Mendelsohn J, et al. Phase II study of weekly intravenous recombinant humanized anti-p185HER2 monoclonal anti-body in patients with HER2/neu-over-expressing metastatic breast cancer. *J Clin Oncol* 1996; 14:737-44.

17. Slamon DJ, Leyland-jones B, Shak S, et al. Use of chemotherapy plus a monoclonal antibody against HER2 for metastatic breast cancer that over-expresses HER2. *N Engl J Med* 2001; 344:783-92.
18. Cobleigh MA, Vogel CL, Tripathy D, et al. Multinational study of the efficacy and safety of humanized anti-HER2 monoclonal antibody in women who have HER-2 over-expressing metastatic breast cancer that has progressed after chemotherapy for metastatic disease. *J Clin Oncol* 1999; 17:2639-48.
19. Seidman AD, Fomier M, Esteva FJ, et al. Weekly trastuzumab and paclitaxel therapy for metastatic breast cancer with analysis of efficacy by HER2 immunophenotype and gene amplification. *J Clin Oncol* 2001; 19:2587-95.
20. Bange J, Zwick E, Ullrich A. Molecular targets for breast cancer therapy and prevention. *Nat Med* 2001; 7:548-52.
21. Esteva FJ, Valero V, Booser D, et al. Phase II study of weekly docetaxel and trastuzumab for patients with HER-2-over-expressing metastatic breast cancer. *J Clin Oncol* 2002; 20:1800-8.
22. Vivanco I, Sawyers CL. The phosphatidylinositol 3-kinase-Akt pathway in human cancer. *Nature Reviews* 2002; 2: 489-501.
23. Vogel CL, Cobleigh MA, Tripathy D, et al. Efficacy and safety of trastuzumab as a single agent in first-line treatment of HER2-over-expressing metastatic breast cancer. *J Clin Oncol* 2002; 2:719-26.
24. Kono K, Sato E, Naganuma H, et al. Trastuzumab (Herceptin) enhances class I-restricted antigen presentation recognized by HER-2/neu-specific T cytotoxic lymphocytes. *Clin Cancer Res* 2004; 10:2538-44.

25. Cuello M, Ettenberg SA, Clark AS, et al. Down-regulation of the erbB-2 receptor by trastuzumab (herceptin) enhances tumor necrosis factor-related apoptosis-inducing ligand-mediated apoptosis in breast and ovarian cancer cell lines that over-express erbB-2. *Cancer Res* 2001; 61:4892-4900.
26. del Peso L, Gonzalez-Garcia M, Page C, Herrera R, Nunez G. Interleukin-3-induced phosphorylation of BAD through the protein kinase Akt. *Science* 1997; 278:687-9.
27. Brunet A, Bonni A, Zigmond MJ, et al. Akt promotes cell survival by phosphorylating and inhibiting a Forkhead transcription factor. *Cell* 1999; 96:857-68.
28. Sun M, Wang G, Paciga JE, et al. Akt1/PKBalpha kinase is frequently elevated in human cancers and its constitutive activation is required for oncogenic transformation in NIH3T3 cells. *Am J Pathol* 2001; 159:431-7.
29. Perez-Tenorio G, Stal O and Southeast Sweden Breast Cancer Group. Activation of Akt/PKB in breast cancer predicts a worse outcome among endocrine treated patients. *Bri J Cancer* 2002; 86:540-5.
30. Tanner M, Kapanen AI, Junttila T, et al. Characterization of a novel cell line established from a patient with Herceptin-resistant breast cancer *Mol Cancer Ther* 2004; 3:1585-92.
31. Nahta R, Hung MC, Esteva FJ. The HER-2-targeting antibodies trastuzumab and pertuzumab synergistically inhibit the survival of breast cancer cells. *Cancer Res* 2004; 64:2343-46.
32. Wen X-F, Yang G, Mao W, et al. HER2 signaling modulates the equilibrium between pro- and antiangiogenic factors via distinct pathways: implications for HER2-targeted antibody therapy. *Oncogene* 2006;[Epub ahead of print]

33. Olayioye MA, Neve RM, Lane HA, Hynes NE. The ErbB signaling network: receptor heterodimerization in development and Cancer. *EMBO J* 2000; 19:3159-67.
34. Yakes FM, Chinratanalab W, Ritter CA, King W, Seelig S, Arteaga CL. Herceptin-induced inhibition of phosphatidylinositol-3 kinase and Akt is required for antibody-mediated effects on p27, cyclin D1, and antitumor action. *Cancer Res* 2002; 62:4132-41.
35. Yang L, Dan HC, Sun M, et al. Akt/protein kinase B signaling inhibitor-2, a selective small molecule inhibitor of Akt signaling with antitumor activity in cancer cells overexpressing Akt. *Cancer Res* 2004; 64:4394-99.
36. Sherr CJ, Roberts JM. CDK inhibitors: positive and negative regulators of G1-phase progression *Gene Dev* 1999; 13:1501-12.
37. Viglietto G, Motti MI, Fusco A. Understanding p27(kip1) deregulation in cancer: down-regulation or mislocalization. *Cell Cycle* 2002;1:394-400.
38. Le XF, Claret FX, Lammayot A, et al. The role of cyclin-dependent kinase inhibitor p27Kip1 in anti-HER2 antibody-induced G1 cell cycle arrest and tumor growth inhibition. *J Biol Chem* 2003; 278:23441-50.
39. Le XF, Pruefer F, Bast Jr RC. HER2-targeting antibodies modulate the cyclin-dependent kinase inhibitor p27Kip1 via multiple signaling pathways. *Cell Cycle* 2005; 4: 87-95.
40. Liang J, Zubovitz J, Petrocelli T, et al. PKB/Akt phosphorylates p27, impairs nuclear import of p27 and opposes p27-mediated G1 arrest. *Nat Med* 2002; 8:1153-60.
41. Faltus T, Yuan J, Zimmer B, et al. Silencing of the HER2/neu gene by siRNA inhibits proliferation and induces apoptosis in HER2/neu-overexpressing breast cancer cells. *Neoplasia*. 2004; 6:786-95

42. Diehl JA, Cheng M, Roussel MF, Sherr CJ. Glycogen synthase kinase-3beta regulates cyclin D1 proteolysis and subcellular localization. *Genes Dev* 1998;12:3499-511.
43. Zhou BP, Liao Y, Xia W, Spohn B, Lee MH, Hung MC. Cytoplasmic localization of p21Cip1/WAF1 by Akt-induced phosphorylation in HER-2/neu-over-expressing cells. *Nat Cell Biol* 2001; 3:245-52.
44. Cheng JQ, Altomare DA, Klein MA. Transforming activity and mitosis-related expression of the AKT2 oncogene:evidence suggesting a link between cell cycle regulation and oncogenesis. *Oncogene* 1997;14:2793-801.
45. West KA, Castillo SS, Dennis PA. Activation of the PI3K/Akt pathway and chemotherapeutic resistance. *Drug Resist Updat* 2002; 5:234-48.

FIGURE LEGENDS

Figure 1. Association of HER2/neu expression and Akt phosphorylation. (A) HER2/neu, pAkt and total Akt levels in MCF7, SKBR3, BT474 and T47D were measured by Western blotting with antibodies against HER2/neu, pAkt (ser473) and Akt. The densitometric levels of HER2/neu, pAkt and Akt were normalized to the corresponding levels of β -actin. The normalized pAkt levels were further adjusted with normalized Akt levels. The bar graphs show adjusted HER2/neu and pAkt levels in each cell line. (B) SKBR3 cells were growing in DMEM/F12 medium containing 10% FCS. After 70% confluence, the cells were changed to serum-free medium for overnight, and then incubated with HRG (1nM) for 20 min. The cells were lysed in cell lysis buffer and 100 μ g protein was immunoprecipitated with anti-HER3 antibody, and then immunoblotted with pTyr antibody (top). The blot was stripped and re-probed with anti-HER2 antibody (middle). The protein was also immunoprecipitated with anti-HER2 and then immunoblotted with pTyr (bottom). (C) SKBR3 cells were incubated with LY294002 or Wortmannin for 18 hrs and then induced with HRG for 20min. The levels of pAkt, Akt, and pGSK-3 β were measured by Western blotting and adjusted with β -actin shown in bar graphs.

Figure 2. Stable expression of Myr-Akt1 and K179M mutant Akt1 in SKBR3 cells. (A) SKBR3 cells were stable transfected with either Myr-Akt1 or K179M mutant Akt1 and selected under G-418. After two months of G-418 selection, RNA was isolated from each positive

transfectant, and analyzed by RT-PCR with primers specific for myc-tag (top panel), Myr-Akt1 (middle panel), and K179M mutant Akt1(dominant negative Akt1) (bottom panel). (B) A sequence from PCR product of positive K179M mutant Akt1 transfectants indicated that nt 1460 AAG was changed to ATG. (C) Relative expression of Akt1 gene level in vector, Myr-Akt1, and K179M Akt1 was quantified by real-time RTPCR and adjusted with reference gene (β -actin). Each bar presented the mean of three amplifications. (D) The levels of pAkt (ser473) in the transfectants were measured by Western blotting. The densitometric levels of pAkt were normalized to the corresponding levels of total Akt and are shown in the bar graph.

Figure 3. Growth characteristics of active Akt1 and dominant negative Akt1 transfected cells in normal growth medium and in serum free medium. (A) SKBR3 cells with active Akt1 transfection (AA28, AA31), dominant-negative transfection (DN6, DN9), and vector only (V33) were plated in 96 well tray at a density 6×10^3 cells per well in growth medium. After 3 days MTT assay was performed, and the optical density was read at 560nm by microplate reader. The bars represented mean of six determinations and standard deviation. The statistical significance was determined by student t test. (B) SKBR3 cells were growing in either complete growth medium (top) or serum-free medium (bottom), and MTT assay was performed on the indicated days. The rate of growth for each clone was compared with their corresponding growth at day 1 under the same growth conditions. (C) The levels of pAkt and total Akt in cells grown in medium containing 10% FCS or in serum-free medium were examined by Western blots analysis using antibodies against pAkt (Ser473) and total Akt. The densitometric levels of pAkt and total Akt of each cell line were first adjusted to the corresponding levels of β -actin

respectively. The adjusted pAkt levels were finally normalized to the corresponding adjusted levels of total Akt and are shown in the bar graph.

Figure 4. Effect of Herceptin on cell proliferation. (A) SKBR3 cells were treated with Herceptin (10 μ g/ml) for 3 days, and mRNA level of HER2/neu was measured by Q-RTPCR with primers HER2/neu and 18S. The bar graph indicated the fold change of HER2/neu mRNA level in Herceptin-treated cells compared with non-treated cells. The level was adjusted by 18S and each bar represents mean of three determinations. (B) SKBR3 cells were plated in 8 well growth chambers at 2000 cells/well, and treated with (b) or without (a) Herceptin for 4 days. The level of HER2/neu protein was determined by IHC with anti-HER2/neu antibody. The arrows indicated positive staining. (C) Five days cell growth in SKBR3 cells treated with or without Herceptin was measured by MTT assay. The bars indicated mean of 6 determinations and standard deviation. The statistical significance was determined by student's t test. (D) SKBR3/AA28, SKBR3/DN9, and SKBR3/V33 cells were incubated with Herceptin at indicated days and cell growth at each indicated days was determined by MTT assay. The growth rate of Herceptin-treated cells was compared with non-treated cells and represented as fold changes. Each value was mean of six determinations. The statistical significance was determined by student's t test. (E) The cells were either incubated with LY294002 or pre-incubated with LY294002 and then treated with Herceptin for the indicated days. The fold changes of cell growth in the treated cells compared with non-treated cells were determined by MTT assay. Each bar was mean of six determinations.

Figure 5. Effect of active Akt1 on Herceptin inhibition of HER2 signaling. (A) SKBR3 cells were either induced with HRG or transfected with active Akt1, dominant negative Akt1, or

vector only. The cells were treated with or without Herceptin for 72 hrs and the levels of pAkt, Akt, pGSK-3 β , and cyclin D1 in the cells were measured by Western blotting. (B) SKBR3/AA28 cells were treated with either Herceptin for 72hrs or with the indicated PI3-kinase inhibitors or API-2 for 24hrs. The levels of pAkt and Akt were measured by Western blotting. (C) The nuclear and cytoplasmic protein from SKBR3/V33, SKBR3/AA28 and SKBR3/DN9 was isolated as described in method section. The levels of p27^{kip} in cytoplasm (c) and nuclear (n) were determined by Western blotting with antibody for p27^{kip}. The antibody for tubulin was used to determine the separation of nuclear and cytoplasmic protein. (D) SKBR3/V33, SKBR3/AA28 and SKBR3/DN9 were treated with Herceptin for 3 days and HER2/neu mRNA levels in the cells were determined by Q-RT-PCR with primers for HER2/neu and 18S. The bars indicated fold changes of HER2/neu mRNA levels compared with untreated SKBR3/V33 cells. Each bar was mean of three determinations.

Figure 6. RNAi silences HER2/neu and down-regulates pAkt in SKBR3 and SKBR3/AA28.

The cells were transfected with either shHER2 or negative sequence (negative control) for 72 hrs. (A) The HER2/neu mRNA levels were measured by Q-RT-PCR with primer for HER2/neu and adjusted with 18S. The fold changes of HER2 mRNA level in the shHER2 transfected cells were compared with non-transfected cells and shown in bar graph. Each bar indicated mean of three determinations. (B) HER2/neu membrane receptor was determined by immunofluorescence analysis with FITC labeled anti-HER2/neu antibody, and the cell nucleus was labeled by propidium iodide (red). The arrows indicated the FITC labeled HER2/neu membrane receptor (green). (C) The cells with positive membrane labeling was counted in five different areas and adjusted with total number of cells. The bars indicated fold changes of cells

transfected with shHER2 or negative sequence compared with non-transfected cells. Each bar represents mean cell number of the five areas. (D) The level of Akt1 in the same transfected cells was determined by Q-RTPCR with primer for Akt1 and adjusted with 18S. The bar graph indicated the fold changes of Akt1 in transfected cells compared with non-transfected cells. Each bar represents mean of three different determinations. (E) The protein levels of pAkt, and Akt were measured by Western blotting with antibodies for pAkt at ser473 and total Akt. The antibody for β -actin was used as a loading control. The densitometric levels of pAkt and total Akt were first adjusted to β -actin, and then the adjusted pAkt levels were finally normalized to the adjusted levels of total Akt and are shown in the bar graph.

Akt level in relation to HER2/neu expression

Figure 1.

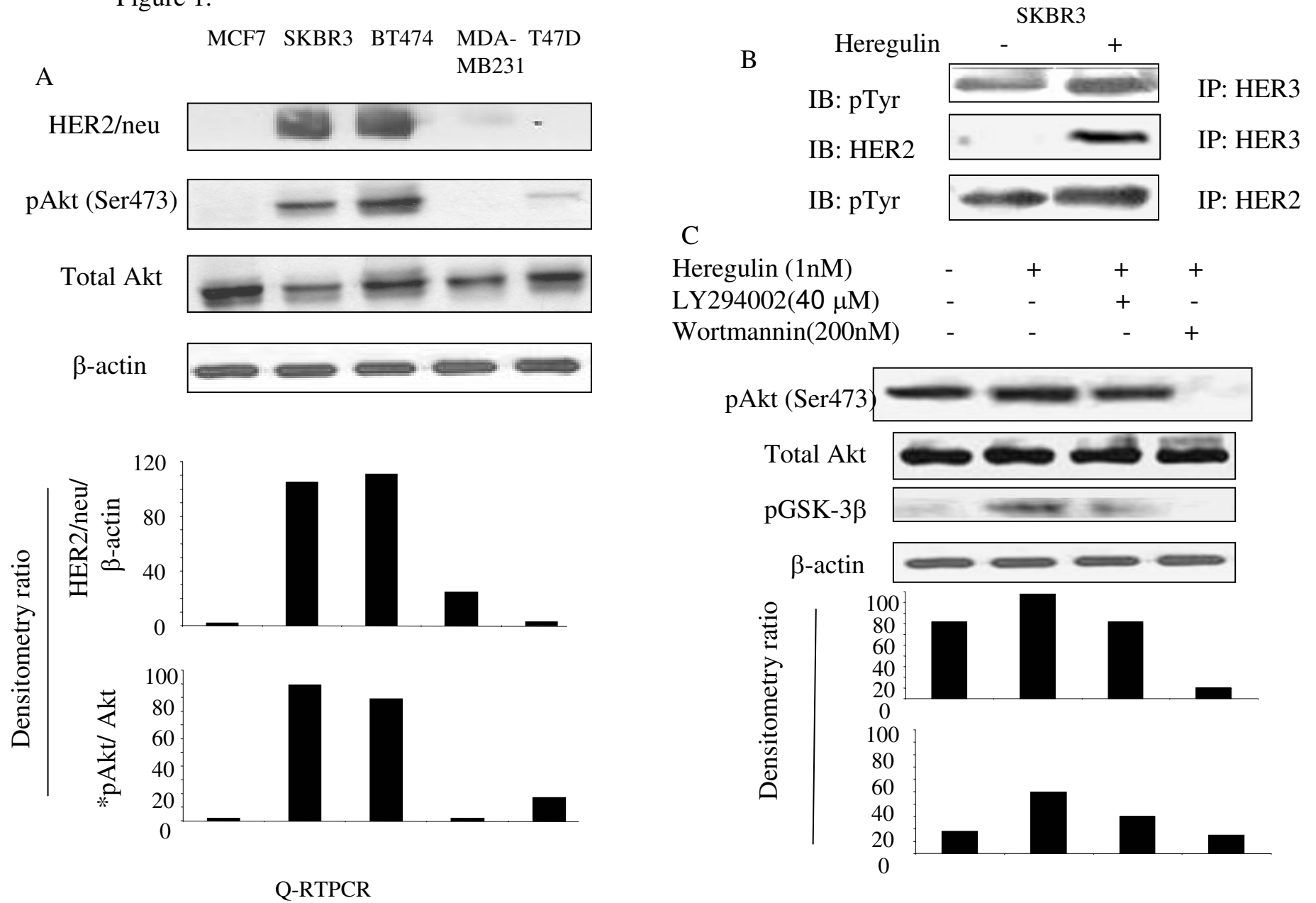


Figure 2. Stable expression of Myr-Akt1 and K179M mutant Akt1 transfectants

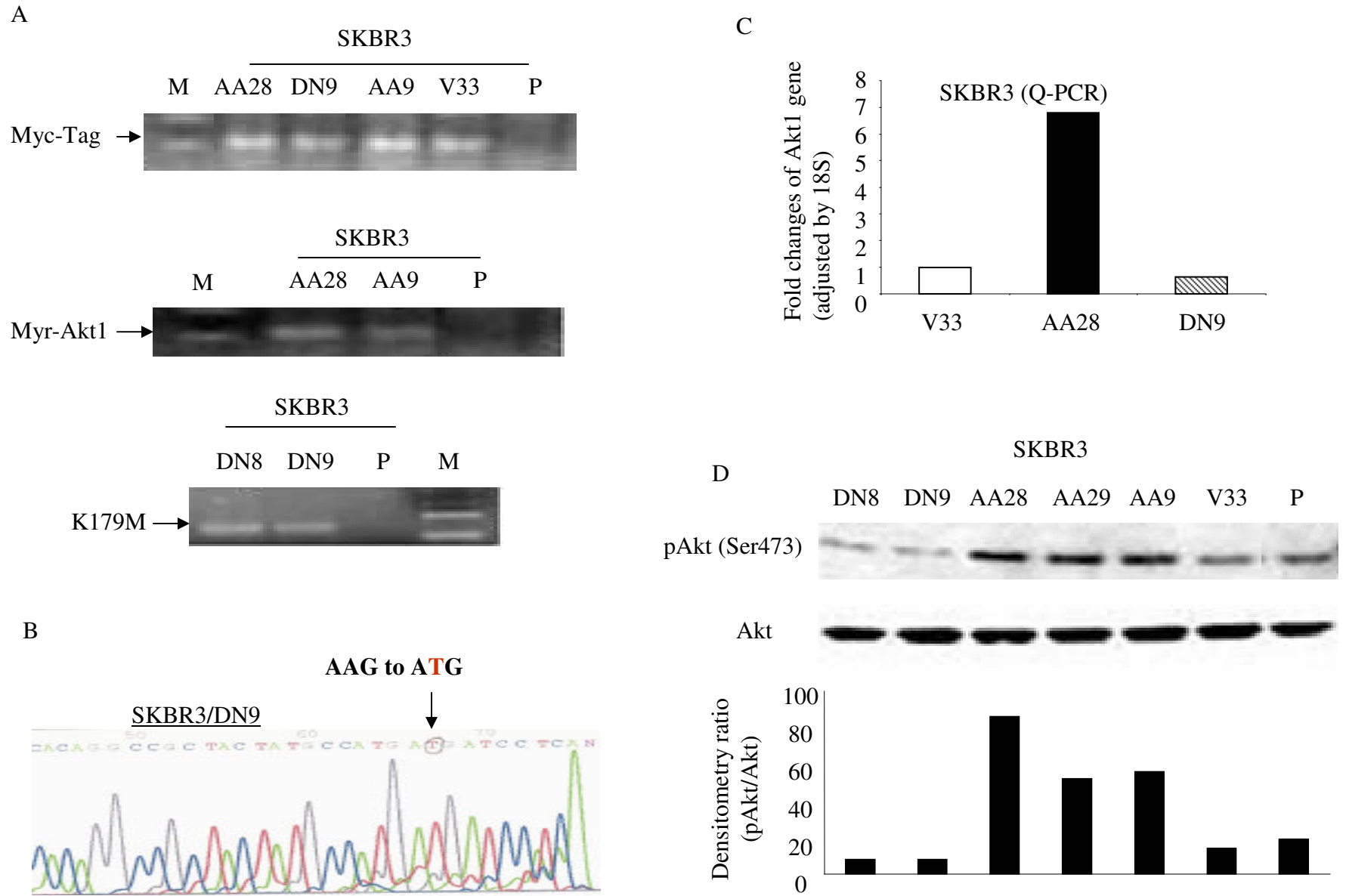


Figure 3

Active Akt1 expression change growth characteristics of SKBR3 cells

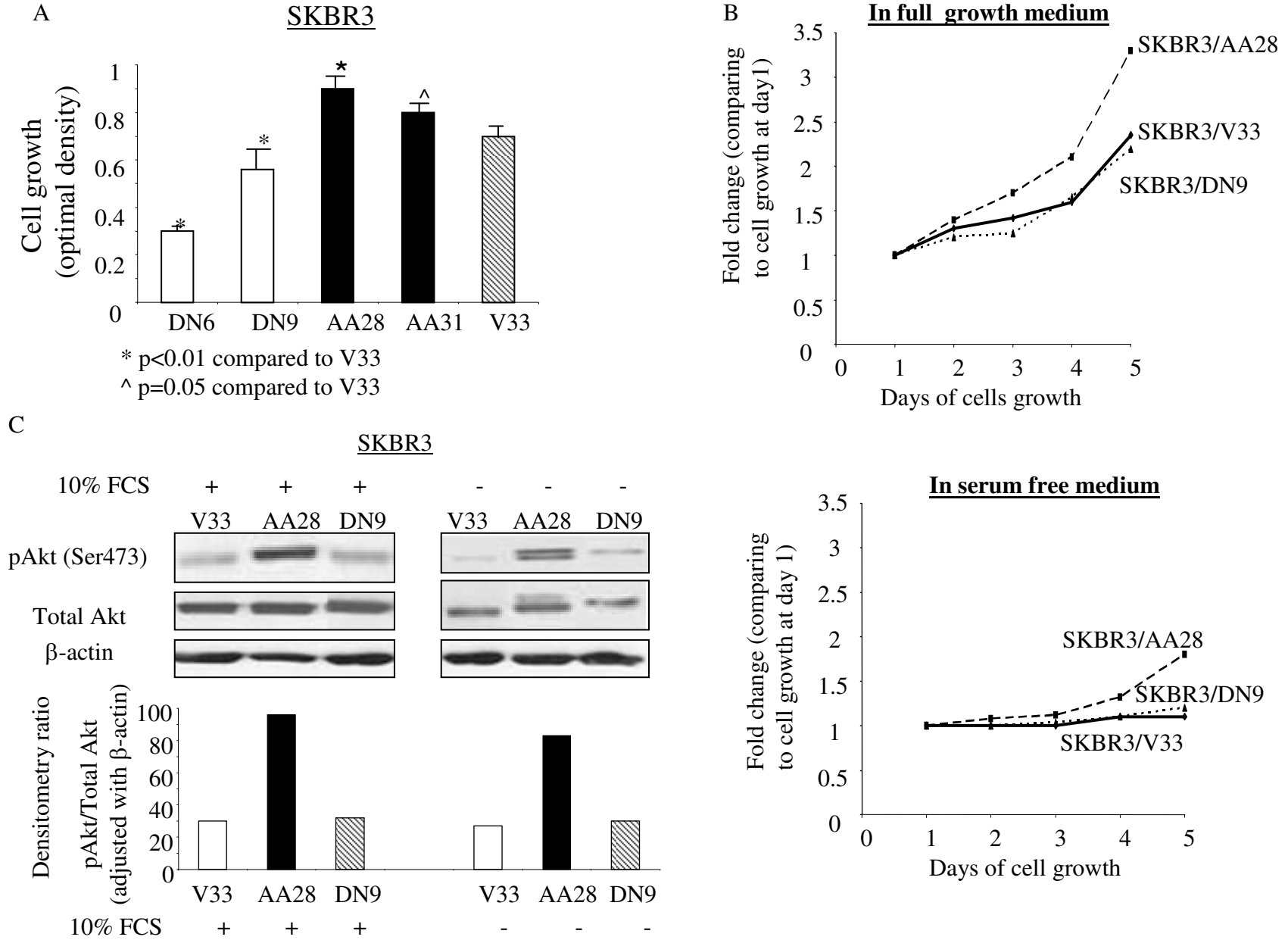


Figure 4

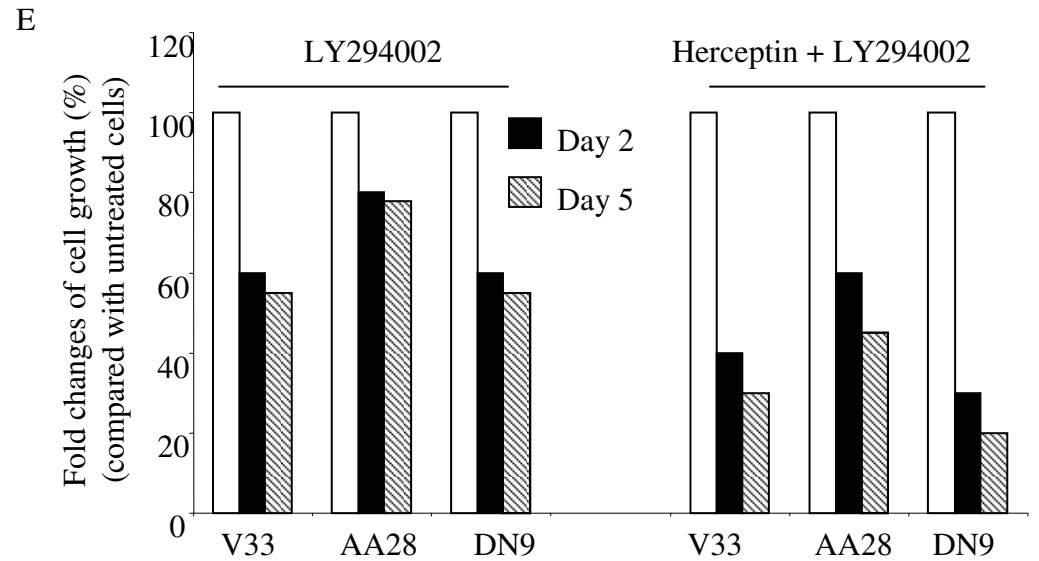
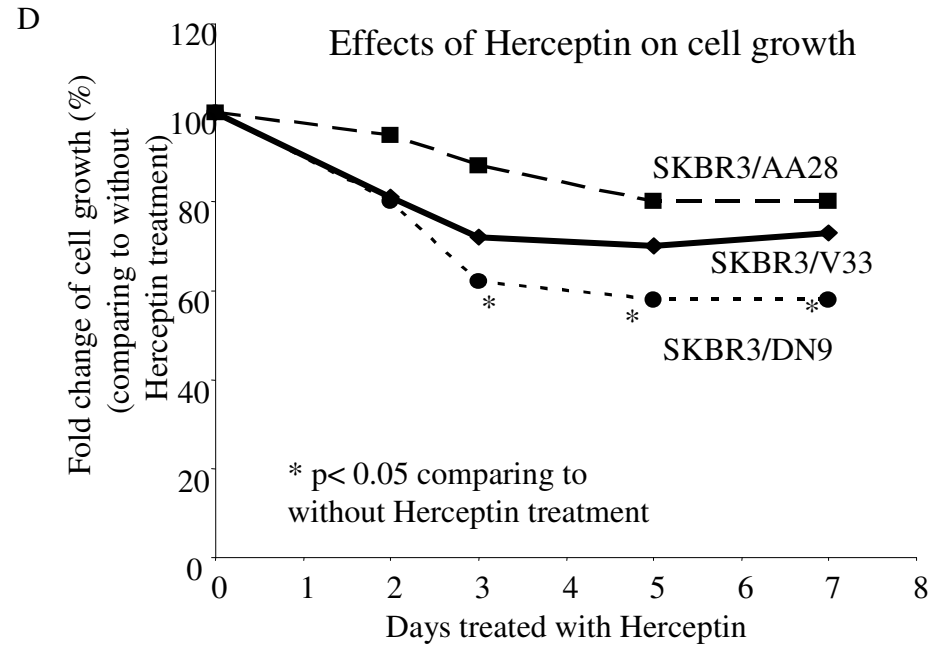
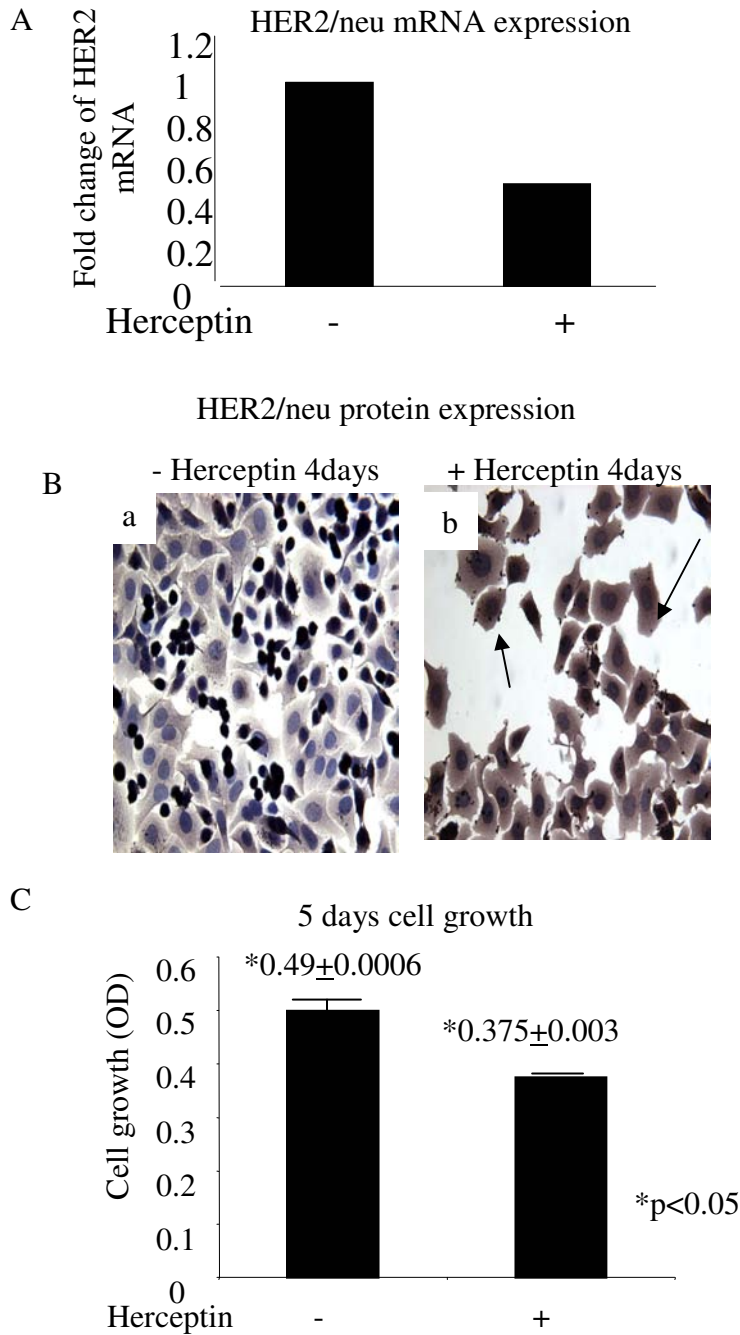
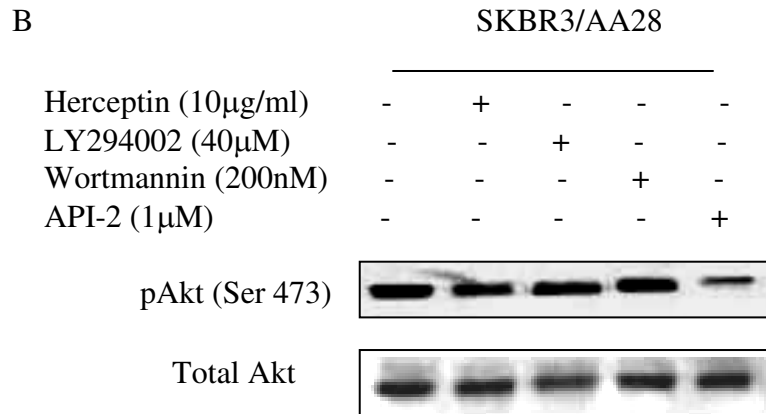
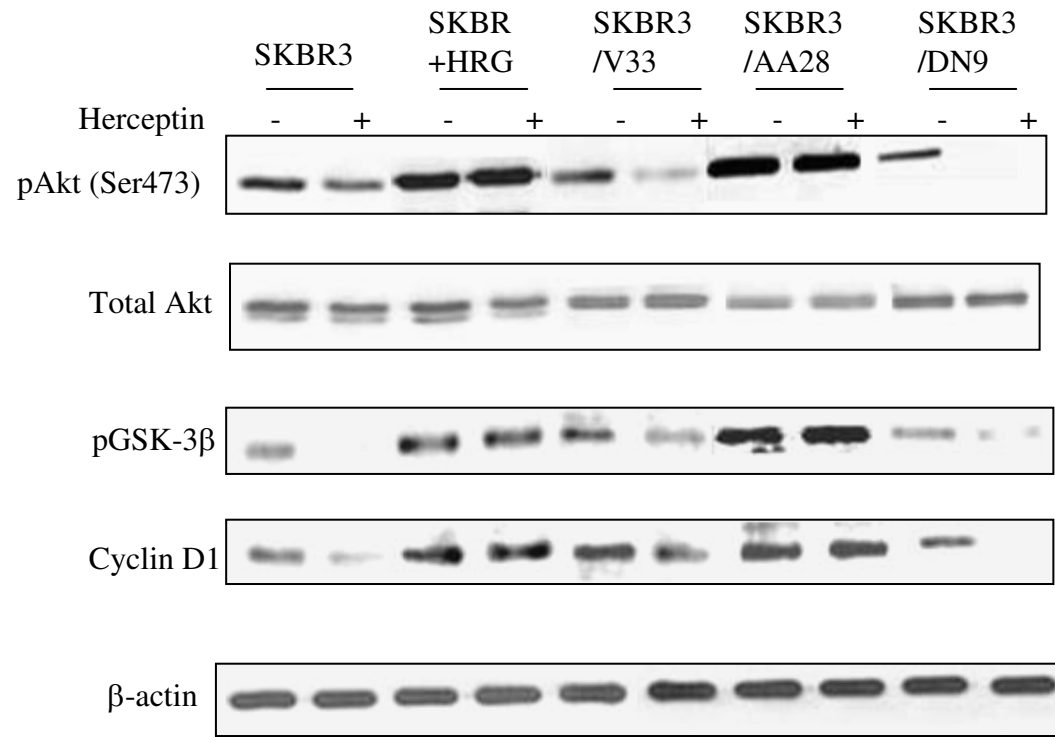


Figure 5

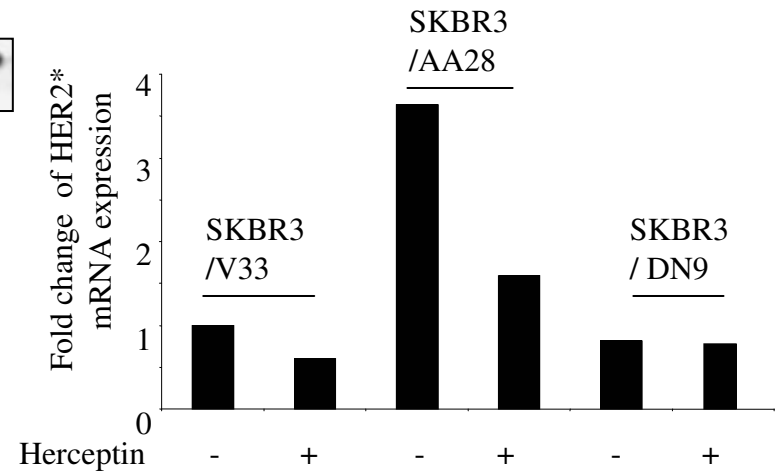
A Effects of Herceptin on PI3-K/Akt pathway in SKBR3 cells



C Active Akt1 translocated p27^{Kip1} from nuclear to cytosol

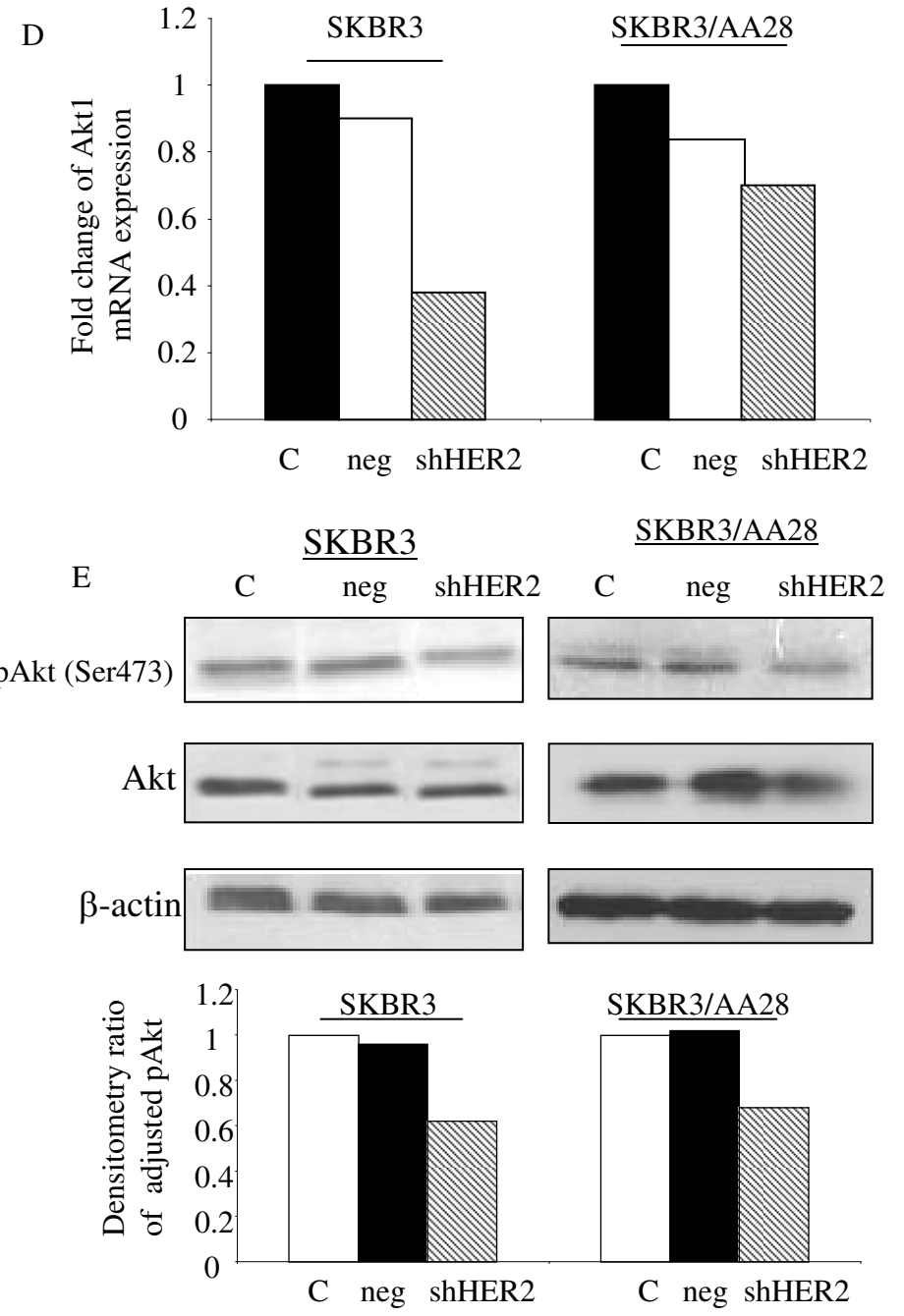
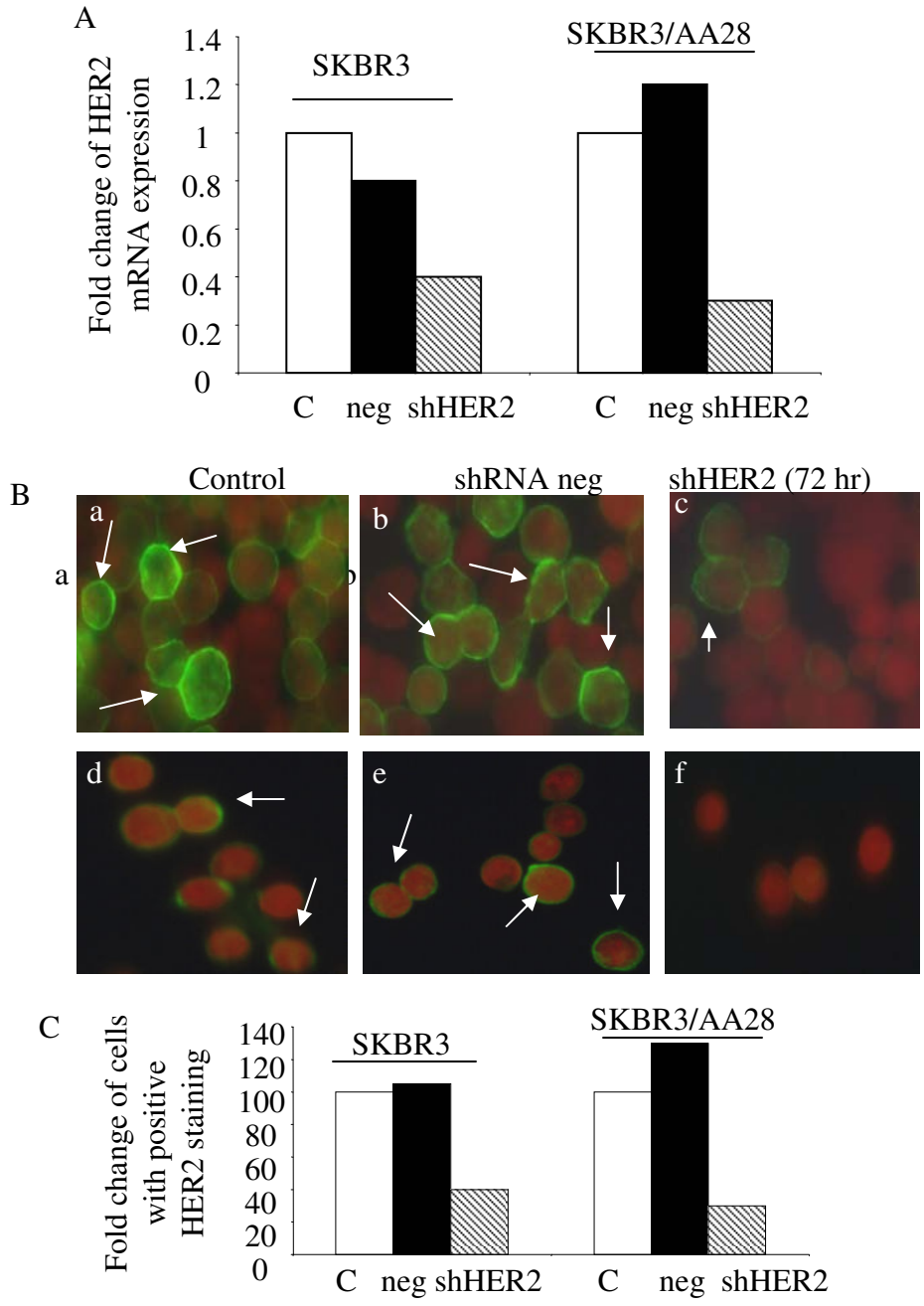


D mRNA expression of HER2



* Compared to vector cells without treatment and adjusted 18S

Figure 6



APPENDIX C

Update HER2/neu and pAkt Clinical Study

Patient's Characteristics

	N (91)	%
Ethnicity		
AA	40	44.0
Hisp	45	49.5
Caucasian	4	4.4
Asian	2	2.2
Age		
<50 yr	51	56.7
≥50 yr	40	43.3

Table 1. pAKT in relation to HER2/neu status

HER2/neu	pAkt		Total
	positive	negative	
positive	36	9	45
	80.0%	20.0%	100.0%
negative	21	25	46
	45.7%	54.3%	100.0%
Total	57	34	91
	62.6%	37.4%	100.0%

P=0.001, OR=4.76, 95%PI (1.87-12.6)

Table 2. pAkt in relation to ER status

ER status	pAkt		Total
	positive	negative	
positive	28	23	51
	54.9%	45.1%	100.0%
negative	27	8	35
	77.1%	22.9%	100.0%
Total	55	31	86
	64.0%	36.0%	100.0%

P=0.042; OR=2.77, 95%PI(1.059-7.260)

Table 3. pAkt in relation to PR status

PR status	pAkt		Total
	positive	negative	
positive	22	18	40
	55.0%	45.0%	100.0%
negative	33	13	46
	71.7%	28.3%	100.0%
Total	55	31	86
	64.0%	36.0%	100.0%

P=0.121, OR=2.077 95% PI (0.849-5.08)

Table 4. pAkt in relation to tumor differentiation grade

Differentiation	pAkt		Total
	positive	negative	
well	2	4	6
	33.3%	66.7%	100.0%
moderate	15	12	27
	55.6%	44.4%	100.0%
poorly	33	17	50
	66.0%	34.0%	100.0%
Total	50	33	83
	60.2%	39.8%	100.0%

P=0.051

Table 5. pAkt in relation to tumor size

	pAkt		Total
	positive	negative	
Tis	0	2	2
	0%	100.0%	100.0%
T0/Tx	0	2	2
	0%	100.0%	100.0%
T1	4	5	9
	44.4%	55.6%	100.0%
T2	25	16	41
	61.0%	39.0%	100.0%
T3	20	5	25
	80.0%	20.0%	100.0%
T4	5	3	8
	62.5%	37.5%	100.0%
Total	54	33	87
	62.1%	37.9%	100.0%

P=0.025

Table 6. pAkt in relation to lymph nodes

node status	pAkt		Total
	positive	negative	
negative	12 44.4%	15 55.6%	27 100.0%
positive	42 68.9%	19 31.1%	61 100.0%
Total	54 61.4%	34 38.6%	88 100.0%

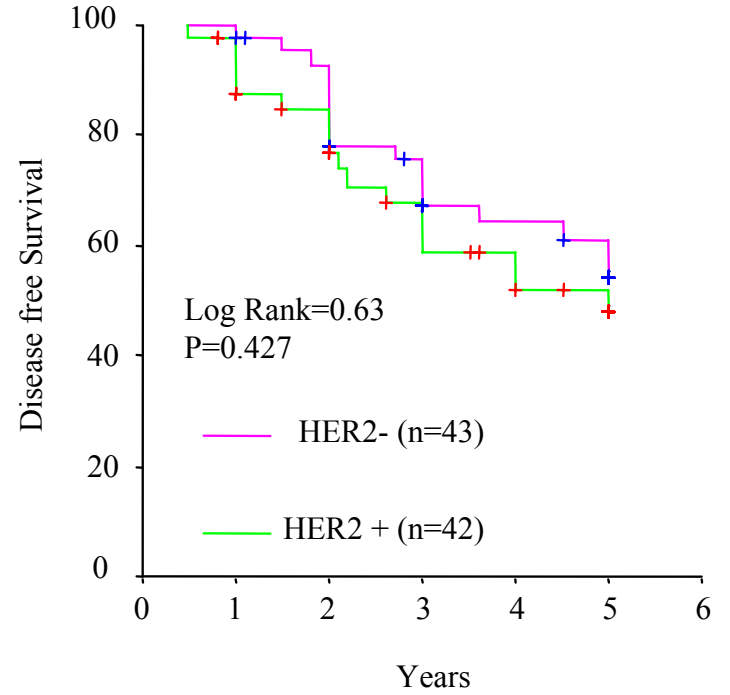
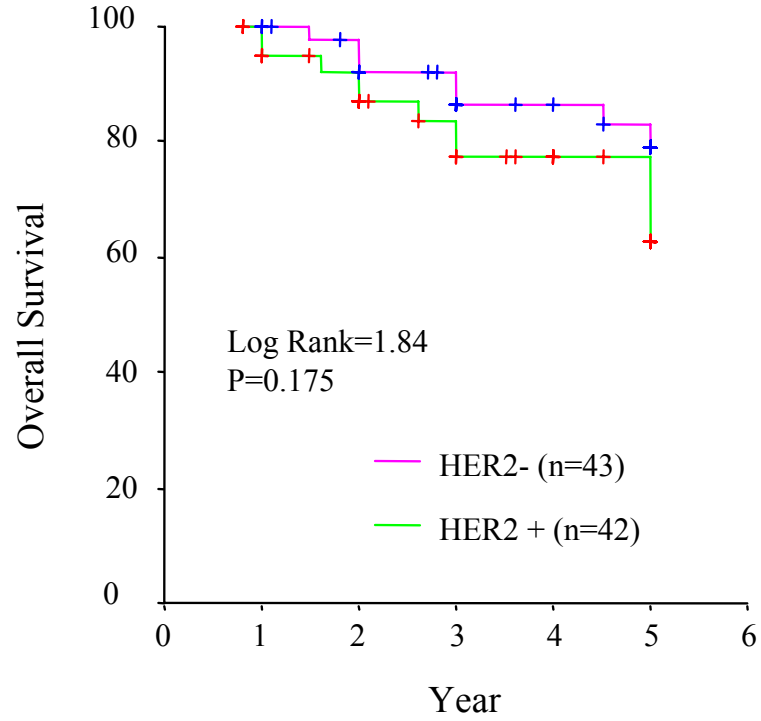
P=0.036 OR=2.763 95% PI (1.087-7.022)

Table 7. pAkt in relation to histology of tumor

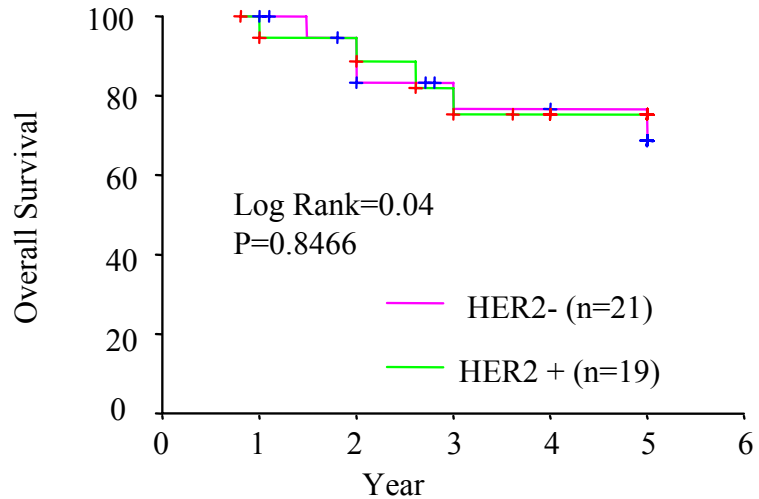
Histology	pAkt		Total
	positive	negative	
Ductal	48	25	73
	65.8%	34.2%	100.0%
Lobular	0	3	3
	0%	100.0%	100.0%
Total	48	28	76
	63.2%	36.8%	100.0%

P=0.047

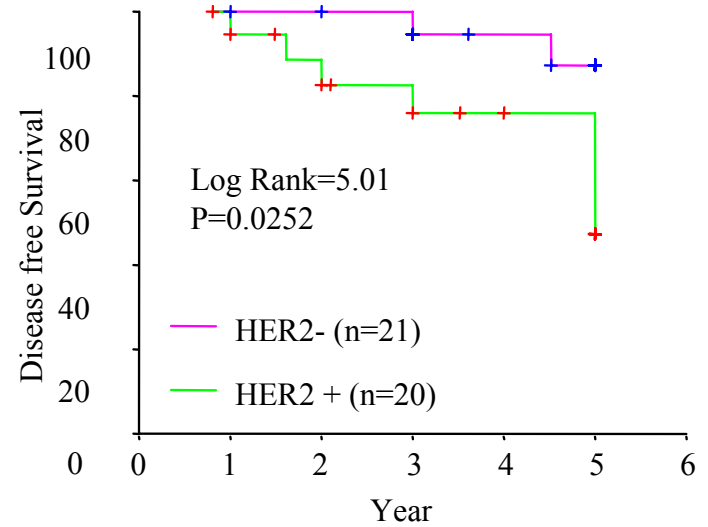
5-year Overall and Disease-free Survival in relation to HER2/neu Status



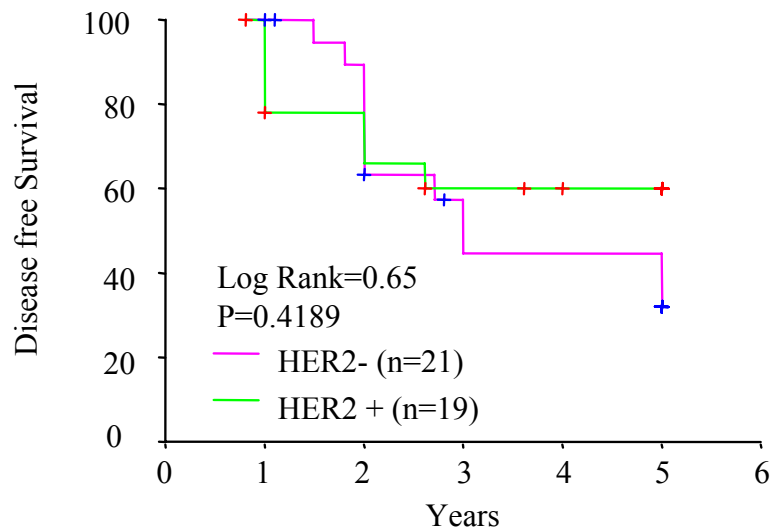
5-year Overall Survival in African American Women with Breast Cancer



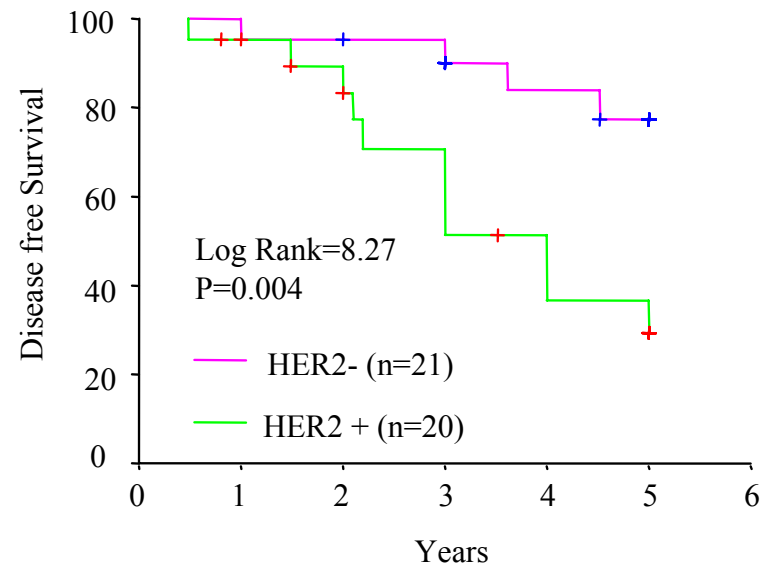
5-year Overall Survival in Latino Women with Breast Cancer



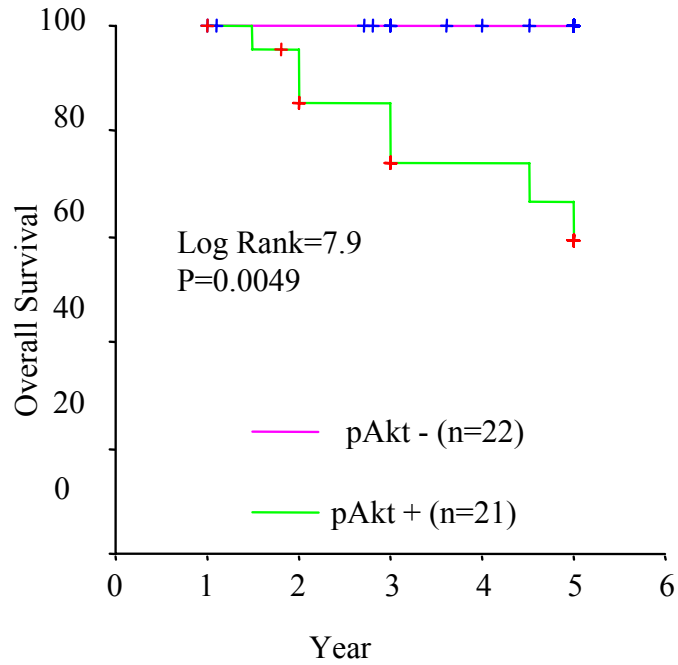
5-year Disease-free Survival in African American Women with Breast Cancer



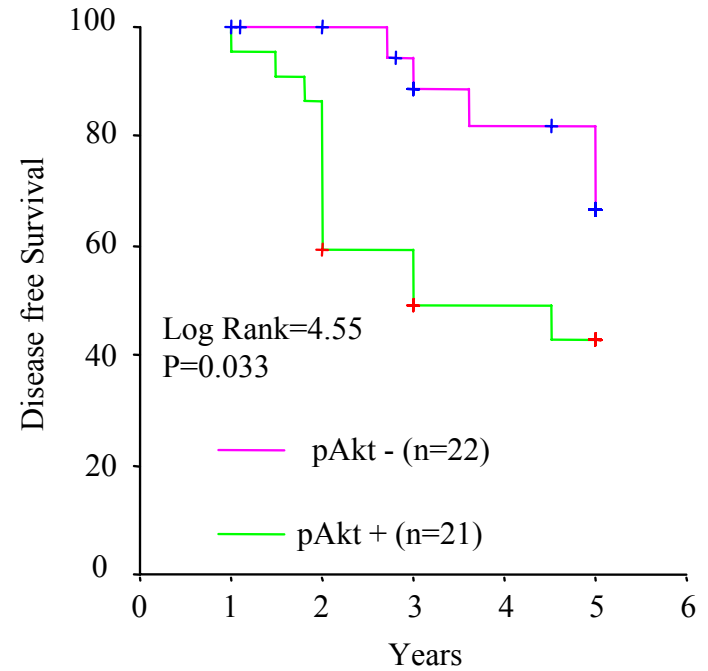
5-year Disease-free Survival in Latino Women with Breast Cancer



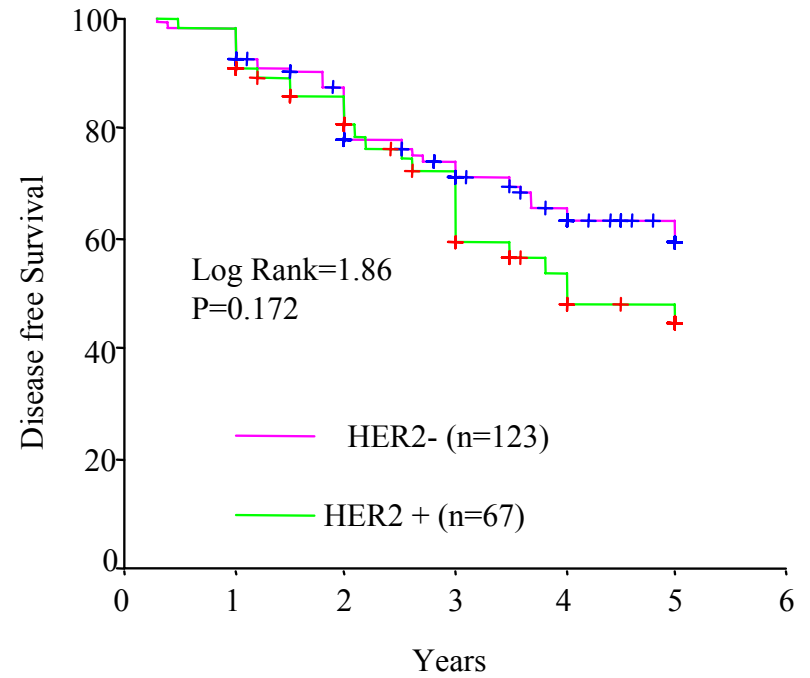
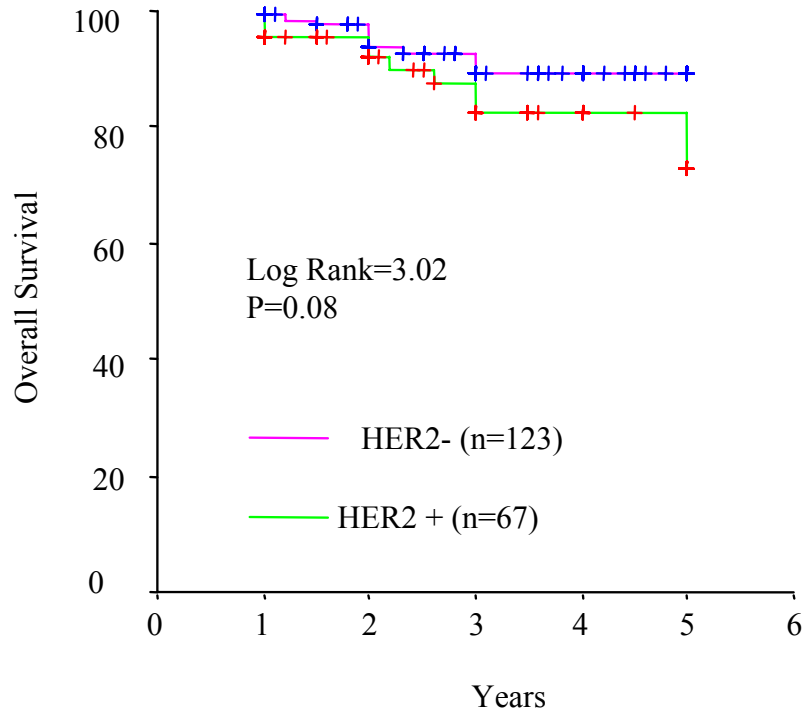
5-year Overall Survival in Patients with HER2/neu negative Breast Cancer in relation to pAkt status



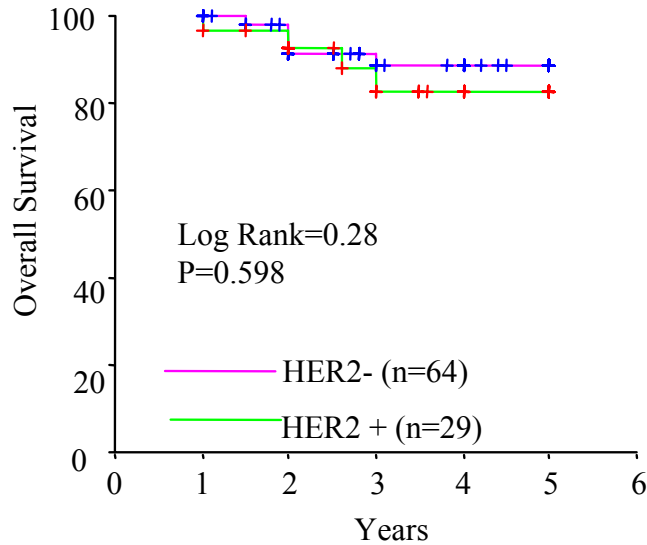
5-year Disease-free Survival in Patients with HER2/neu negative Breast Cancer in relation to pAkt status



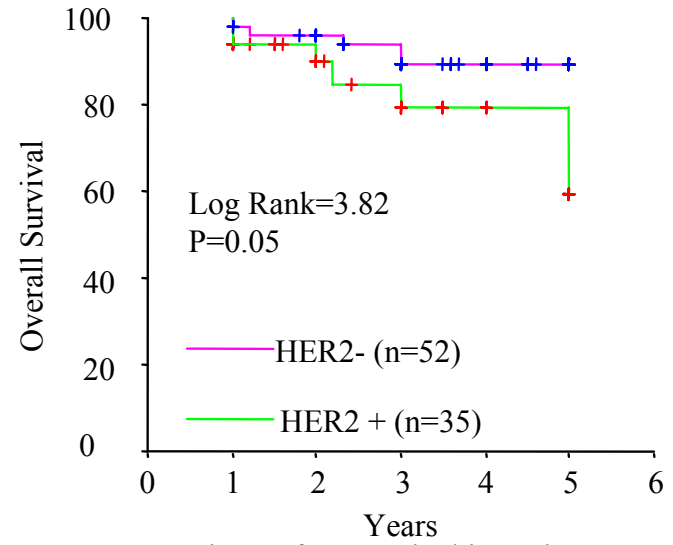
5-year Overall and Disease-free Survival in relation to HER2/neu Status



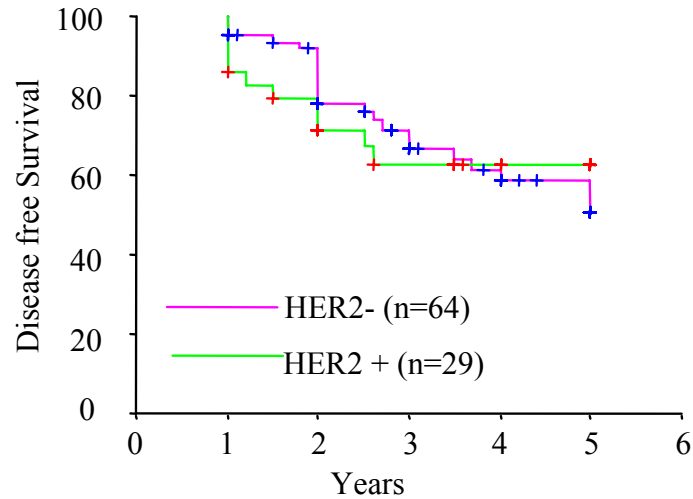
5-year Overall Survival in African American Women with Breast Cancer



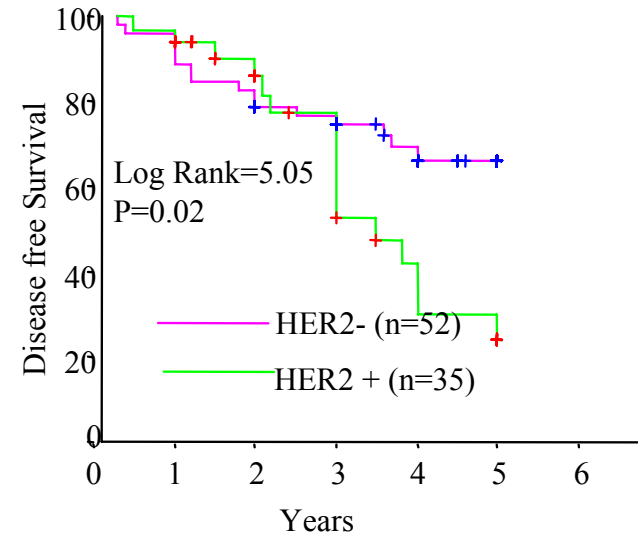
5-year Overall Survival in Latino Women with Breast Cancer



5-year Disease free Survival in African American Women with Breast Cancer



5-year Disease free Survival in Latino Women with Breast Cancer



46 patients pAkt status were analyzed at before and after treatment:

	N	%
pAkt level decreased	9	19.6
No change	37	80.4
Total	46	100.0

Table 8. pAkt in relation to IGF-IR status

IGF-IR status	pAkt		Total
	positive	negative	
positive	15 65.2%	3 42.9%	18 60.0%
negative	8 34.8%	4 57.1%	12 40.0%
Total	23 100.0%	7 100.0%	30 100.0%

P=0.392

Table 10. HER2/neu status in relation to IGF-IR status

HER2/neu status	IGF-IR		Total
	positive	negative	
positive	6	4	10
	60.0%	40.0%	100.0%
negative	7	11	18
	38.9%	61.1%	100.0%
Total	13	15	28
	46.4%	53.6%	100.0%

P=0.4

APPENDIX D

Cell Lines Containing Activated AKT and Dominant Negative AKT Mutations

Microarray Studies of
MCF7, BT474 and SKBR3

Cell Lines

MCF7/V8	Grown in the presence and absence of Herceptin
MCF7/DN2	Grown in the presence and absence of Herceptin
MCF7/AA13	Grown in the presence and absence of Herceptin
SKBR3/V23	Grown in the presence and absence of Herceptin
SKBR3/DN9	Grown in the presence and absence of Herceptin
SKBR3/AA28	Grown in the presence and absence of Herceptin
BT474/V1	Grown in the absence of Herceptin
BT474/DN4	Grown in the absence of Herceptin
BT474/AA5	Grown in the absence of Herceptin

The RNA Quality

- RNA was extracted from each cell line using the RNeasy Kit (Qiagen)
- The quality and quantity of RNA were determined using a Nanodrop spectrophotometer and a capillary electrophoresis apparatus Bioanalyzer 2000 (Agilent)

Nanodrop and Bioanalyzer

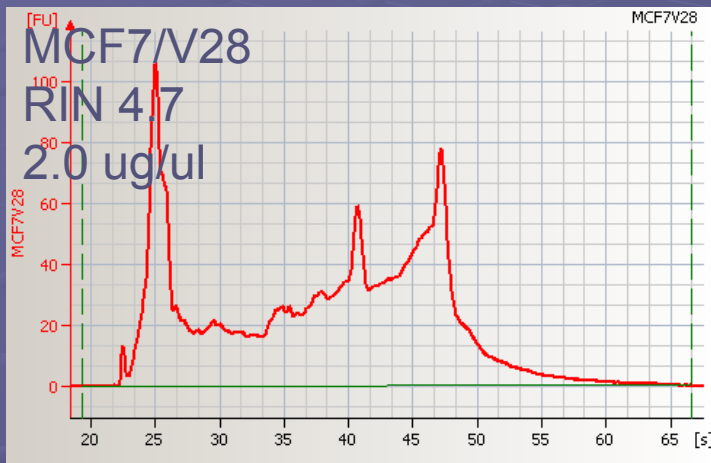


Diode array spectrophotometer
Accurately measures cyanine dye
and RNA concentration
Requires only 1-2 ul of sample

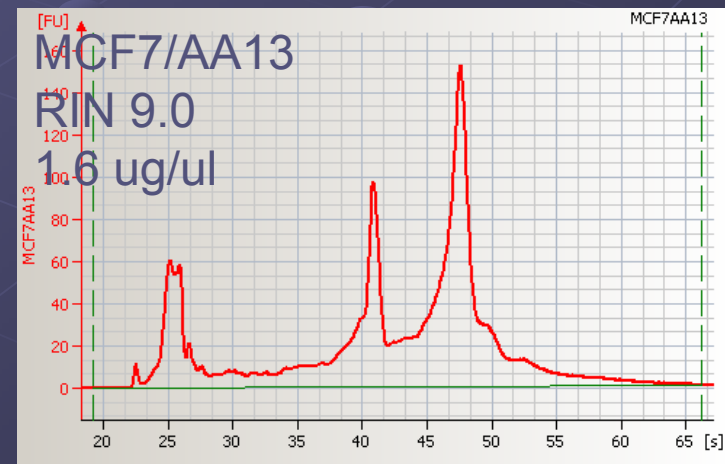
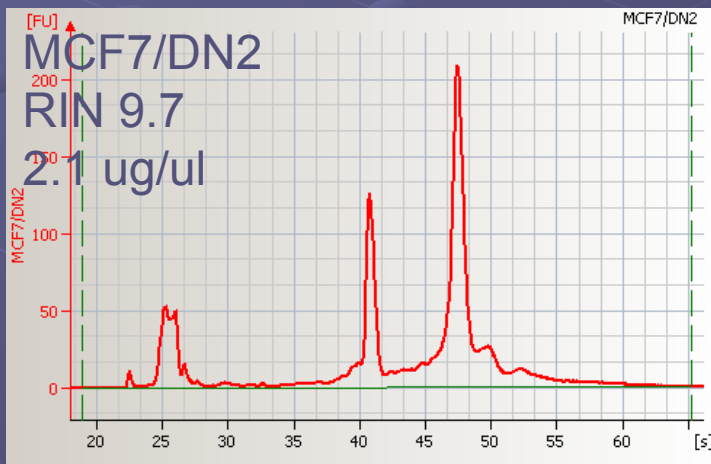


Capillary electrophoresis gel
Measures quality of RNA using
1 ul of sample
12 samples per run

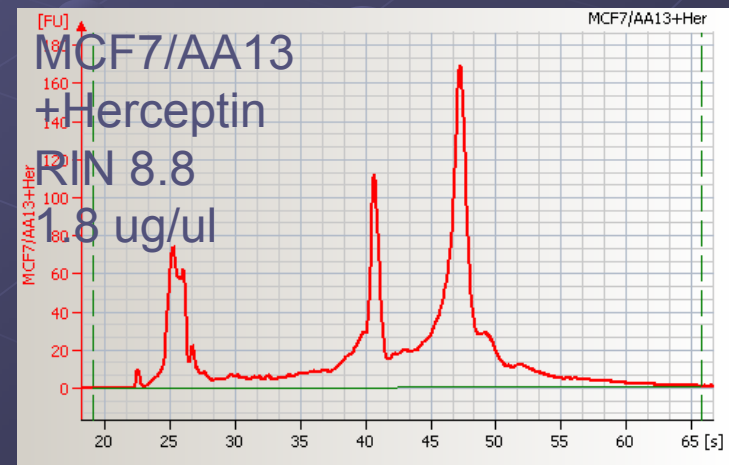
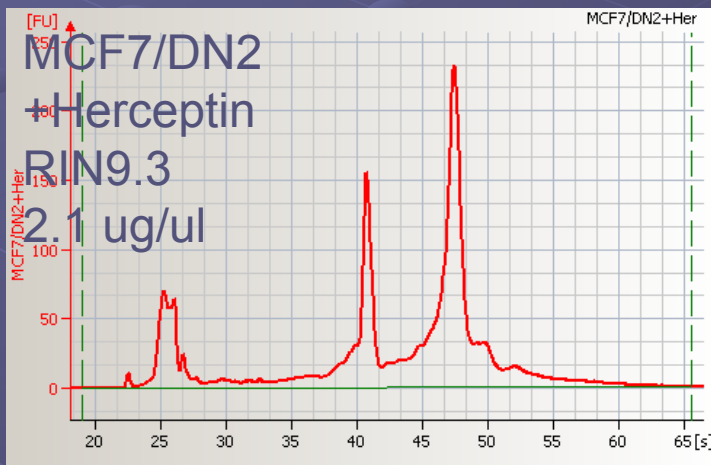
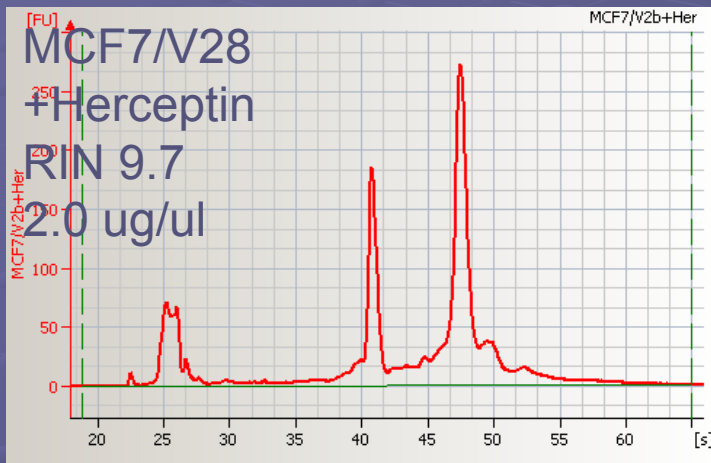
MCF7



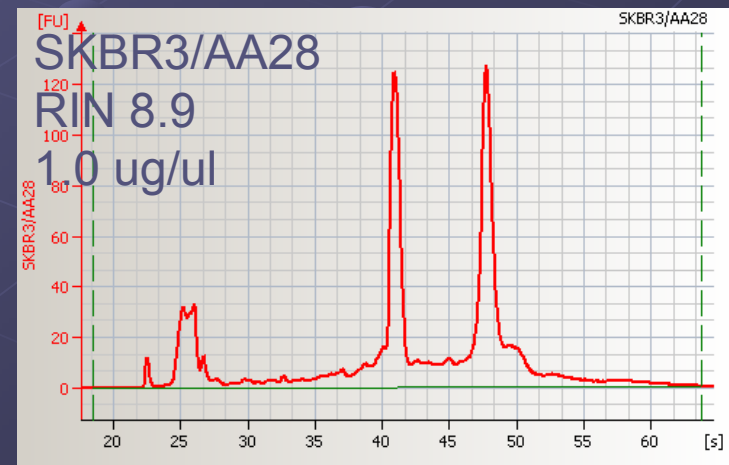
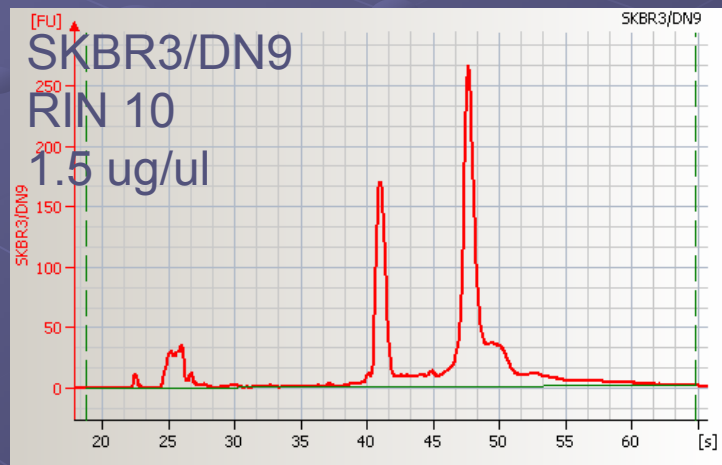
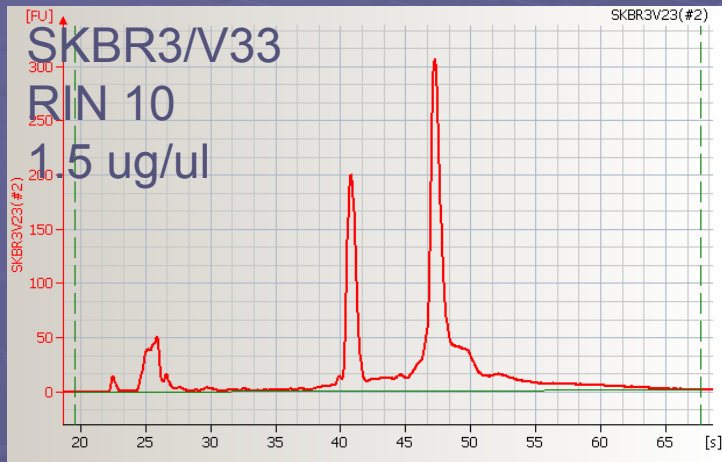
COMMENT: The quality of MCF7/V28 RNA is very low. I repeated the Bioanalyzer run three times, and all gave the same result. It also yielded poorly labeled RNA. I used it for the microarray, but it may have to be repeated.



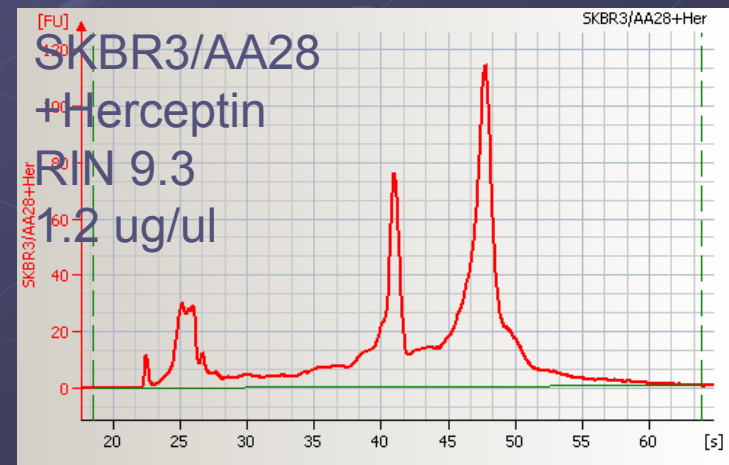
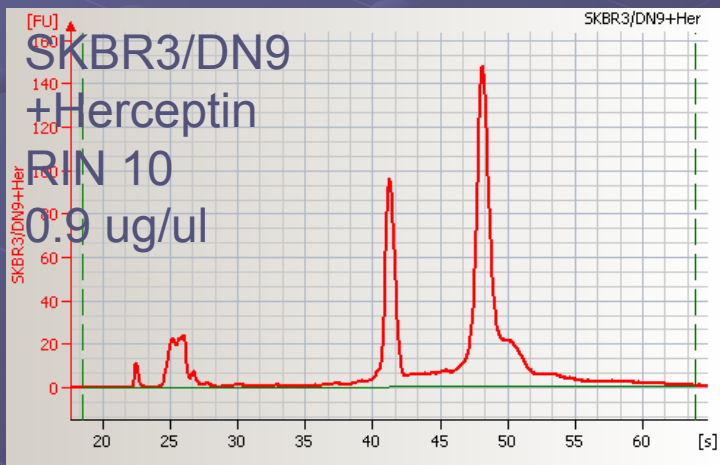
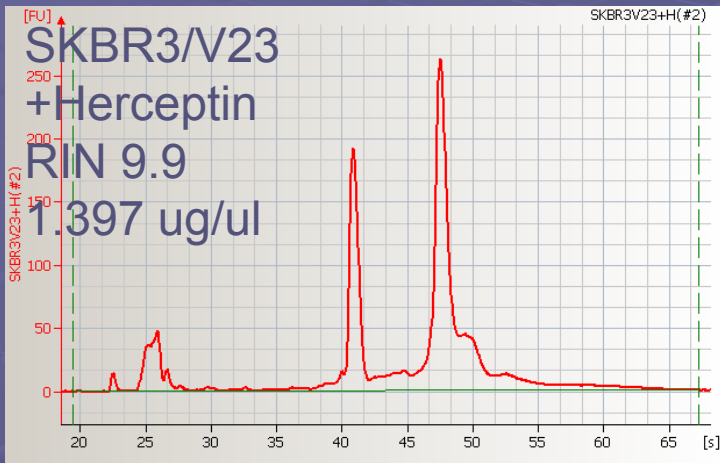
MCF7 + Herceptin



SKBR3 RNA



SKBR3 + Herceptin

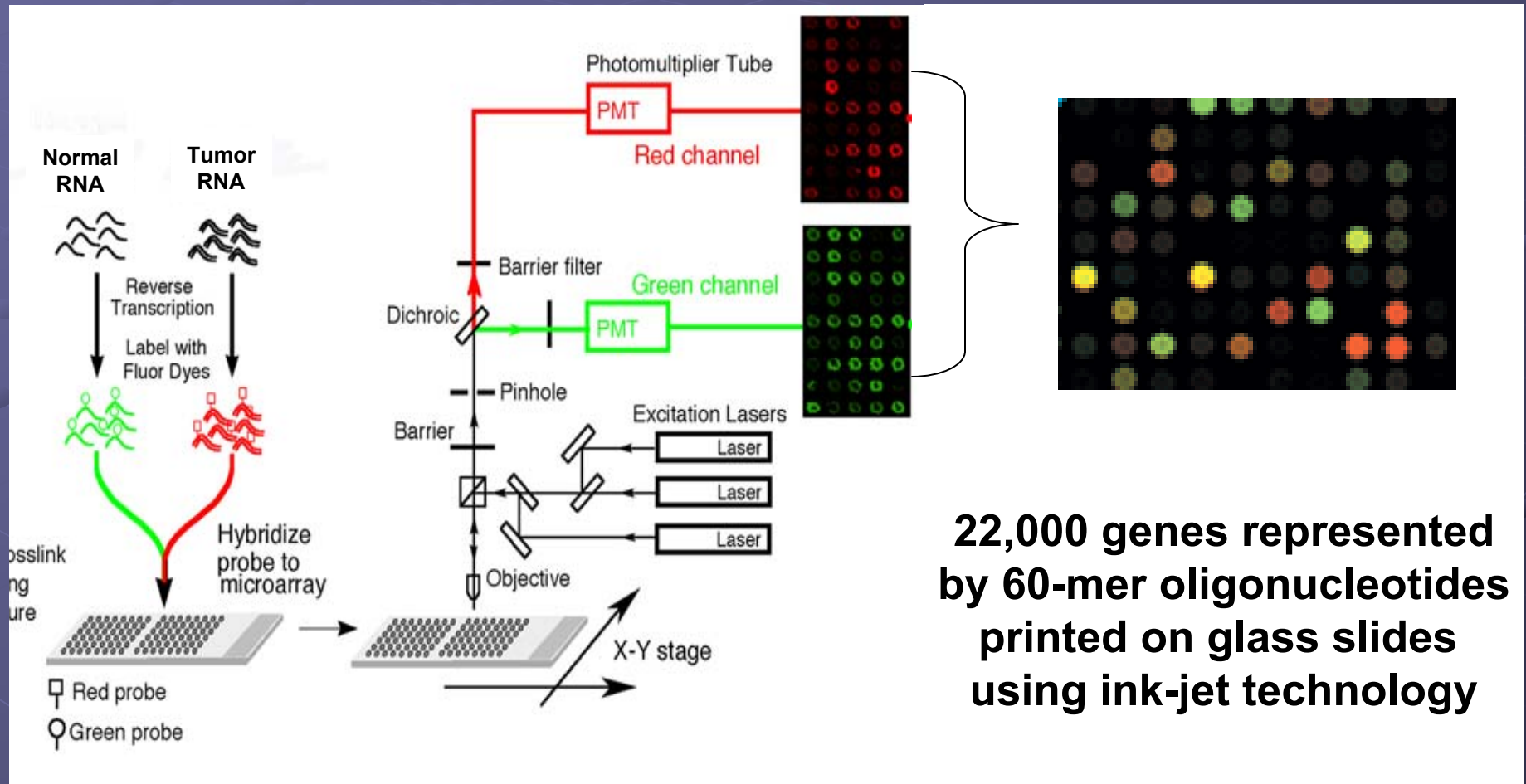


Labeling Efficiency of the RNA

SAMPLE	Cy Label pmole/ul	RNA ng/ul	260/280	FOI
MCF7/V8(Cy3)	4.57	359.44	2.29	4.13
MCF7/V8+H(Cy3)	7.43	609.93	2.27	3.95
MCF7/DN2(Cy5)	7.05	519.40	2.28	4.40
MCF7/DN2+H(Cy5)	6.77	463.21	2.26	4.74
MCF7/AA13(Cy5)	6.75	474.14	2.23	4.62
MCF7/AA13+H(Cy5)	7.31	502.61	2.28	4.72
SKBR3/V23 (Cy30				
SKBR3/V23+H (Cy3)				
SKBR3/DN9 (Cy5)				
SKBR3/DN9+H (Cy5)				
SKBR3/AA28 (Cy5)				
SKBR3/AA28+H (Cy5)				
BT474/V1(Cy3)	6.44	534.10	2.27	3.91
BT474/DN4(Cy5)	7.01	494.66	2.28	4.60
BT474/AA5(Cy5)	8.32	541.20	2.29	4.99

NOTE: FOI (Frequency of Incorporation) is approximately the number of cyanine labeled nucleotides incorporated into the RNA per 1000 bases.

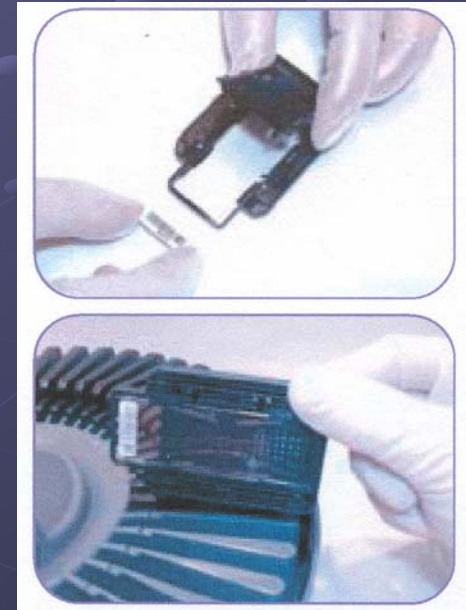
Agilent Microarrays



Agilent Scanner



48-Position Slide Carousel



Dual-laser scanner

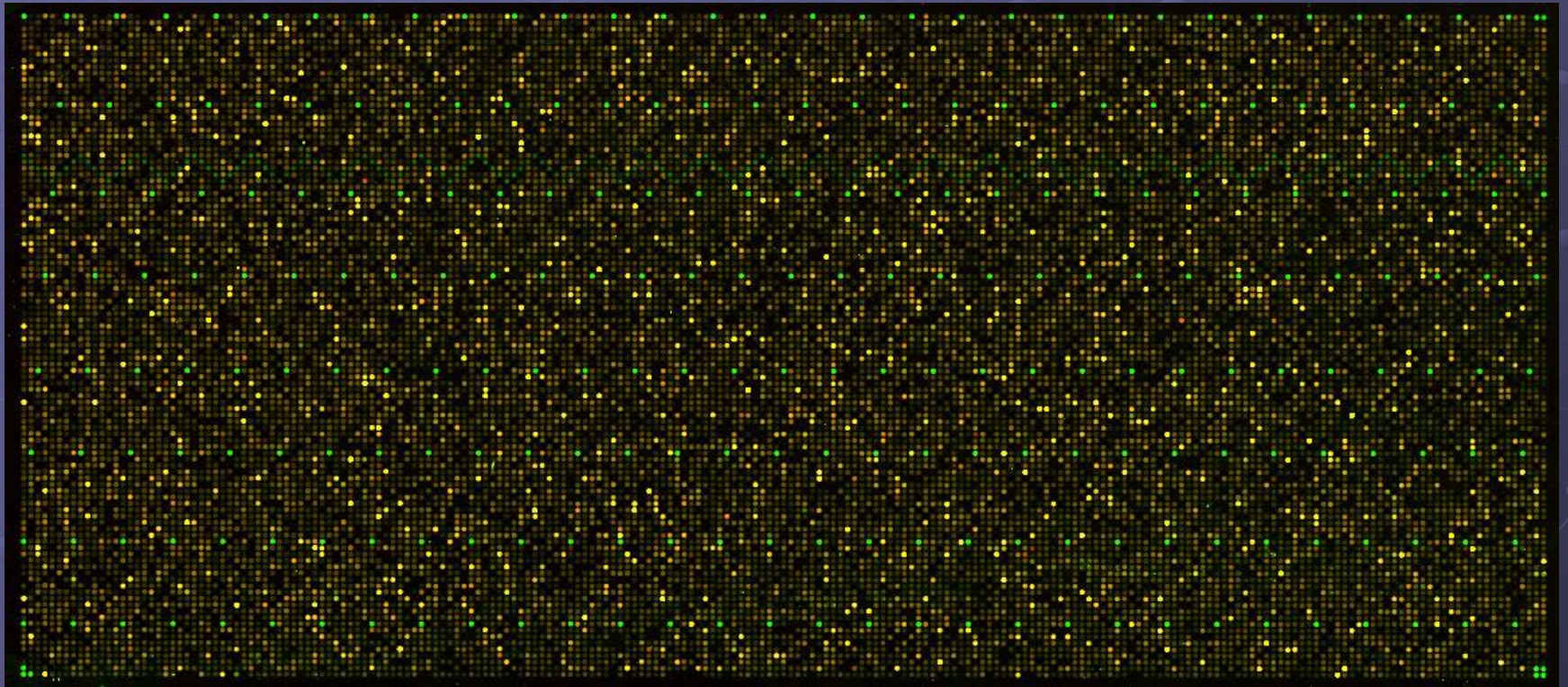
Programmable for minimal interaction (walk-away system)

Autofocus scanning system (continual focusing during scanning process)

Barcode reader

Feature Extraction Software for Image Analysis

Agilent Microarray Image file for MDA468 ZD1839 5 μ M vs MDA468 DMSO



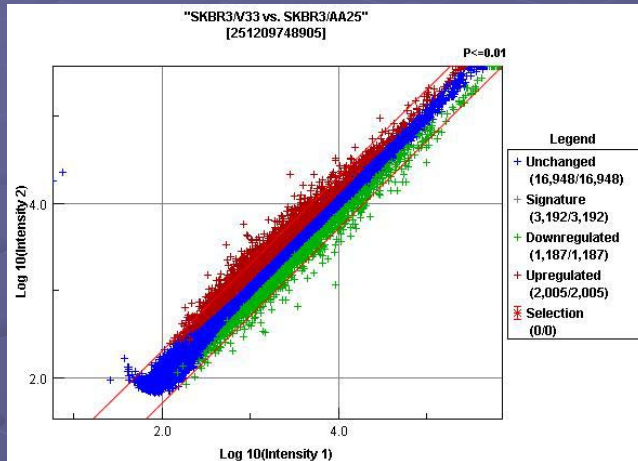
Uniform spot size, clear pattern of control probe
signals

Microarray Chips

1. BT474/V1 (Cy3) x BT474/DN4 (Cy5)
2. BT474/V1 (Cy3) x BT474/AA5 (Cy5)
3. MCF7/V8 (Cy3) x MCF7/DN2 (Cy5)
4. MCF7/V8 (Cy3) x MCF7/AA13 (Cy5)
5. MCF7/V8+Her (Cy3) x MCF7/DN2+Her (Cy5)
6. MCF7/V8+Her (Cy3) x MCF7/AA13+Her (Cy5)
7. SKBR3/V23 (Cy3) x SKBR3/DN9 (Cy5)
8. SKBR3/V23 (Cy3) x SKBR3/AA28 (Cy5)
9. SKBR3/V23+Her (Cy3) x SKBR3/DN9+Her (Cy5)
10. SKBR3/V23+Her (Cy3) x SKBR3/AA28+Her (Cy5)

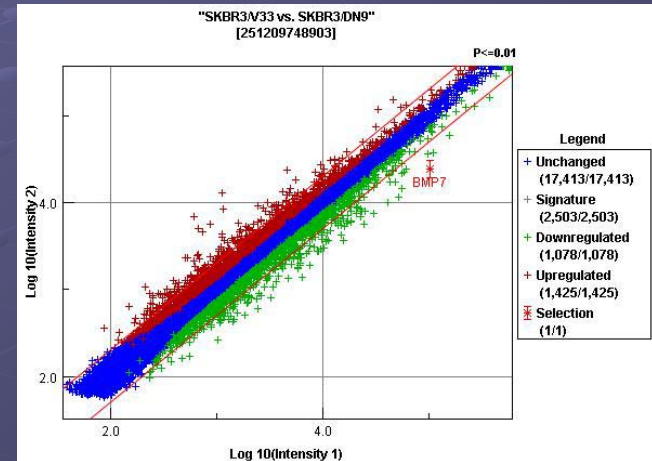
Intensity Blots Represent Differences of in Expression Between Samples: SKBR3

AA
25



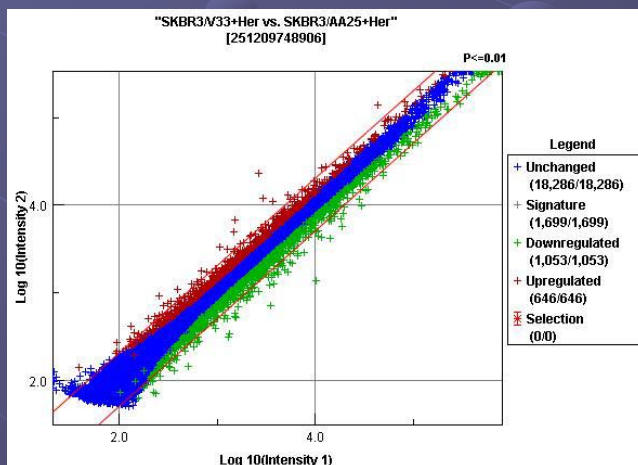
V33

DN
9



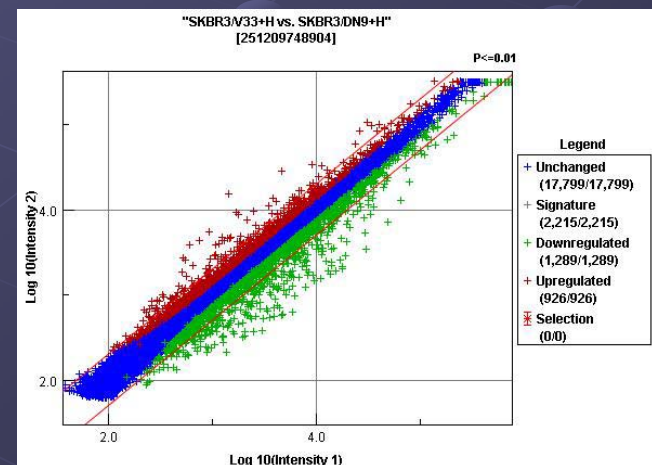
V33

AA
25
+H



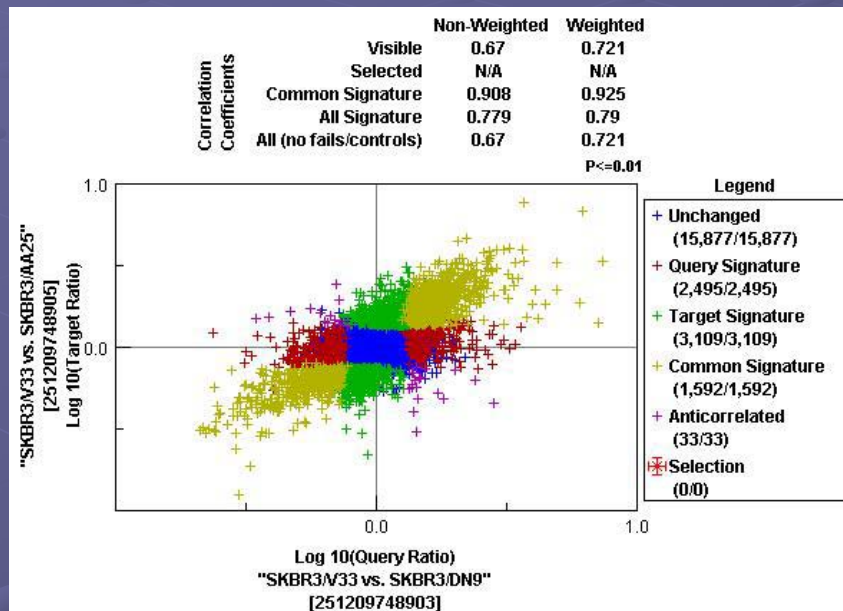
V33+H

DN
9
+H

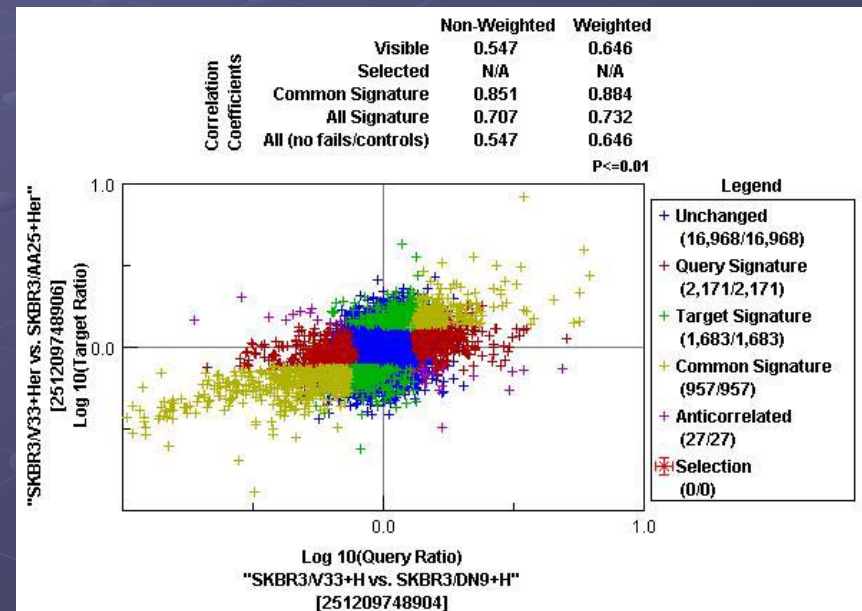


V33+H

Comparison Plots Represent Data Differences Between Microarrays

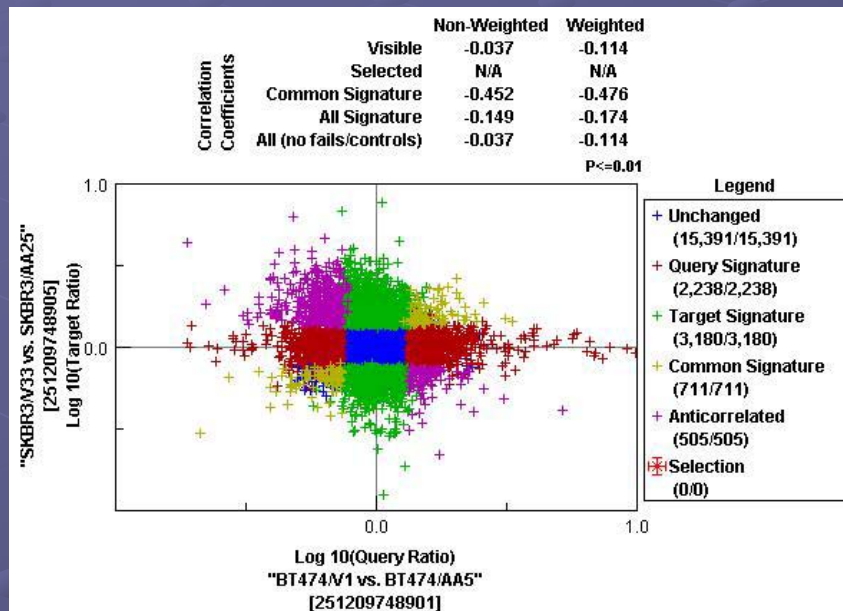


SKBR3/V33 vs. SKBR3/AA25
Compared to
SKBR3/V33 vs. SKBR3/DN9
Correlated 0.779

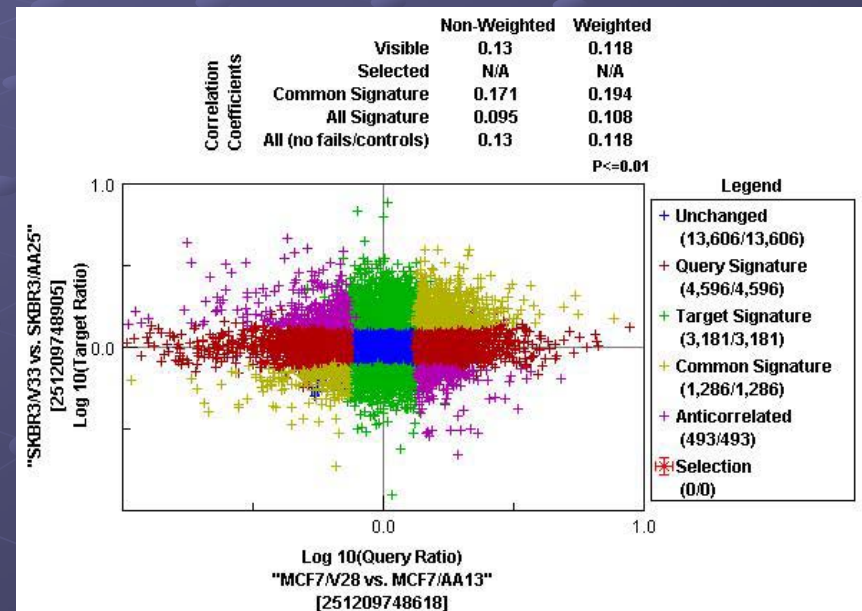


SKBR3/V33+H vs. SKBR3/AA25+H
Compared to
SKBR3/V33+H vs. SKBR3/DN9+H
Correlated 0.707

Comparison Between Cell Lines Do Not Show High Expression Correlation

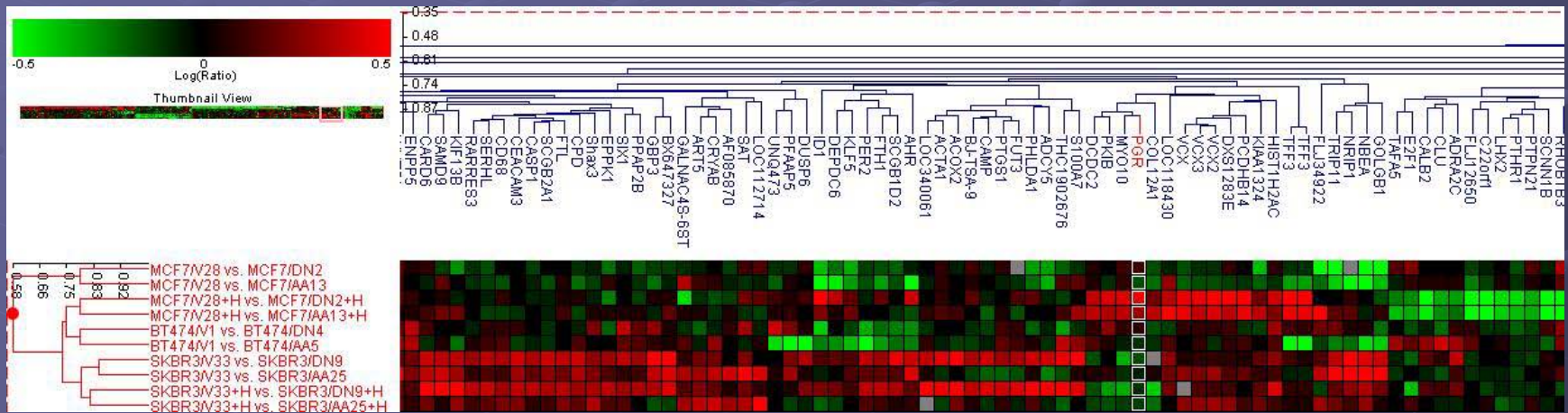


SKBR3/V33 vs. SKBR3/AA25
 Compared to
 BT474/V1 vs. BT474/AA5
 Correlation -0.149



SKBR3/V33 vs. SKBR3/AA25
 Compared to
 MCF7/V28 vs. MCF7/AA13
 Correlation 0.095

The PGR Region



Similarly, note that in the region of PGR, there are also a group of genes that are up regulated in SKBR3/DN9, but down regulated in SKBR3/AA25, independent of the presence or absence of Herceptin. The story is complex in that MCF7, BT474 and SKBR3 do not change expression in the same way when a particular AKT mutation is present.

APPENDIX E

NAME	EMAIL	PHONE NUMBER	CLUSTER
Allen, Bruce	brallen@cdrewu.edu	323-563-5872	Cancer
Alexander, Gail Orum	gailorum@cdrewu.edu	x5851	Cancer
Ali, Ishrat	iali@ladhs.org	310-668-3469	Cancer
Bazargan, Mohsen	mobazarg@cdrewu.edu	310-761-4722	HIV-Cancer
Bazargan-Hejazi, Shahrzad	shbazarg@cdrewu.edu	323-357-3464	HIV-Cancer
Cadavid, Nestor-Gonzales			
Calderon, Jose	drcalderon@cdrewu.edu	310-761-4729	Cancer
Chen, Zujian	zujianchen@cdrewu.edu	323-563-5947	Cancer
Chillar, Ram	rchillar@ladhs.org	310-668-3469	Cancer
Chowdhary, Supurna			
Clayton, Sheila	shclayton@cdrewu.edu	(310) 668-3144	Cancer
Datta, Nand	nanddatta@cdrewu.edu	(310) 668-4545	Cancer
Davis, Jean	ijeandavis@cdrewu.edu	323-563-5826	Cancer
Ghoneum, Mamdooh	mghoneum@ucla.edu	x5953	Cancer
Giannikopolous, Ioannis	iogianni@cdrewu.edu		
Junko, Nishitani	jnishitani@cdrewu.edu	323-563-5935	Cancer
Kim, Junyeop	junyeopkim@cdrewu.edu	323-357-3458	HIV-Cancer
Mehta, Manan	msmehta@gmail.com		
Mishra, Dhruva	dhruvamishra@cdrewu.edu	323-563-5947	Cancer
Mohamed, Hezla	hezlamohamed@cdrewu.edu ; hmohamed@cdrewu.edu	310-668-4445	Cancer
Norris, Keith	knorris@ucla.edu	323-249-5702	
Padda, Manmeet	paddamd@yahoo.com		
Robinson, Paul	paulrobinson@cdrewu.edu	310-761-4731	All 3 Major Clusters
Rodriguez, Elizabeth	elizabethrodriguez@cdrewu.edu	323-563-4853	
Sanchez, Kathleen	ksanchez61@sbcglobal.net	323-497-4055	
Sarkesian, Armene	armsark@sbcglobal.net		
Sarkissyan, Mariana	mariansark@hotmail.com	323-563-5947	Cancer
Shaheen, Magda	magdashaaheen@cdrewu.edu	310-761-4727	Cardio/Metab-Cancer
Singh, Rajan	rajansingh@cdrewu.edu	323-563-3928	Cardio/Metab-Cancer
Vadgama, Jay	javadgam@cdrewu.edu	323-563-4853	Cancer
Williams, Imani			Cancer
Wu, Yanyuan	yanyuanwu@cdrewu.edu	323-563-9893	Cancer

DIVISION	DEPARTMENT	
Tobacco Research	OBGYN	
Dean	College of Science and Health	
Hem/Onc	Internal Medicine	
RCMI	Family Medicine	
RCMI	Psychiatry	
RCMI	Ophthalmology	
Cancer Res/Training	Internal Medicine	
Hem/Onc	Internal Medicine	
Surgical/Onc	Surgery	
Surgical/Urology	Surgery	
	ENT	
Gastroenterology	Internal Medicine	
IRB/Otololaryn	ENT	
Cancer Res/Training	Internal Medicine	
Cancer Res/Training	Internal Medicine	
	Pathology	
Vice President	Internal Medicine	
Gastroenterology	Internal Medicine	
RCMI		
Cancer Res/Training	Internal Medicine	
Cancer Res/Training	Internal Medicine	
RCMI		
Endocrinology	Internal Medicine	
Chief, Cancer Res	Internal Medicine	
& Training		
Cancer Res/Training	Internal Medicine	

APPENDIX F

DREW-UCLA BREAST CANCER RESEARCH AND TRAINING PARTNERSHIP: MOLECULAR/CELLULAR PATHOGENESIS MODEL

Summary of Tasks (3) proposed in the original application:

- 1) Identify established UCLA researchers conducting innovative breast cancer research.
 - 2) within this pool of researchers, identify research projects with the best potential to provide experiences for Drew trainees to create their own focus and compete for independent funding.
 - 3) develop mentor/trainee relationships that will not only transfer knowledge from UCLA scientists to Drew trainees, but also offer career development and research opportunities for trainees.
 - 4) create or establish access to workshops, seminars, scientific meetings, journal clubs, and coursework geared toward developing Drew trainees.
 - 5) conduct a specialized and innovative breast cancer research project that will stimulate future breast cancer research at Drew and will use Drew's Tissue Repository as its greatest resource.
- This research program will focus on cell and molecular biology, detection, diagnosis, etiology, and treatment of HER2/neu expressing breast tumors in minority and underserved women.

**DREW-UCLA BREAST CANCER RESEARCH AND TRAINING
PARTNERSHIP: MOLECULAR/CELLULAR PATHOGENESIS MODEL**

Drew-UCLA Partnership - Funding Progress from March 2005	
Activity at Drew	Number
<i>Funding:</i>	
Active grants	4
Newly approved	2
Pending	14

**DREW-UCLA BREAST CANCER RESEARCH AND TRAINING
PARTNERSHIP: MOLECULAR/CELLULAR PATHOGENESIS MODEL**

Drew-UCLA Partnership - Recruitment Progress from March 2005	
Activity at Drew	Number
<i>Faculty recruited:</i>	6
New Assistant Professor	3
Current Senior fellows Promoted to Assistant Professor	3

**DREW-UCLA BREAST CANCER RESEARCH AND TRAINING
PARTNERSHIP: MOLECULAR/CELLULAR PATHOGENESIS MODEL**

Drew-UCLA Partnership - Training Progress from March 2005	
Activity at Drew	Number
<i>In Training (Directly involved):</i>	27
Clinical Fellows	4
Postdoctoral fellows	4
Clinical Residents (were 4, 3 moved onto clinical fellowship)	1
Medical Students	2
Undergraduate Students (Includes summer students)	10
High School Students (Includes summer students)	6

**DREW-UCLA BREAST CANCER RESEARCH AND TRAINING
PARTNERSHIP: MOLECULAR/CELLULAR PATHOGENESIS MODEL**

Drew-UCLA Partnership - Training Progress from March 2005	
Activity at Drew since March 2005	Number
<i>Participation in Research Seminars, Workshops, Journal Club, lab Meetings, between the partnership sites</i>	
Faculty (senior and junior), fellows (clinical and basic), and students attend a number of above activities. These are in addition to those listed above as “directly involved”	>40

**DREW-UCLA BREAST CANCER RESEARCH AND TRAINING
PARTNERSHIP: MOLECULAR/CELLULAR PATHOGENESIS MODEL**

Drew-UCLA Partnership - Publications Progress from March 2005	
Activity at Drew since March 2005	
<i>Publications</i>	Number
Published – In press	4
Accepted with minor revisions	2
Under review	2
In preparation	3
Abstracts presented/published	4

Evaluation of Partnership Funding activity

Funding Activity at Drew since March 2005 (Total of 17)				
Investigator Role	Academic Status	Title of Application	Funding Agency / Funding Period	Status
Vadgama, PI/Co-PI	Professor and PI	Drew-UCLA U56 Partnership Program	NCI / 2005-2010	Approved
Vadgama, PI/Co-PI	Professor and PI	Drew-UCLA U56 Partnership Program	NCI / 2006-2011	Pending
Vadgama, Co-PI Koeffler Co-PI	Professor and PI	Role of CCN Proteins in Breast Cancer	NCI /2005-2010	Approved
Vadgama, PI Koeffler Co-PI	Professor and PI	Pre-proposal: DOD-Prostate Cancer Partnership Program HBCU-Cancer Center	DOD / 2006-2011	Pending

APPENDIX F1

Evaluation of Partnership Funding activity

Wu, Co-PI Slamon, Co-PI Mentors: Vadgama, Pegram	Assistant Professor	Cellular and Molecular studies to investigate the Role of AKT/Protein Kinase B in HER-2/neu Over-expressing Breast Tumors	NCI U56 2005-2010	Approved
Wu, PI Mentors: Vadgama, Slamon	Assistant Professor	Oncogenic Role of Akt1 in HER2/neu overexpressing Breast Tumors, Target for Treatment	MBRS/NIH (SOI) 2007-2011	Pending
Troutman, PI Mentors: Vadgama	Assistant Professor	The Use of Toll-like Receptors in Ovarian Cancer Detection	MBRS/NIH 2007-2011	Pending
Troutman, Co-PI Walsh, Co-PI Mentors: Koeffler	Assistant Professor	Identification of risk factors for aggressive endometrial cancer in minority women	NCI / 2006- 2009	Pending

Evaluation of Partnership Funding activity

Chakrabarti, PI Mentors: Koeffler, Vadgama	Senior Postdoctoral Fellow/ Assistant Professor	Influence of Normal and Tumor Breast Epithelial Cells on Hematopoietic and Mesenchymal Stem Cell Plasticity	RCMI/NIH Stem Cell Program 2007-2011	Pending
Chakrabarti, PI Mentors: Vadgama, Srivastavan	Senior Postdoctoral Fellow/ Assistant Professor	Identification of LOH in African American and Hispanic women with breast cancer	MBRS/NIH 2007-2011	Pending
Zhong, PI Mentors: Vadgama	Assistant Professor	Mechanism of alcohol-induced RNA pol III dependent gene transcription	MBRS/NIH (SO1) 2007-2011	Pending

Evaluation of Partnership Funding activity

<p>Park Co-PI; Penichet, Co-PI Mentors: Vadgama</p>	<p>Assistant Professor</p>	<p>Antibody-cytokine fusion proteins to enhance the immune response against MRB/Robo4</p>	<p>NCI / 2006-2009</p>	<p>Pending</p>
<p>Thant, PI Mentors: Vadgama</p>	<p>Senior Postdoctoral Fellow/ Assistant Professor</p>	<p>Role of VEGF and MMPs in metastatic colorectal cancer</p>	<p>MBRS/NIH 2007-2011</p>	<p>Pending</p>
<p>Romero, PI Mentors: Slamon, Vadgama</p>	<p>Clinical Fellow/ Assistant Professor</p>	<p>Epidermal Growth Factor Receptor Tyrosine Kinase Inhibitors for the Treatment of Esophageal Adenocarcinoma, a Pre-Clinical Study</p>	<p>MBRS/NIH 2007-2011</p>	<p>Pending</p>

Evaluation of Partnership Funding activity

<p>Duong, Co-PI Black, Co-PI</p>	<p>Associate Professor</p>	<p>Development of Novel Classification and Identification of Aberrant genes in Glioblastoma multiforme (GBM)</p>	<p>NCI / 2006-2009</p>	<p>Pending</p>
<p>Zhong PI Mentors: Tripathi Vadgama</p>	<p>Assistant Professor</p>	<p>JNK1 and JNK2 differently regulate expression of Brf1 to result in change in RNA polymerase III-dependent transcription</p>	<p>RCMI / NIH Transgenic Animal Studies Program 2007-2011</p>	<p>Pending</p>
<p>Park PI Mentors: Koeffler, Vadgama</p>	<p>Assistant Professor</p>	<p>Enhanced Self-Renewal of Embryonic Stem Cells</p>	<p>RCMI/NIH Stem Cell Program 2007-2011</p>	<p>Pending</p>